

UNCLASSIFIED

DTIC FILE COPY

1

SECURITY CLASSIFICATION OF THIS PAGE (When Data Entered)

AD-A196 700

REPORT DOCUMENTATION PAGE		READ INSTRUCTIONS BEFORE COMPLETING FORM
1. REPORT NUMBER AFIT/CI/NR 88- 97	2. GOVT ACCESSION NO.	3. RECIPIENT'S CATALOG NUMBER
TITLE (and Subtitle) A COMPUTER MODEL FOR ANALYSIS OF DIELECTRICALLY ENHANCED SINGLE-ZONE TUNNEL DIODES		5. TYPE OF REPORT & PERIOD COVERED MS THESIS
		6. PERFORMING ORG. REPORT NUMBER
AUTHOR(s) WILLIAM MELENDEZ		8. CONTRACT OR GRANT NUMBER(s)
PERFORMING ORGANIZATION NAME AND ADDRESS AFIT STUDENT AT: UNIVERSITY OF TEXAS - AUSTIN		10. PROGRAM ELEMENT, PROJECT, TASK AREA & WORK UNIT NUMBERS
CONTROLLING OFFICE NAME AND ADDRESS		12. REPORT DATE 1988
		13. NUMBER OF PAGES 120
MONITORING AGENCY NAME & ADDRESS (if different from Controlling Office) AFIT/NR Wright-Patterson AFB OH 45433-6583		15. SECURITY CLASS. (of this report) UNCLASSIFIED
		15a. DECLASSIFICATION/DOWNGRADING SCHEDULE
16. DISTRIBUTION STATEMENT (of this Report) DISTRIBUTED UNLIMITED: APPROVED FOR PUBLIC RELEASE		
17. DISTRIBUTION STATEMENT (of the abstract entered in Block 20, if different from Report) SAME AS REPORT		
18. SUPPLEMENTARY NOTES Approved for Public Release: IAW AFR 190-1 LYNN E. WOLAVER <i>Lynn Wolaver</i> 20 July 88 Dean for Research and Professional Development Air Force Institute of Technology Wright-Patterson AFB OH 45433-6583		
19. KEY WORDS (Continue on reverse side if necessary and identify by block number)		
20. ABSTRACT (Continue on reverse side if necessary and identify by block number) ATTACHED		

DTIC  
SELECTED  
AUG 03 1988  
S & D

**A COMPUTER MODEL FOR ANALYSIS OF DIELECTRICALLY  
ENHANCED SINGLE-ZONE TUNNEL DRYERS**

Accession For	
NTIS CRA&I	<input checked="" type="checkbox"/>
DTIC TAB	<input type="checkbox"/>
Unannounced	<input type="checkbox"/>
Justification	
By _____	
Distribution/	
Availability Codes	
Dist	Avail and/or System
<b>A-1</b>	

APPROVED:

\_\_\_\_\_

\_\_\_\_\_



**A COMPUTER MODEL FOR ANALYSIS OF DIELECTRICALLY  
ENHANCED SINGLE-ZONE TUNNEL DRYERS**

by

**WILLIAM MELENDEZ , B.S.**

**THESIS**

Presented to the Faculty of the Graduate School of

The University of Texas at Austin

in Partial Fulfillment

of the Requirements

for the Degree of

**MASTER OF SCIENCE IN ENGINEERING**

**THE UNIVERSITY OF TEXAS AT AUSTIN**

August 1988

## ACKNOWLEDGEMENTS

I would like to extend my appreciation to my supervising professor, Dr. Philip S. Schmidt, for guiding me towards the completion of this research. Also, I would like to thank Dr. Theodore L. Bergman for his technical advice and Mrs. Brenda Fondren for her assistance in the editing of this report.

Special appreciation goes to my wife, Maida, for her emotional support and for assisting in the typing of this thesis.

This work was supported by the U.S. Air Force through The Air Force Institute of Technology, Civilian Institution Program, Wright-Patterson AFB, OH.

William Melendez

The University of Texas at Austin  
August, 1988

## ABSTRACT

### A COMPUTER MODEL FOR ANALYSIS OF DIELECTRICALLY ENHANCED SINGLE-ZONE TUNNEL DRYERS

by

WILLIAM MELENDEZ, B.S.

SUPERVISING PROFESSOR: PHILIP S. SCHMIDT, Ph.D.

Dielectric heating was incorporated into the existing continuous single-zone convective dryer model. The energy balance equation for a control volume around the drying product was nondimensionalized, and the resulting dimensionless parameters were used to generate a "unique" characteristic drying curve and to define drying regimes for dielectrically enhanced drying. Numerical models were developed to represent the heat generation inside the wet product and the position of the evaporative front as a function of moisture content. The governing equations were modified to account for the thermal influence of vapor flux in the dry region. The enhanced computer code is capable of predicting the drying rate and temperature history for the product, and calculating the required dryer length, and the drying time for dielectrically enhanced drying.

*Keywords: This computer program, dielectric heating, (K.C.)*

## TABLE OF CONTENTS

Acknowledgments	iii
Abstract	iv
List of Figures	vii
Nomenclature	ix
Chapter 1 Introduction	1
1.1 Dryer Models	1
1.2 Objectives of the Present Work	4
Chapter 2 Theoretical Background	6
2.1 Drying Rate, Vapor Flux Equation	6
2.2 The Characteristic Drying Curve Principle.	7
2.3 Application of Dielectric Heating to Drying	10
2.3.1 Principles of Dielectric Heating	10
2.3.2 Boiling Point Drying	11
2.3.3 Dielectrically Enhanced Drying Systems	12
2.4. Application of the Characteristic Drying Curve Principle to Dielectric Drying	15
Chapter 3 Characteristic Drying Curve for Dielectrically Enhanced Drying	16
3.1 Nondimensionalization of the Problem.	16
3.1.1 Relative Warm-Up Rate, $f_w$	20
3.1.2 Relative Drying Rate, $f_r$	23
3.2 Drying Mode Factor, $\phi$	25
3.2.1 Physical Significance	25
3.2.2 Drying Regimes	28
3.3 Procedure for Normalizing Experimental Data	29
3.4 Normalization Results of Experimental Data	32

Chapter 4 Modification of the Dryer Model	36
4.1 Product Model	36
4.1.1 Evaporative Front	36
4.1.2 Governing Dryer Equations	41
4.1.3 Temperature Profile	44
4.2 Heat Generation Term	47
Chapter 5 The Modified Dryer Code	51
5.1 Introduction	51
5.2 Subprograms in the Enhanced Dryer Code	51
5.3 Validation of the Computer Code	54
5.3.1 Introduction	54
5.3.2 Case 1 Drying Without an Evaporative Front	54
5.3.3 Case 2 Drying With an Evaporative Front	56
5.3.4 Case 3 Determination of P for Equivalent Drying Rates	64
5.4 Dryer Performance Under Varying Drying Regimes	64
5.4.1 Dryer Code Results for Different Drying Mode Factors	64
5.4.2 Vapor Flux Effect in Dry Region	65
Chapter 6 Conclusions and Recommendations.	67
6.1 Conclusions	67
6.2 Recommendations	68
Appendix A	73
A.1 Variables Dictionary	74
A.2 Listing of The Enhanced Dryer Code	83
A.3 Listing of The Normalizing Code	101
Appendix B	104
B.1 Heat and Mass Balances	105
B.2 Summary of the Equations Used by the Dryer Code	111
References	114

## LIST OF FIGURES

<u>Figure</u>		<u>Page</u>
1.1	Components and elements of a fundamental dryer model	3
1.2	Continuous convective tunnel dryer	3
2.1	Typical convective drying test data, the drying rate curve and the characteristic drying curve for fixed air conditions	8
2.2	Schematic representation of the dependence of $\epsilon''$ on T and X	11
2.3	Relationship between $Q_v$ , $Q_g$ and X	13
3.1	Control volume for the wet product	17
3.2	Normalized temperature gradient vs X	22
3.3	The relative warm-up rate vs X	22
3.4	Experimental drying rate data, $P = 0.5 \text{ kW}$ , $T_a = 93^\circ\text{C}$	24
3.5	Control volume for the dry region	26
3.6	Typical characteristic functions for the relative drying rate during the warm-up period	33
3.7	Typical experimental drying rate curves	35
3.8	Drying curves from 3.7 after normalization	35
4.1	Illustration of the receding plane model	37
4.2	Moisture distribution in Lyons' experiment	40
4.3	Evaporative front position as a function of X	40
4.4	Control volumes and energy terms	49
4.5	Temperature history for drying glass beads with $1.0 \text{ kW}$ and $65^\circ\text{C}$ air	46
4.6	Graphical representation of the heat generation model	49
5.1	Computational flow chart for the University of Texas dryer code	52
5.2	Temperature history prediction for Case 1	57
5.3	Drying rate prediction for Case 1	57
5.4	Drying rate curve for polyurethane foam, $P = 0.5 \text{ kW}$ , $T_a = 150^\circ\text{C}$	59



5.5	Normalized drying curve for Case 2	59
5.6	Characteristic function in the falling rate period for Case 2	60
5.7	Moisture content history for Case 2	63
5.8	Temperature history as a function of moisture content for Case 2	63

## NOMENCLATURE

A	Evaporative surface area ( $m^2$ )
b	Product depth (m)
Bi	Heat transfer Biot number (dimensionless)
Bi <sub>m</sub>	Mass transfer Biot number (dimensionless)
C	Specific heat (kJ/kg K)
C <sub>a</sub>	Specific heat of dry air (kJ/kg K)
C <sub>w</sub>	Specific heat of saturated liquid water (kJ/kg K)
C <sub>s</sub>	Specific heat of dry product (solid) (kJ/kg K)
C <sub>v</sub>	Specific heat of water vapor (kJ/kg K)
D	Diffusion coefficient ( $m^2/s$ )
D	Molecular weight ratio of water to air (dimensionless)
E	Electric field (Volts/m)
f	Frequency (Hz)
f <sub>f</sub>	Final Relative drying rate (dimensionless)
f <sub>o</sub>	Initial Relative drying rate (dimensionless)
f <sub>r</sub>	Relative drying rate (dimensionless)
f <sub>w</sub>	Relative warm-up rate (dimensionless)
h	Convective heat transfer coefficient ( $kW/m^2 K$ )
h <sub>a</sub>	Total air enthalpy, (air and vapor) (kJ/kg dry air)
h <sub>f</sub>	Saturated liquid water enthalpy (kJ/kg)
h <sub>v</sub>	Vapor enthalpy (kJ/kg)
K <sub>o</sub>	Mass transfer coefficient ( $kg/m^2-s$ )
M <sub>a</sub>	Dry air mass flow rate per unit of dryer width (kg dry air / s-m)
M <sub>s</sub>	Dry product mass flow rate per unit of dryer width (kg dry product/s-m)
m <sub>o</sub>	Initial mass of water inside the product (kg)
m <sub>w</sub>	Mass of water inside the product (kg)
m <sub>s</sub>	Mass of dry product (kg)
N <sub>v</sub>	Drying rate flux ( $kg/m^2 s$ )
N <sub>vo</sub>	Maximum drying rate flux ( $kg/m^2-s$ )

P	Dielectric forward power in dryer (kW)
$Q_{as}$	Heat source in air stream (kW/m <sup>2</sup> )
$Q_g$	Dielectric heat flux in wet product (kW/m <sup>2</sup> )
$Q_c$	Convective heat flux (kW/m <sup>2</sup> )
$Q_\delta$	Conductive heat flux (kW/m <sup>2</sup> )
$Q_e$	Evaporative heat flux (kW/m <sup>2</sup> )
$Q_s$	Sensible heat flux for the dry product (kW/m <sup>2</sup> )
$Q_T$	Total heat flux going into the wet product (kW/m <sup>2</sup> )
$Q_v$	Volumetric heat generation (kW/m <sup>3</sup> )
$Q_w$	Sensible heat flux for the wet product (kW/m <sup>2</sup> )
t	Time (s)
$T_a$	Air temperature (°C)
$T_{as}$	Adiabatic saturation temperature (°C)
$T_B$	Boiling (saturation) temperature (°C)
$T_{dp}$	Dew point temperature (°C)
$T_m$	Mean temperature (°C)
$T_o$	Product initial temperature (°C)
$T_p$	Wet product temperature (°C)
$T_s$	Product surface temperature (°C)
$T_{wb}$	Wet bulb temperature (°C)
$U_s$	Product velocity (m/s)
$U_a$	Air velocity (m/s)
$V_p$	Volume of product (m <sup>3</sup> )
$V_w$	Volume of the wet region (m <sup>3</sup> )
X	Product moisture content, (kg water/kg dry product)
$X^*$	Nondimensionalized moisture content in the warm-up region
$X_B$	Moisture content at which product reaches boiling point (kg/kg)
$X_c$	Critical moisture content for convective drying (kg/kg)
$X_{cd}$	Critical moisture content for dielectrically enhanced drying (kg/kg)
$X_o$	Initial moisture content (kg/kg)
Y	Air humidity, dry air mass basis (kg water/kg dry air)
$Y_s$	Humidity at product surface (kg/kg)

$z$  Distance from product inlet (m)

Greek and Other Symbols

$\beta$  Evaporative front coefficient (dimensionless)  
 $\Delta h_v$  Latent enthalpy of vaporization (kJ/kg)  
 $\delta$  Depth of evaporative plane (m)  
 $\delta^*$  Relative depth of dry region (dimensionless)  $\delta/b$   
 $\epsilon_0$  Permittivity of free space (Farad/m)  
 $\epsilon''$  Effective dielectric loss factor (dimensionless)  
 $\Phi$  Characteristic moisture content (dimensionless)  
 $\phi$  Drying Mode Factor (dimensionless)  
 $\gamma$  Evaporative resistance coefficient (dimensionless)  
 $\lambda_a$  Air thermal conductivity (kW/m K)  
 $\lambda_s$  Dry product thermal conductivity (kW/m K)  
 $\rho_s$  Density of dry solid on total volume basis (kg/m<sup>3</sup>)  
 $\rho_w$  Density of water on a wet region volume basis (kg/m<sup>3</sup>)  
 $\Omega$  Drying intensity (dimensionless)  
 $\psi$  Relative humidity (dimensionless)  
 $\zeta$  Relative depth of wet region =  $1 - \delta^*$  (dimensionless)

## CHAPTER 1

### INTRODUCTION

The use of dielectric heating in drying processes has been an area of research interest for several years. A number of papers have been published on the enhancing effects of dielectric drying. Research and industrial experience has shown that dielectrically enhanced drying can reduce thermal degradation, producing a better quality product than conventional drying methods. In addition, dielectric heating allows the use of smaller ovens, attains faster drying rates, and maintains a cleaner environment relative to conventional drying. The combination of these factors can result in a more efficient drying plant.

Despite the high efficiency and operational advantages of dielectric drying, its adoption in industry has been slow for two main reasons: 1) high capital cost of dielectric heating equipment, and 2) lack of predictive tools to assess the best dielectrically assisted drying configuration for a particular product. Incorporation of dielectric heating involves a relatively large capital investment, and therefore, must be judiciously evaluated and optimized for its successful implementation.

#### 1.1. DRYER MODELS

In the pursuit of more efficient dryer operation and less expensive dryer development, process engineers have developed models with the objective of predicting the behavior of a particular dryer under specified operating conditions. As documented by Reay [1], there are three types of dryer models : 1) the scale-up factor model used to design dryers; 2) the input/output model used to operate dryers; and 3) the fundamental model based on the fundamental physics of the drying process. The scale-up factor model is used when pilot plant tests are conducted and the operating conditions are varied until product specification is met; then, the dimensions of the full-scale dryer are estimated using empirical scale-up rules based on past experience. The input/output model is based on an intuitive

understanding gained from learning the impact of changes on product and operating conditions through a posteriori correlation of inputs and outputs. The fundamental model is based on a mathematical representation of the physical processes occurring in the dryer, but, it may also require some experimental data on the characteristics of the product. The scale-up factor and input/output models cannot be extrapolated outside the range of past experience; the fundamental model, however, should be a more powerful tool since its range of application is not circumscribed by past experience [1].

The dryer model discussed in this report is of the fundamental type. A fundamental dryer model must have two components: a product model and an equipment model. Figure 1.1 depicts the relationship between these two model elements. The product model characterizes the drying kinetics of the product independently of the dryer type. Its parameters can be attained from bench scale tests performed on a small quantity of product. The function of the product model is to determine drying rates at any moisture content, temperature, dielectric power, or local drying air conditions. Three elements are necessary for a complete product model: 1) a drying rate function for a small quantity of the product as a function of temperature, air psychrometric properties and dielectric heating rate; 2) an algorithm for predicting the drying rate at any given operating condition and moisture content; 3) information on hygroscopicity and thermophysical changes of the product with respect to its moisture content.

The equipment model represents the interaction between the product model and any energy source (air, dielectric, hot plate) independently of the particular product. This model relies on the product model for the numerical values of drying rate and product properties. The equipment model must be able to determine the heat transfer rate from the air to the product, calculate the change in product and air moisture content and the necessary dryer length or drying time needed to accomplish the desired final product moisture content.

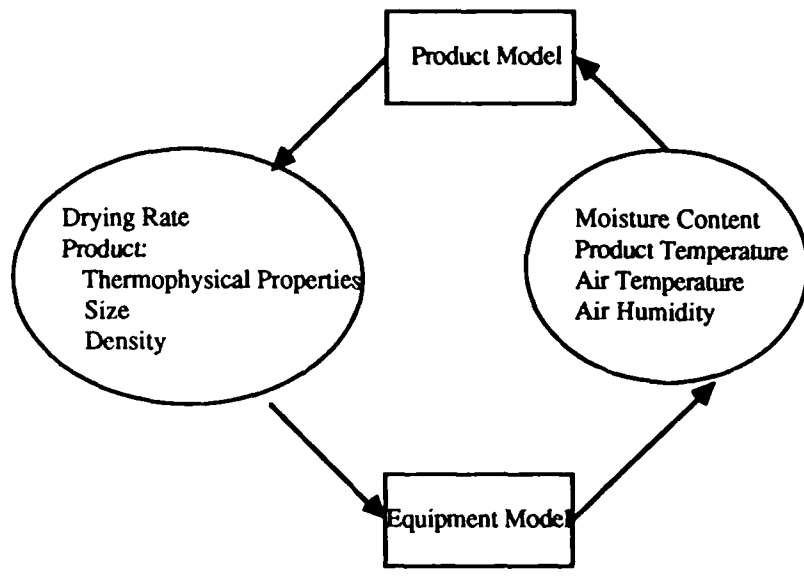


Figure 1.1 Components and elements of a fundamental dryer model [1].

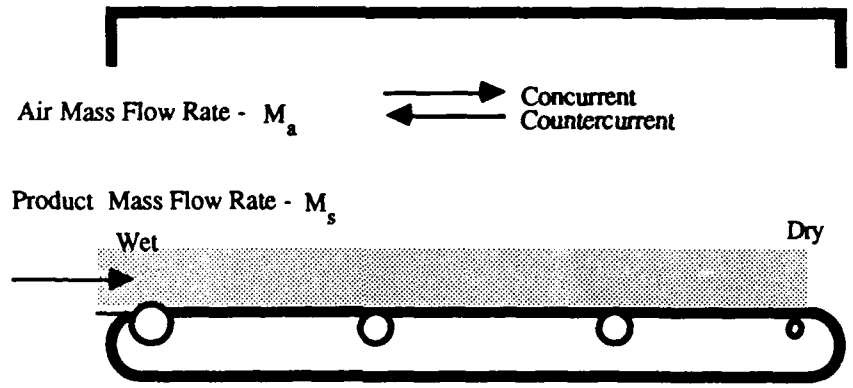


Figure 1.2 Continuous convective tunnel dryer. Adapted from Reference [2].

### 1.1.2 University of Texas Dryer Model

The University of Texas dryer model and its computer code algorithm are the results of efforts to develop a fundamental model of the drying process. This model was documented by Flake [2].

The product model is based on the characteristic drying curve principle, as predicated by Keey [3,4,5,6] for convective drying. The equipment model interfaces the drying process with the product's drying kinetic model in a continuous convective, single-zone tunnel dryer, which is shown in Figure 1.2. The existing dryer model is able to handle drying with concurrent or countercurrent air flow and with isothermal or adiabatic air conditions. The convective heat transfer and mass transfer coefficients are estimated from Nusselt number correlations. The equipment model predicts all the air conditions in the dryer, including the wet bulb temperature, adiabatic saturation temperature and regions where condensation is imminent.

There are certain drying conditions that Flake's dryer model cannot handle. First, the code cannot handle boiling point drying (i.e., conditions where the product reaches saturation temperature). Second, though provisions were made to account for internal heat generation, a product model with dielectric heating is not available. The effect of dielectric heating on the characteristic drying curve is unknown since Keey formulated the characteristic drying curve for convective drying only. These limitations form the basis for the objectives of this research.

### 1.2. OBJECTIVES OF THE PRESENT WORK

The major long-range objective of the Dielectric Heating Research Program at the University of Texas at Austin is to develop a complete predictive capability for dielectric heating applications in industrial heating and drying processes. One step toward this goal was the development of a fundamental dryer model for a continuous convective tunnel dryer, and a computer code capable of interfacing the tunnel dryer model with the product kinetics model [2]. The overall



objective of the present study is to incorporate dielectric heating into the existing dryer model. To achieve this goal, the effects of dielectric heating on the existing product model and equipment model need to be explored in detail.

The specific objectives of the present work are:

- Determine pertinent parameters to normalize dielectrically assisted drying curves and produce a "characteristic drying curve" which accounts for the effects of dielectric heating.
- Incorporate the characteristic drying curve into the product model of the existing computer code.
- Incorporate the heat generation term into the equipment model of the existing computer code.
- Demonstrate the application of the proposed normalization scheme to a limited set of experimental data for dielectrically enhanced drying.
- Modify the existing single-zone computer code to handle dielectrically assisted drying.

## CHAPTER 2

### THEORETICAL BACKGROUND

#### 2.1 DRYING RATE, VAPOR FLUX EQUATION

Keey [3] develops a detailed derivation of the drying rate from a wet surface based on Fick's law. The drying rate is expressed as

$$N_v = K_o D \ln \left[ \frac{D + Y_s}{D + Y} \right] \quad (2.1)$$

Equation 2.1 gives the maximum drying rate when the surface humidity is evaluated at the wet bulb temperature inside the dryer, since at this condition  $Y_s$  becomes the saturation humidity. Three major assumptions are necessary to derive Equation 2.1. First, the density of the vapor and the diffusion coefficient are assumed constant. Second, the vertical velocity at the concentration boundary layer is assumed to be negligible. Third, the difference between the self-diffusivity ( $D_{aa}$ ) and the limiting interdiffusivity ( $D_{ab}$ ) is assumed to be negligible [22]. In the case of drying with dielectric heating, the assumptions inherent in Equation 2.1 are no longer valid. Drying rates are much higher in dielectric heating due to higher heat input; hence, the convective vapor flux will affect the concentration boundary layer on top of the product surface. In addition, dielectric drying can occur at temperatures well above the wet bulb temperature, and in fact above the dry bulb temperature of the airstream. When  $T_a \geq 100^\circ\text{C}$ , the difference between the self-diffusivity and the limiting interdiffusivity is no longer negligible [22].

When dielectric heating is employed, the internal drying mechanisms can become more complicated since other vapor transport drivers, besides Fickian diffusion, begin to dominate. Pressure gradients and thermal gradients may play significant roles in the determination of the total moisture transport within the

product [17], and therefore, models for dielectrically enhanced drying should allow for the influence of these effects.

## 2.2 THE CHARACTERISTIC DRYING CURVE PRINCIPLE

### 2.2.1 Introduction

The characteristic drying curve principle was first introduced by van Meel in 1958 [21]. Since then, its application to industrial drying has been extensively studied and elaborated on by many researchers, especially R.B. Keey whose work forms the basis for the product model used in the University of Texas dryer model. The principle of the characteristic drying curve states that, for a given material, it is possible to develop a normalized drying rate curve which is nearly independent of external drying conditions [4].

### 2.2.2 Background

The theory behind the characteristic drying curve is well-documented by Keey in several articles [3,5,6]; a review of key concepts follows. To derive the drying rate curve for a given material using experimental data, the slope of the mass-time curve obtained at fixed conditions of air temperature, velocity and humidity is calculated and plotted against the moisture content as presented in Figure 2.1. This plot of  $N_v$  vs.  $X$ , called the drying rate curve, is used extensively in the design and evaluation of conventional drying equipment [2].

In many drying processes, an initial constant rate period occurs. This constant drying rate,  $N_{v0}$ , is the maximum drying rate at which a wet surface reaches the wet bulb temperature under convective conditions. This rate is used to normalize the drying rate curve. The constant drying rate period is represented by the wet surface model which assumes that evaporation takes place only at the surface of the product and that surface liquid is replenished with liquid from the interior of the product by capillary action.

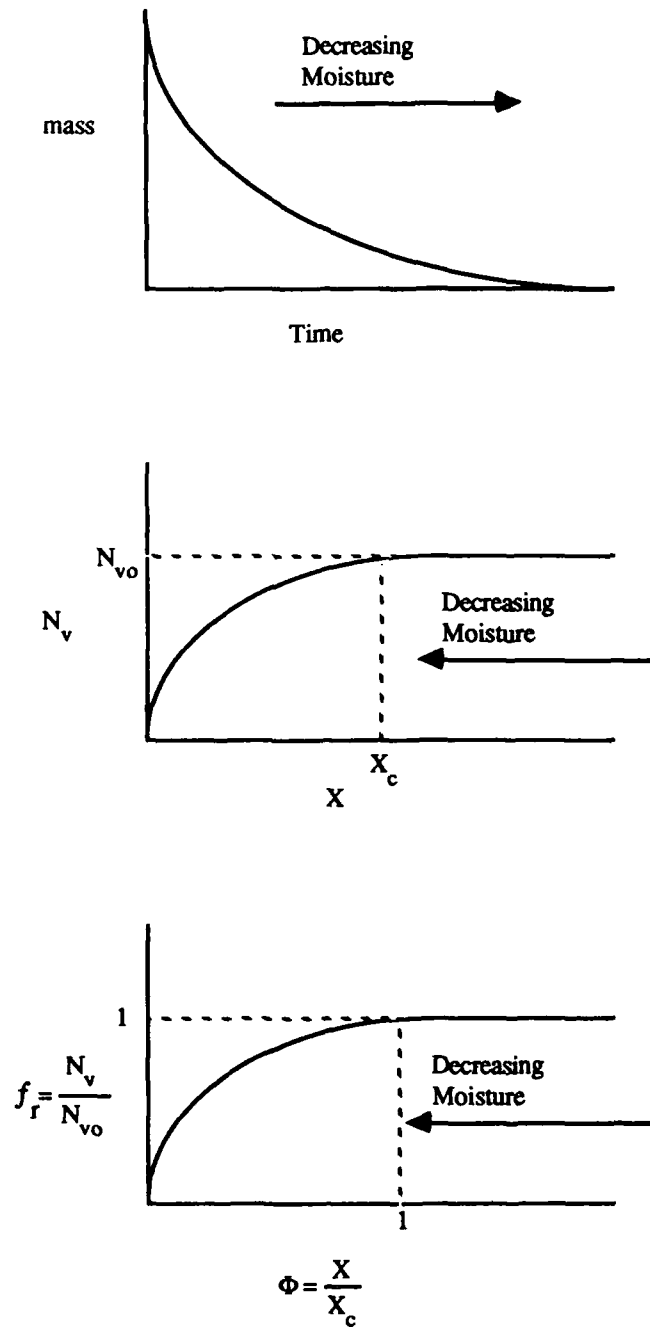


Figure 2.1 Typical convective drying test data, the drying rate curve and the characteristic drying curve for fixed air conditions.

At some point in the convective drying process, capillary action is not sufficient to keep the surface wet, and dry spots appear on the surface. With time, a dry region develops between the interior of the wet product and the surface. This dry region acts as a resistance to vapor transport, and the drying rate decreases. During this period, called the falling rate period, the evaporation rate falls as the moisture content decreases. This period is often characterized by a "receding moisture front" in which evaporation occurs at the surface of a shrinking wet core topped by a dry shell of material [1]. Some materials may experience more than one falling rate period due to different internal moisture migration mechanisms.

The critical moisture content,  $X_c$ , is defined as the average moisture content of the product at the transition point between the constant drying rate and the falling rate period. As stated by Keey,  $X_c$  is not a physical property of the material, since its value depends on the thickness, initial drying rate, and diffusivity of moisture inside the material. However, it is an identifiable feature of the drying rate curve for a given material dried under fixed conditions.  $X_c$  is the scaling factor for the normalized moisture content,  $\Phi$ .

The drying intensity,  $\Omega$ , is defined as the ratio of the drying rate at the surface of the product to the moisture diffusion rate inside the material. Its value will determine if a receding front will be observed during the drying process. If  $\Omega$  is much greater than 2, a sharp, well-defined front will sweep down the product; if  $\Omega$  is much less than 2, a sharp front will not be observed [3].

The characteristic drying curve is defined as the normalized drying rate,  $f_r$ , plotted against  $\Phi$ , as indicated in Figure 2.1. When using this curve, it is assumed that a change in external conditions will have the same proportional effect on the falling rate period as on the constant rate period. Keey states that there is no single characteristic drying curve for a given material and that a single curve will be observed only when  $\Omega$ , the heat transfer Biot number,  $Bi$ , and the evaporative resistance coefficient,  $\gamma$ , assume some value [6,16].

## 2.3 APPLICATION OF DIELECTRIC HEATING TO DRYING.

Dielectric heating has been proposed for drying applications due to the high affinity of water for electromagnetic energy at microwave and radio frequencies. Dielectric heating can be advantageous under the following conditions [11]:

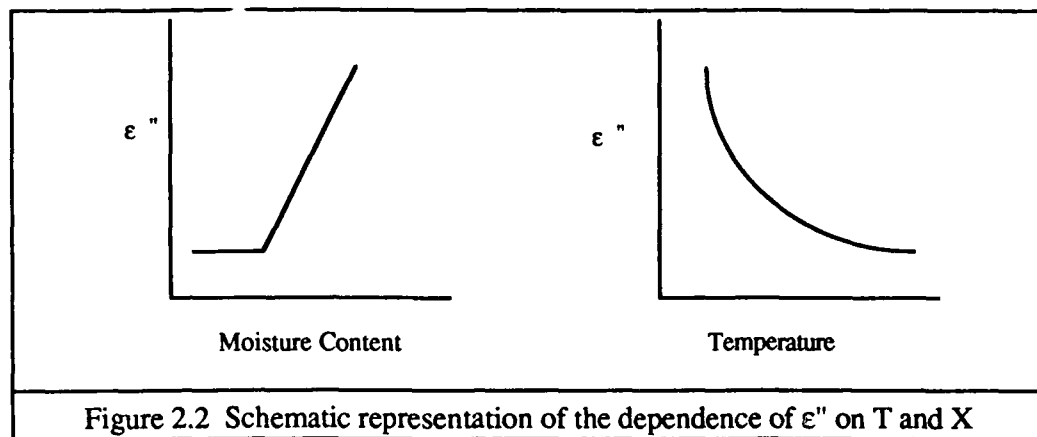
- There is inadequate heat transfer due to internal resistance to heat flow.
- There is inadequate heat transfer due to a small external heat transfer coefficient.
- The internal mass transfer is slow due to the moisture being held in the pendular state and/or the moisture movement is limited by vapor diffusion.
- The resulting quality of the dried product is poor due to the conventional drying system.

### 2.3.1 Principles of dielectric heating

Dielectric heating serves to volumetrically heat a material by electromagnetic energy generated at radio (3-300 MHz) or microwave (300-3000 MHz) frequencies. This form of heating does not depend on the thermal conduction properties of the material, and thus, can be particularly advantageous in processing low thermal conductivity materials. The electromagnetic power density deposited in the material is given by Vankoughnett [8].

$$P = 2\pi f \epsilon_0 \epsilon'' E^2 \quad \frac{\text{Watts}}{\text{cubic meter}} \quad (2.2)$$

The effective dielectric loss factor,  $\epsilon''$ , a property of the material, its moisture content, and moisture distribution, determines the magnitude of dielectric heating for a given frequency and electromagnetic field intensity. Materials with a high affinity for electromagnetic energy are called lossy materials. The  $\epsilon''$  depends on the frequency, temperature, moisture content, and electrical conductivity of the



material, and may also vary locally within the material where moisture and temperature gradients exist. Figure 2.2 shows a typical dependence of  $\epsilon''$  on X and T. For most practical purposes, an average  $\epsilon''$  through the material may be used and may be taken to be a linear function of X; consequently,  $Q_g$  may be approximated as a linear function of X, provided that T and E remain relatively constant.

### 2.3.2 Boiling Point Drying

Heating of moist materials with electromagnetic energy is so effective that reaching the boiling point is the most common mode of operation rather than the exception. When the product reaches the boiling point, mass transfer of moisture into the adjacent air is rapid, and the possibility of saturating the airstream becomes significant. Therefore, the air inside the dryer must be monitored if condensation is to be avoided.

Boiling point drying, characterized by high internal temperatures and rapid mass transfer due to high energy input and pressure build-up in the material, can induce damaging stresses in the internal structure of the product. The feasibility of boiling point drying is dictated by the product's thermal and physical characteristics. Granular and other porous materials are well-suited for boiling point drying since internal pressure build-up is not severe. Compacted materials are more sensitive to internal pressure build-up, thereby limiting the level of power

input. Materials that are sensitive to high temperatures may require drying under subcooled conditions (i.e., conditions in which the internal temperature is intentionally kept below the boiling point).

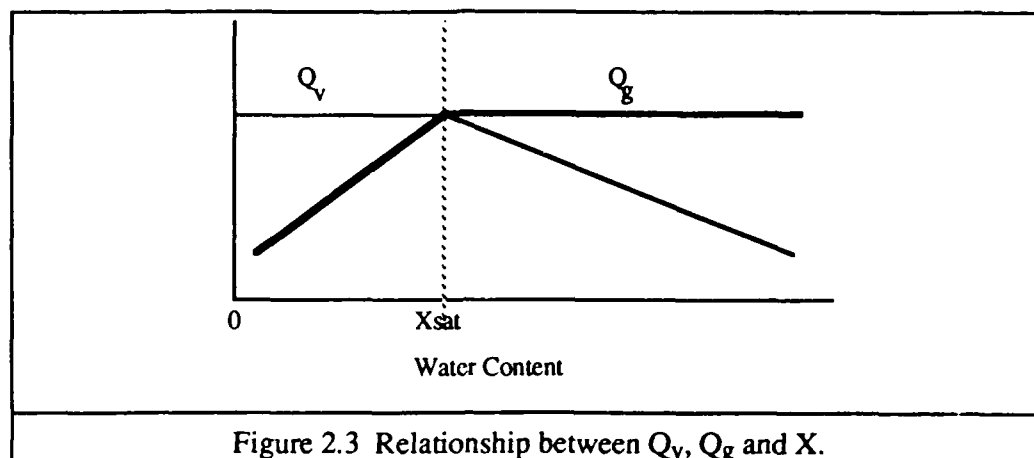
### 2.3.3 Dielectrically Enhanced Drying Systems

A hybrid system is a convective dryer assisted by dielectric heating. The temperature difference between the air and the product will help or hinder dielectric drying. If  $T_a > T_p$ , evaporation will take place on the surface and dielectric drying will be enhanced. The use of dielectric heating can accelerate the migration of water to the surface due to internal pressure build-up and capillary effects. Removal of water by evaporation requires more energy than by migration (mechanical means). Taking into consideration the high capital cost of dielectric heating equipment, it is generally less costly to produce hot air than electromagnetic energy. Therefore, the most efficient way to dry a material is to use dielectric heating to induce migration and to use hot air for evaporation. Migration versus evaporation is discussed by Lefeuvre [10], but he does not consider the possibility of having a dry region (evaporative front) hindering the diffusion of heat and moisture. If a dry region does exist, the comparison just made between hot air and dielectric heating needs to be re-evaluated because less heat from the hot air is being utilized for evaporation due to the dry region's conductive resistance.

If  $T_a < T_p$ , condensation of the moisture vapor from the warm interior of the product will take place at the surface and a part of the dielectrically induced heating will be used to replace the sensible heat lost by the material. There are cases, however, in which the cooling effect of the air is desired to control the temperature of the product. The way that air temperature is coupled with dielectric heating will be an important factor in the successful utilization of dielectric energy in the drying industry.

Schmidt and Accad [9] have surveyed dielectric drying modeling and experimental work. They carried out parametric studies to explore the sensitivity of the evaporation rate from a pan of water to changes in  $U_a$ ,  $T_a$ ,  $\psi$ , and  $Q_g$ . These





studies showed that similar evaporation rates can be obtained for pure convective, high-temperature air drying and dielectric drying with ambient air. A “saturation point” was defined for a dielectric dryer when all the incident power is being absorbed by the load; above the “saturation” moisture content,  $Q_v$  increases as the water volume decreases while  $Q_g$  stays approximately constant. When the water volume is less than the “saturation point”, only part of the incident power is absorbed and the rest is reflected away or absorbed by the surroundings. At this point,  $Q_v$  stays constant (given that  $E$  stays constant), but  $Q_g$  decreases as water volume decreases. Figure 2.3 presents a schematic representation of the relationship between  $Q_g$ ,  $Q_v$  and  $X$ . The value of  $X_{sat}$  will later be shown to represent an important transition point in the characterization of dielectrically enhanced drying curves.

Perkin [11] presents the continuum equations for mass flow of moisture, heat flow, and total pressure in which the transport coefficients are a function of moisture content and temperature and must be determined experimentally.

Perkin defines the parameter  $Q_g/h$ , which is the equilibrium temperature difference between the product surface and the air. Three drying regimes are identified using this parameter:

- $Q_g/h > 500^\circ\text{C}$ : Drying characteristics are due to electromagnetic energy alone, as drying is insensitive to air temperature and air humidity. The principal role of the airstream is to remove the evaporating moisture from the dryer.
- $Q_g/h < 50^\circ\text{C}$ : Drying is sensitive to changes in humidity and air temperature. Hot air contributes to the evaporative energy.
- $50^\circ\text{C} < Q_g/h < 500^\circ\text{C}$ : Behavior is in-between the above two cases.

Perkin uses  $Bi_m$  to classify the materials into either low vapor flow internal resistance or high vapor flow internal resistance. The extreme cases for  $Q_g/h$  and  $Bi_m$  are used to simplify the governing equations of the drying problem and to obtain estimates of the drying behavior of the product.

Pourhiet and Bories [12] use a mathematical model originally established by Luikov and experimentally validated by Bories. The model describes the physical laws of heat and mass transfer, taking into consideration electromagnetic power deposition. Pourhiet and Bories developed a relationship between  $Q_g$  and  $X$  and speculated that:

- the moisture distribution inside the material can be monitored using  $Q_g$ ,
- the appearance of a dried zone near the surface can be avoided by controlling  $Q_g$ , and
- a uniform distribution of the humidity inside the product can be attained by controlling  $Q_g$ .

They also found the equivalent airstream temperature for a given microwave power, which would give the same drying rate without microwaves. Therefore, dielectric drying transfer units can be converted into conventional drying transfer units, allowing for direct comparison of the two methods.

Pourhiet and Bories also compared a hybrid heating system to a conventional one to determine which would be more economical if both achieved

the same drying time. Results showed that a minimum installed power is necessary to break even.

#### 2.4. APPLICATION OF THE CHARACTERISTIC DRYING CURVE PRINCIPLE TO DIELECTRIC DRYING

No literature is currently available to guide the development of characteristic drying curves associated with dielectrically assisted drying. Statistical analysis techniques, however, were used by Meiners [7] in an attempt to normalize the drying curve for a bed of 3 mm glass beads under 0.5 kW of microwave power and different air temperatures. While the technique is useful in attempting to extrapolate data from a limited series of tests to a wider range of conditions, it does not provide the physical basis needed to generalize to conditions well outside the limits of available data.

The general concept of the characteristic drying curve may apply to dielectric heating for several reasons:

- Under many conditions, the drying rate will be dominated by the heat generation term, which does not depend on the hygrothermal characteristics of air.
- Conduction of convective heat into the material will, in many cases, not be the primary driving force for evaporation; therefore, the depth of the dry region, which is established by  $\Omega$ , will not be the thermally limiting element.

Key [6,16] considered these parameters as impediments to the development of a single characteristic drying curve for a particular product. In dielectrically enhanced drying, the dielectric response characteristic of the material and the interrelationship between internal and surface heating (or cooling) are expected to play the primary role in defining drying behavior. These parameters will be considered in detail in Chapter 3.

## CHAPTER 3

### CHARACTERISTIC DRYING CURVE FOR DIELECTRICALLY ENHANCED DRYING

#### 3.1 NONDIMENSIONALIZATION OF THE PROBLEM.

Proper selection of normalizing scales produces variables of comparable magnitude over a range of operating conditions. The pertinent parameters for nondimensionalization of a problem can be found either by bringing into play information provided by basic physical laws, or assumptions about the functional form of the result [18]. The objectives of nondimensionalizing the problem are to reduce the number of variables, to simplify the mathematical structure of the problem to make results more widely applicable, and to keep experimental runs to a minimum. In drying processes, the main motivation for this approach is to limit the amount of experimental data needed to extrapolate results from a particular drying condition to other drying conditions. Eckert [19] discusses the nondimensionalization of a convective drying problem in which the difference between the wet bulb temperature and the product's initial temperature is used to make the conservation equations dimensionless. The nondimensionalization of the problem allowed Eckert to perform parametric studies by varying a few dimensionless parameters instead of the numerous variables in the problem.

In this chapter, an energy balance, performed on a control volume element representative of the wet product with convection and dielectric heating, is used to develop dimensionless parameters with the intention of using these parameters to produce a characteristic drying curve.

Referring to Figure 3.1, an energy balance on the control volume around the wet product yields

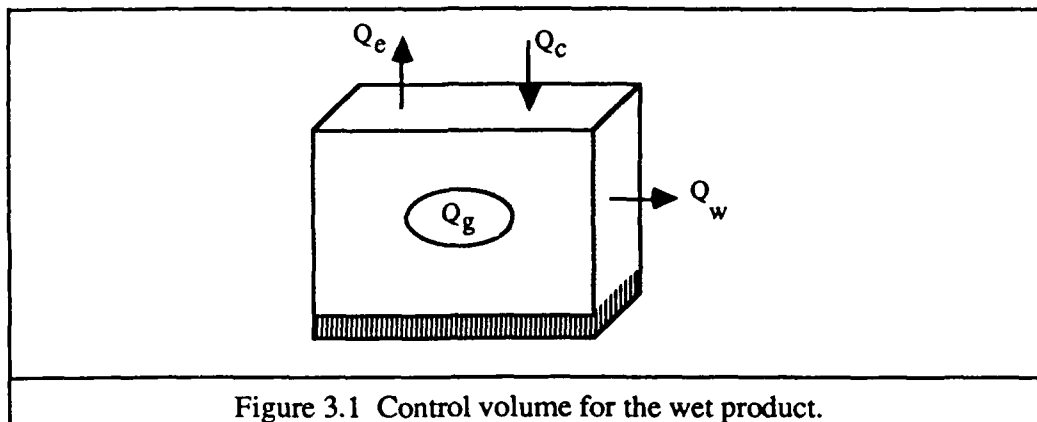


Figure 3.1 Control volume for the wet product.

$$Q_c + Q_g = Q_e + Q_w \quad (3.1)$$

where all the fluxes are based on the evaporative surface area, and

$$Q_c = h (T_a - T_s) \quad \text{and} \quad Q_g = \frac{P}{A} \quad (3.2), (3.3)$$

$$Q_e = N_v \Delta h_v \quad Q_w = \rho_s b (C_s + X C_w) \frac{\partial T_p}{\partial t} \quad (3.4), (3.5)$$

In Equation 3.1, the change of energy content associated with water vapor, air, and phase transformation of the solid species has been neglected. Note that in Equation 3.3,  $Q_g$  was defined in terms of the dielectric forward power which is assumed to be constant and completely absorbed by the moist product in the initial drying stage; for later stages where  $Q_g$  is expected to decrease, the characteristic drying curve concept will be used to represent the decline in  $Q_g$  departing from the maximum value calculated in Equation 3.3. Some of the

variables in Equation 3.1 are hard to normalize because they do not have an obvious scaling factor. An evident choice for a normalizing parameter would be a direct operating condition since it is known and can usually be set to a constant value. Examples of such operating conditions are air temperature, air humidity, microwave or radio frequency forward power, air velocity, and initial moisture content.

The characteristic drying curve is defined in terms of  $N_v$  and  $X$ , as discussed in Chapter 2. For convenience, therefore, Equations 3.1–3.5 will be transformed from their independent variable,  $t$ , to the more significant variable,  $X$ . To transform from “time domain” to “moisture content domain”:

$$\frac{\partial T}{\partial t} = \frac{\partial X}{\partial t} \frac{\partial T}{\partial X} = \frac{-N_v}{\rho_s b} \frac{\partial T}{\partial X} \quad (3.6)$$

Therefore, Equation 3.5 can now be expressed in terms of  $X$ ;

$$Q_w = -N_v (C_s + X C_w) \frac{\partial T_p}{\partial X} \quad (3.7)$$

Combining Equations 3.7, 3.4 and 3.1,

$$Q_c + Q_g = N_v \Delta h_v \left[ 1 - \frac{(C_s + X C_w)}{\Delta h_v} \frac{\partial T_p}{\partial X} \right] \quad (3.8)$$

The LHS of Equation 3.8 is the total energy,  $Q_T$ , going into the product. The RHS of Equation 3.8 will depend on  $Q_T$  regardless of the heat source, dielectric or convective.  $Q_T$  could be dominated by  $Q_c$  or  $Q_g$ ; in this case,  $Q_T$  will be normalized on the dielectric heat flux.

$$\phi = \frac{Q_T}{Q_g} = \frac{Q_g + Q_c}{Q_g} = 1 + \frac{Q_c}{Q_g} \quad (3.9)$$

Note that if  $Q_T$  is dielectrically dominated,  $\phi \approx 1$ , and if  $Q_T$  is convectively dominated,  $\phi \gg 2$ . This normalized parameter will be termed the “drying mode factor”. Its physical significance in dielectrically assisted drying will be discussed at length in Section 3.2.

Using Equation 3.9 to replace  $(Q_c + Q_g)$  and dividing Equation 3.8 by  $\phi Q_g$ :

$$1 = \frac{N_v \Delta h_v}{Q_g \phi} \left\{ 1 - \left[ \frac{(C_s + X C_w)}{\Delta h_v} \frac{\partial T_p}{\partial X} \right] \right\} \quad (3.10)$$

The quantity within the squared brackets is the specific energy (kJ/kg) gained by the wet product normalized by the latent heat of vaporization of water. This term includes a temperature gradient characteristic of the warm-up period. Define the bracketed term as,

$$f_w = \frac{(C_s + X C_w)}{\Delta h_v} \frac{\partial T_p}{\partial X} \quad (3.11)$$

The dimensionless variable,  $f_w$ , will be called the “relative warm-up rate”. This parameter is not found in the drying literature; its physical significance in dielectric drying is discussed in detail in Section 3.1.1.

Going back to Equation 3.10, the first term in the RHS of the equation is the drying rate,  $N_v$ , normalized by the maximum drying rate when the moisture in the solid reaches saturation temperature. Define the dimensionless variable,  $f_r$ , as:

$$f_r = \frac{N_v \Delta h_v}{Q_g \phi} \quad (3.12)$$

$f_r$ , will be called the "relative drying rate", which behaves similarly to its counterpart in convective drying. Finally, the energy balance equation, 3.1, takes the normalized form:

$$1 = f_r (1 - f_w) \quad (3.13)$$

The following sections explore the relationship of the normalized parameters,  $f_w$ , and  $f_r$ , to the characteristic drying curve concept.

### 3.1.1 Relative warm-up rate, $f_w$

To study the physical meaning of  $f_w$ , the variables  $T_p$  and  $X$  will be nondimensionalized using the range of these variables during the drying process as scaling factors. For  $T_p$ , the scaling variable is the water's local saturation temperature,  $T_B$ , and the reference variable is the initial product temperature,  $T_o$ . For  $X$ , scaling is done by the boiling point moisture content,  $X_B$ , and the reference value is given by the initial moisture content,  $X_o$ . That is,

$$T_p^* = \frac{T_p - T_o}{T_B - T_o} \quad \text{and} \quad X^* = \frac{X - X_o}{X_B - X_o} \quad (3.14)$$

Performing a variable transformation from the pair  $(X, T)$  to the pair  $(X^*, T^*)$  the following expression is obtained for  $f_w$ :

$$f_w = \frac{C_w (T_B - T_o)}{\Delta h_v} \left[ \frac{C_s + X_o C_w}{C_w (X_B - X_o)} + X^* \right] \frac{\partial T_p^*}{\partial X^*} \quad (3.15)$$



Two groups of variables generated by the normalization are further defined:

$$Q^* = \frac{C_w (T_B - T_0)}{\Delta h_v} \quad C^* = \frac{C_s + X_0 C_w}{C_w (X_B - X_0)} \quad (3.16), (3.17)$$

Now Equation 3.15 reads:

$$f_w = Q^* (C^* + X^*) \frac{\partial T^*}{\partial X^*} \quad (3.18)$$

The quantity  $Q^*$  is the dimensionless ratio of the average sensible heat gained by the water inside the material from  $t = 0$  to saturation to the latent heat of vaporization.  $C^*$  is the ratio of the initial thermal mass of the wet product to the total thermal mass of the evaporated water from  $t = 0$  to saturation.

The normalized temperature gradient in Equation 3.18 will now be examined. From a purely intuitive point of view, it can be argued that if  $Q_T$  increases,  $\Delta T_p$  will increase, but  $\Delta X$  will also increase, making their ratio constant for a given material at a given moisture content. Therefore,  $\partial T / \partial X$  is only a function of  $X$  and the properties of the material. Furthermore,  $Q^*$  and  $C^*$  depend only on the material properties and the initial conditions. From these observations, the following assertion is made: for a given material, the relative warm-up rate is independent of air temperature and dielectric power and only depends on the moisture content. To test this hypothesis,  $\partial T^* / \partial X^*$  vs.  $X$  and  $f_w$  vs.  $X$  were plotted in Figures 3.2 and 3.3 respectively, using drying data for 3 mm glass beads from several experiments run at different air temperatures and power densities, with  $T_0 = 25^\circ\text{C}$ . As expected,  $\partial T^* / \partial X^*$  and  $f_w$  behaved in the same fashion regardless of the power density or air temperature. Therefore, at least for the limited set of data given here, the relative warm-up rate is a function only of  $X$  during the warm-up period.

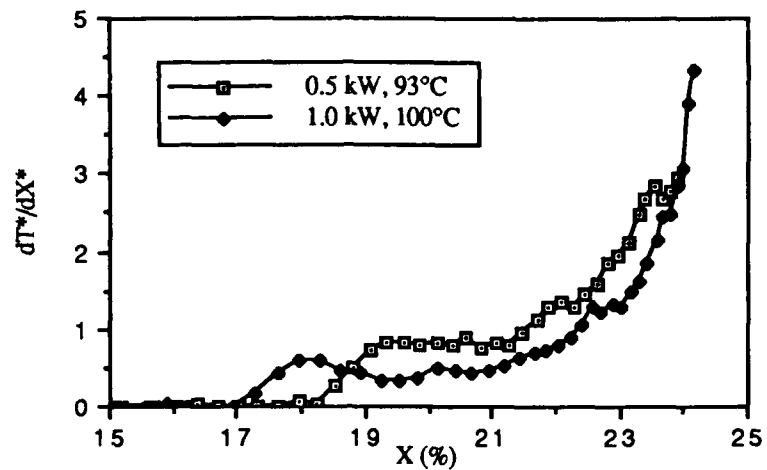


Figure 3.2 Normalized temperature gradient vs.  $X$

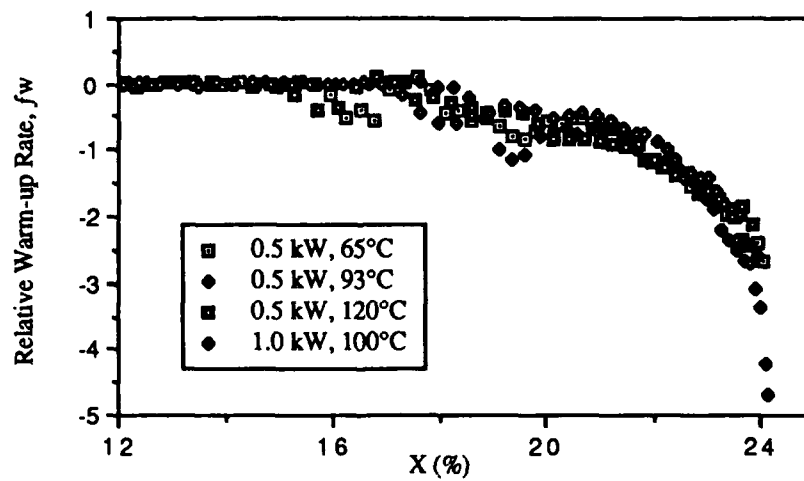


Figure 3.3 The relative warm-up rate vs.  $X$ .

### 3.1.2 Relative Drying Rate, $f_r$

The normalized drying rate,  $f_r$ , called the relative drying rate, approaches one as the relative warm-up rate approaches zero. At this point, in boiling point drying, the drying rate is observed to become constant. Figure 3.4 was generated using drying data for a bed of glass beads  $0.1 \text{ m}^2$  in surface area and 5 cm deep, subject to 0.5 kW microwave power and  $T_a = 93^\circ\text{C}$ . Note that the constant drying rate begins approximately at the point where the wet product reaches saturation temperature.

At a certain moisture content, all the forward dielectric power cannot be absorbed by the sample, and some of the power is reflected. The generated power starts decreasing as  $\epsilon''$  decreases with decreasing  $X$  (see discussion in Chapter 2). At this point,  $N_v$  starts decreasing proportionally to  $Q_g$  since no sensible heating is occurring. This period of the dielectric drying process is referred to as the falling rate period. The falling rate period in this case is produced primarily by a decline in  $Q_g$  and not by limitations on moisture diffusion in the product. The moisture content at which the power deposition starts decreasing is here called the "critical moisture content",  $X_{cd}$ . It has the same characteristics as the critical moisture content in conventional drying, but the mechanisms behind them are completely different. It can be inferred that during the falling rate period,  $f_r$  is only a function of  $X$ .

In summary, Sections 3.1.1 and 3.1.2 have asserted that  $f_r$  is a function only of  $X$  throughout the drying process which implies that there is a unique characteristic drying curve for materials dried under dielectric power. Experimental evidence was presented for a typical nonhygroscopic material. Going back to Equation 3.13,  $f_r$  will be a maximum when  $f_w = 0$ ; then,  $f_r = 1$  until  $X = X_{cd}$ . At this point, the power input is no longer constant and  $f_r$  decreases until  $X = 0$ . Since it was demonstrated that  $f_r$  and  $f_w$  only depend on  $X$  for a given material, the following expression can be stated:

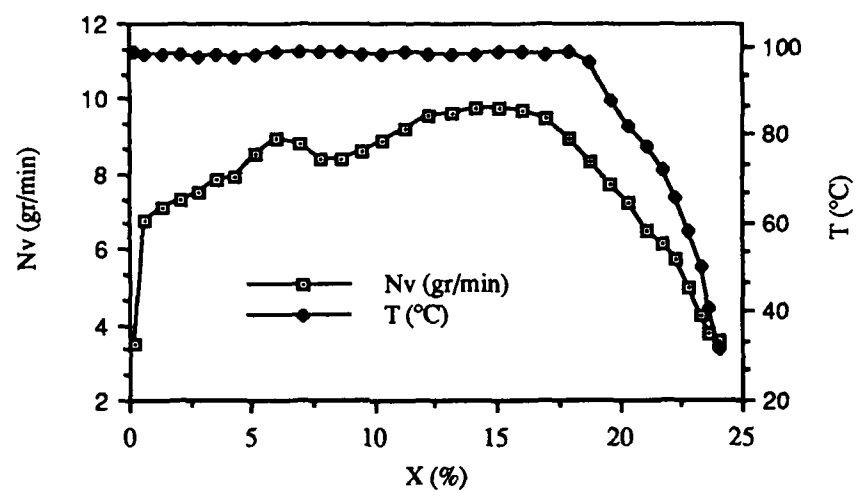


Figure 3.4 Experimental drying rate data,  $P = 0.5$  kW,  $T_a = 93^\circ\text{C}$ .

$$f_r = \frac{1}{1 - f_w} = \mathfrak{R}(X) \quad (3.19)$$

where  $\mathfrak{R}(X)$  is obtained by means of curve fitting or estimating techniques performed on experimental test data as discussed in Section 3.3. Note that  $\mathfrak{R}(X)$  goes from  $\approx 0$  to 1 in the warm-up period; is equal to one in the constant rate period; and goes from 1 to  $\approx 0$  in the falling rate period.

### 3.2 DRYING MODE FACTOR, $\phi$

#### 3.2.1 Physical significance

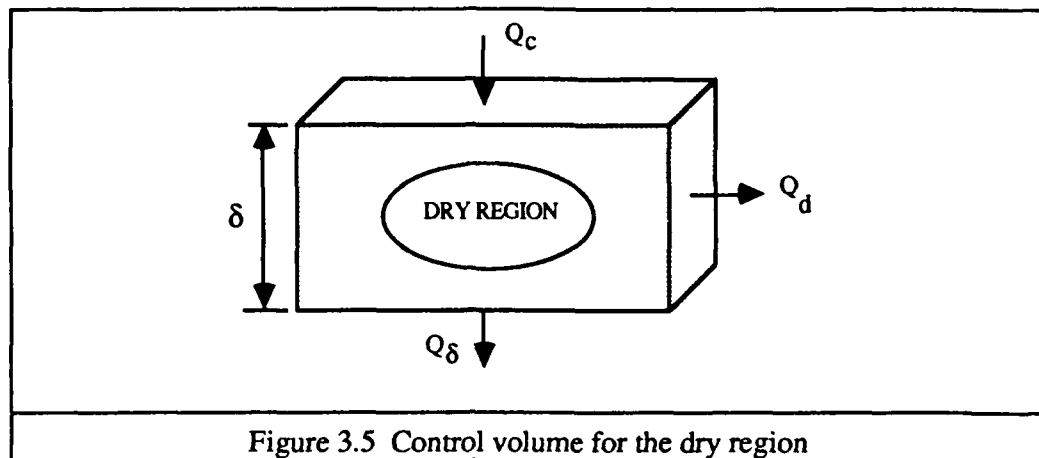
The drying mode factor indicates whether drying is dominated by convective or dielectric heating. This parameter is also used as a scale to normalize different convective and conductive conditions, and to define different drying regimes that arise as a consequence of dielectric heating. Also,  $\phi$  is used to estimate the temperature profile in the product's dry region. This particular effect is explored in Section 4.1.3.

Note that  $\phi$  is the normalized  $Q_T$  going into the wet product which is influenced by the presence or absence of an evaporative front due to the conductive resistance imposed by the dry region. If a dry region is not present then Equation 3.9 becomes

$$\phi = 1 + \frac{h(T_a - T_s)}{Q_g} \quad (3.19)$$

However, if a dry region develops inside the material, the expression for  $Q_T$  will change because the convective heat flux is now being used for both sensible heating in the dry region and sensible heating and evaporation in the wet region.

Therefore, if a dry region is present,



$$\phi' = 1 + \frac{Q_{\delta}}{Q_g} = 1 + \frac{\lambda_s}{Q_g} \frac{\partial T_s}{\partial \delta} \quad (3.20)$$

Note that  $\phi = \phi'$  when an evaporative front is not present since  $Q_c = Q_{\delta}$ . Also,  $\phi$  and  $\phi'$  approach infinity as  $Q_g$  approaches zero. This singularity does not present a problem because as  $\phi$  approaches infinity, the product  $\phi Q_g$  approaches  $Q_c$  in Equation 3.10.

To calculate  $\phi'$ , it is necessary to know the instantaneous position of the evaporative front and the temperature profile inside the dry region. If this information is not available, and the thermal mass of the dry product is relatively small, the convective heat flux can be used as an approximation for the conducted heat without incurring a large error. The energy balance on the dry region will be used to establish the relationship between  $\phi$  and  $\phi'$ . From Figure 3.5:

$$Q_{\delta} = Q_c - Q_d \quad (3.21)$$

where

$$Q_d = \rho_s \delta C_s \frac{\partial T_m}{\partial t} \quad (3.22)$$

Equation 3.22 gives the sensible heat gained by the dry region based on the mean temperature of the region; the thermal effect of the region's growth was not included. Transforming from time domain to moisture content domain,

$$\frac{\partial T_m}{\partial t} = \frac{-N_v}{\rho_s b} \frac{\partial T_m}{\partial X} \quad (3.23)$$

Combining Equations 3.21, 3.22, and 3.23, dividing by  $Q_g$ , adding one to both sides and using Equation 3.19 and 3.20, the following expression is obtained:

$$\phi' = \phi + \frac{C_s \delta N_v}{Q_g b} \frac{\partial T_m}{\partial X} \quad (3.24)$$

From equation 3.24,  $\phi = \phi'$  as long as:

- $\partial T_m / \partial X \approx 0$ , which translates into negligible sensible heating in the dry region
- $\delta / b$  is very small, or
- $Q_g$  is much bigger than  $Q_c$  ( $\phi \approx 1$ )

A drying mode factor cannot be calculated for cases in which the dry region thickness is large and unknown. For such cases, a reasonable assumption would be  $\phi' \approx 1$  since a large conductive resistance is expected, making the conduction heat transfer small. Note that the drying mode factor is not necessarily

constant, since it depends on  $T_s$ . Product temperatures need to be measured and an empirical or analytical expression is needed to estimate the position of the evaporative front.

### 3.2.2 Drying Regimes

Perkin [11] discusses the usefulness of defining drying regimes for dielectrically assisted drying. To define the regimes, he uses the ratio  $Q_g/h$ . To date, Perkin's approach has been the only effort to quantify the importance of the complimentary relationship between dielectric heating and convective heating in terms of efficient drying. The disadvantage of the  $Q_g/h$  approach is that it is not dimensionless and does not take into account the relationship between the product and air temperatures.

The drying mode factor will be used to define distinct drying regimes that arise from dielectric drying. The following is a compilation of limiting cases and the significance of the drying mode factor for each regime.

- Convective Regime ( $\phi \gg 2$ ): The product experiences a high rate of convective heating and the convective heat flux is much higher than the dielectric heat flux. This regime corresponds to Perkin's drying regime defined by  $Q_g/h < 50^\circ\text{C}$ . Drying is sensitive to changes in air conditions.
- Mixed Regime ( $\phi \approx 2$ ): Convective and dielectric heating are approximately equal in magnitude.
- Dielectric Regime ( $\phi \approx 1$ ): This regime is characterized by high dielectric heating ( $Q_g \gg Q_c$ ) or negligible convective heating. This corresponds to Perkin's drying regime defined by  $Q_g/h > 500^\circ\text{C}$ . Drying is relatively insensitive to air conditions, and the principal function of the air is to serve as a moisture sink.
- Subcooled Regime ( $\phi < 1$ ): The product experiences convective cooling. If  $\phi \approx 0$ , the convective cooling and dielectric heating are approximately equal in



magnitude. The product temperature is higher than the dry bulb temperature of the air which can only occur when dielectric heating is applied.

- Cooling Regime ( $\phi < 0$ ): This implies that the product temperature is decreasing as it is being dried. An example of this regime is the cool-down zone in a multi-zone dryer, where the product is allowed to approach ambient temperature, eliminating remaining moisture without dielectric heating.

### 3.3 PROCEDURE FOR NORMALIZING EXPERIMENTAL DATA

#### 3.3.1 Collection of experimental data

The experimental data required are  $m_w$ ,  $T_s$ ,  $T_a$ ,  $U_a$ , and  $P$ , as a function of  $t$ . The data are recorded using a computerized data acquisition system. After placing the wet sample on top of the digital balance, the balance is tared to monitor the amount of water that has evaporated. Temperature probes, connected to a Luxtron fiber-optic temperature measurement system, are placed on the surface and in the middle of the wet sample. A velocity probe is used to monitor the air velocity, and a dual channel microwave power meter is used to monitor the forward and reflected power going into the dryer. The data are written to magnetic media at predetermined time intervals.

#### 3.3.2 Data transformation.

The experimental data must be transformed into  $X$  and  $N_v$  terms. To obtain  $X$ ,

$$X_i = \frac{m_o - m_i}{m_s} \quad (3.25)$$

where  $m_i$  is the mass of the evaporated water at  $t_i$ . To obtain  $N_v$ ,

$$N_{v,i} = \frac{-(X_{i+1} - X_i)}{A(t_{i+1} - t_i)} \quad (3.26)$$

A smoothing technique is used to reduce extrinsic noise inherent in the experimental procedure. An average value from  $n$  consecutive data points is used to represent an interval.

$$N_{v,(i+\frac{(n-1)}{2})} = \frac{1}{n} \sum_{j=i}^{(i+n-1)} N_{v,j} \quad (3.27)$$

For example if  $n = 5$  and  $i = 7$  then

$$\bar{N}_{v,9} = \frac{1}{5} (N_{v,7} + N_{v,8} + N_{v,9} + N_{v,10} + N_{v,11}) \quad (3.28)$$

Finally, a data file is created containing  $X$ ,  $N_v$ ,  $T_s$ , and  $T_p$ , for a particular  $T_a$  and  $P$ .

### 3.3.3 Data normalization

The data file is read by the normalizing code, and the normalizing parameters are calculated for each data point. Letting  $Q_g = P/A$ ,

$$\phi_i = 1 + \frac{h_i (T_a - T_{s,i})}{Q_g} \quad (3.29)$$

where  $h_i$  is calculated by a subroutine based on empirical correlations of the Nusselt number given in the form

$$\text{Nu} = C_1 \text{Re}^m \text{Pr}^n \quad (3.30)$$

Finally, the empirical data are normalized by the expression,

$$f_{r,i} = \frac{N_{v,i} \Delta h_v}{\phi_i Q_g} \quad (3.31)$$

The code used to normalize the data is listed in Appendix A.

### 3.3.4 Characteristic Drying Curve Function

The normalized data must be plotted to assess the accuracy of the normalization and to obtain the characteristic drying curve equation. For the warm-up period, a characteristic function is determined from  $X_0$  to  $X_B$ . Typically a linear, parabolic or cubic function is obtained; so,  $f_r$  can be represented as:

$$f_r = (1-f_0) X^* + f_0 \quad (3.32)$$

or

$$f_r = -(1-f_0) X^{*2} + 2(1-f_0) X^* + f_0 \quad (3.33)$$

or

$$f_r = (1-f_0) X^{*3} - 3(1-f_0) X^{*2} + 3(1-f_0) X^* + f_0 \quad (3.34)$$

where  $f_0$  is the initial relative drying rate. Functions 3.32 through 3.34 are graphed in Figure 3.6, where it was assumed that  $f_0 = 0$ . Note that  $X^*$  is only defined for the warm-up period.

For the falling rate period, Accad and Schmidt [9] and others (Figure 3.4) have observed that the drying rate decreases linearly with decreasing  $X$  (See Chapter 2); however, cubic functions have also been obtained for the falling rate period (see Section 5.3.3). The characteristic drying curve function can be obtained by applying either equation 3.32, 3.33, or 3.34 and by substituting  $f_0$  by  $f_f$ . The normalized  $X$  for the falling rate period is given by

$$\Phi = \frac{X - X_f}{X_{cd} - X_f} \quad (3.35)$$

Note that for  $X_f = 0$ ,  $\Phi$  becomes the normalized moisture content as defined for convective drying of nonhygroscopic materials.

#### 3.4 NORMALIZATION RESULTS OF EXPERIMENTAL DATA

To illustrate the proposed normalization scheme, existing sets of experimental data on a bed of 3 mm glass beads 0.1 m<sup>2</sup> in area and 5 cm deep, subject to different microwave power levels and air temperatures, are normalized. The experimental data are limited in the sense that it only covers the range of  $0.8 < \phi < 1.25$ , but it does demonstrate the normalization scheme for different power levels and air conditions. Since the bed of glass beads is a coarse nonhygroscopic material, an evaporative front is expected to develop inside the product. The function proposed in Equation 4.10 is used to estimate the front position, with the evaporative front coefficient,  $\beta$ , estimated on the basis of air temperature and delivered microwave power (see Section 4.1.1). Evidence of the existence of an evaporative front in the material can be observed in Figure 3.7 where the drying rate curves for different temperatures and power densities have been plotted. Note that for  $P = 0.5$  kW, the drying curves start together, grow apart from each other in proportion to  $(T_a - T_s)$ , and finally converge into one

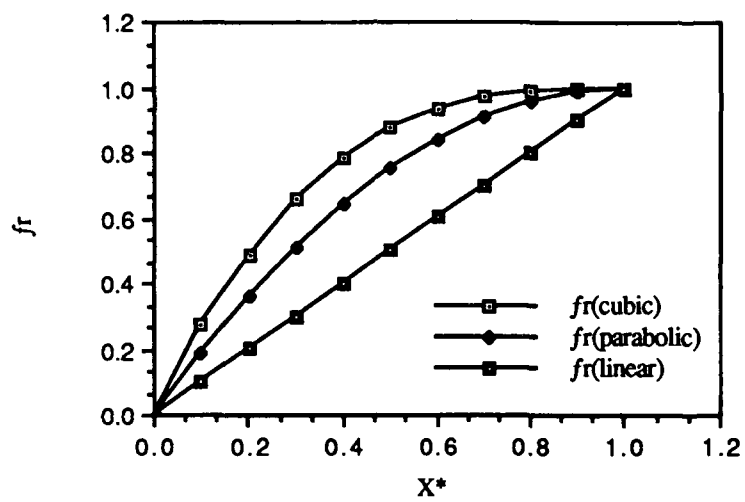


Figure 3.6 Typical characteristic functions for the relative drying rate during the warm-up and falling rate periods.

again. If a drying test could be set up where the air temperature is always equal to the product temperature, the convective heat flux would be zero at all times. Under these conditions, the drying rate curve is expected to rise until no sensible heating is occurring. At this point, all the energy input goes into evaporation, and the drying rate will be constant. However, heating or cooling effects will cause the drying rate to depart from the pure dielectric drying behavior. If convective cooling is present, the energy left for evaporation is less than the heat generated and the drying rate will be proportionally lower; if convective heating is present, the energy available for evaporation will be more than the heat generated, and the drying rate will be proportionally higher. This observation can be seen in Figure 3.7. The curves grow in proportion to the heat input until a moisture content of about 15% is reached. After this point, the curves tend to converge and follow the same path regardless of the air temperature; therefore,  $Q_c$  is not contributing to  $Q_T$ . At the beginning of the drying period, the dry region is relatively small and the heat conduction into the material is not hindered. At some point, the dry region becomes large enough to impede the conduction of heat to or from the wet region, and dielectric heating is practically the only source of evaporation. This situation resembles the hypothetical case of pure dielectric drying mentioned earlier and all the drying curves will converge into one.

The data collected for the drying tests were transformed from the parameters  $(t, m_w, T)$  to the parameters  $(X, N_v, T)$  and input into the normalizing code. Figure 3.8 shows the results of the normalization. Despite the experimental uncertainties of the measuring devices, the warm-up rate period normalized fairly well. A constant drying rate period was not observed for the 0.5 kW curves whereas a well-defined constant drying rate was observed for the 1.0 kW curves.

The results shown in Figures 3.7 and 3.8 support the hypothesis that the normalization procedure outlined in this chapter can be used to characterize drying rates for combined dielectric heating and convective conditions.

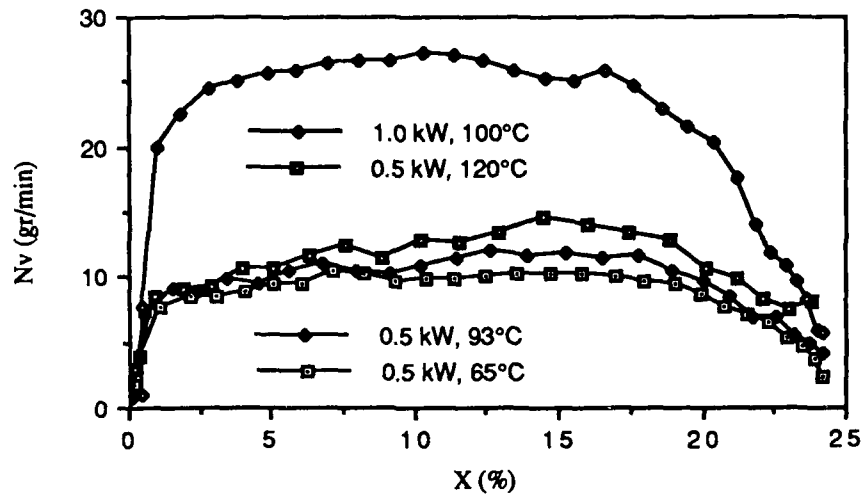


Figure 3.7 Typical experimental drying rate curves.

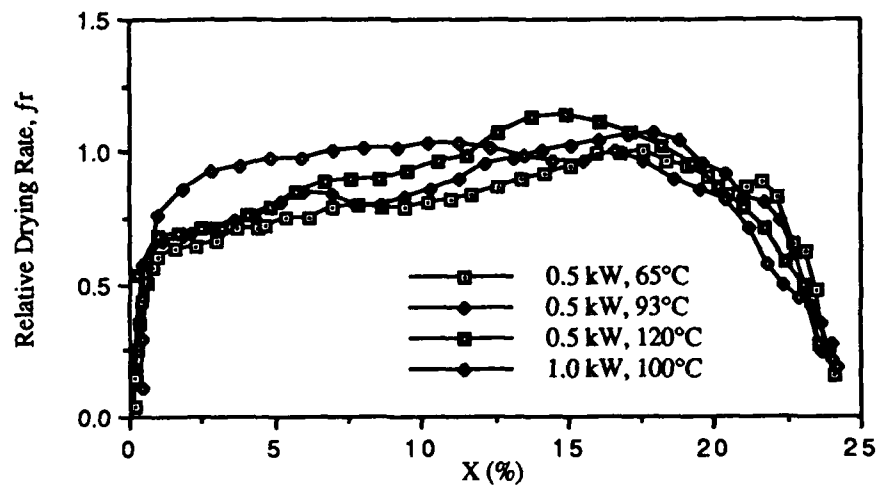
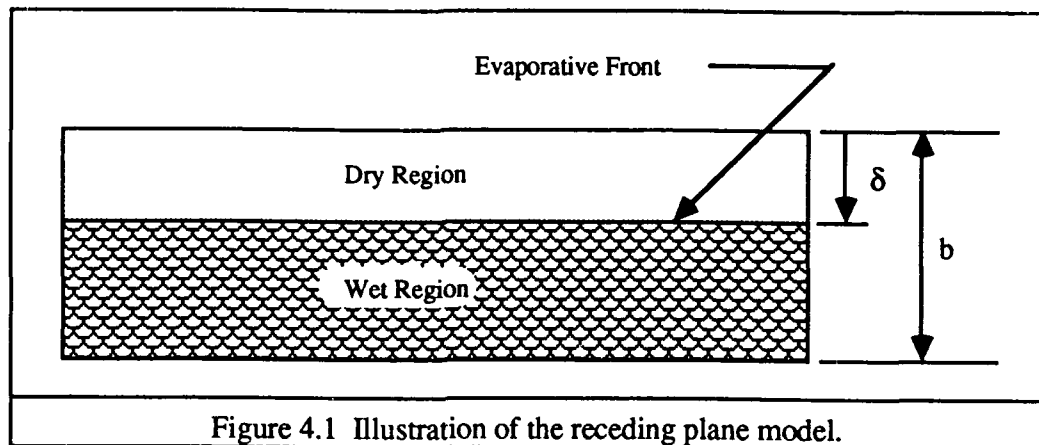


Figure 3.8 Drying curves from Figure 3.7 after normalization.



The following equation relates the drying rate to the product's physical dimensions and the main independent variable, X:

$$A N_v = \frac{-\partial m_w}{\partial t} = \frac{-\partial (X \rho_s V_s)}{\partial t} = -\rho_s b A \frac{\partial X}{\partial t} \quad (4.1)$$

Equation 4.2 relates the drying rate to the physical dimensions of the wet product.

$$A N_v = \frac{-\partial m_w}{\partial t} = \frac{-\partial (\rho_w V_w)}{\partial t} = -\rho_w \frac{\partial V_w}{\partial t} - V_w \frac{\partial \rho_w}{\partial t} \quad (4.2)$$

Note that  $\rho_w$  is defined as the mass of water per unit volume of the wet region (not total product volume), and hence, depends on how the moisture is distributed in the product. Consider the two extreme cases:

Case 1. Constant water density. This case is characterized by a well-defined evaporative front sweeping down the product with the wet region pore volume totally saturated. Equation 4.2 reduces to:



$$A N_v = -\rho_w A \frac{\partial (b - \delta)}{\partial t} = \rho_w A \frac{\partial \delta}{\partial t} \quad (4.3)$$

Combining Equation 4.1 and 4.3 and solving for  $\partial \delta$ :

$$d\delta = -b \frac{\rho_s}{\rho_w} dX \quad (4.4)$$

The ratio of the densities in Equation 4.4 is given by:

$$\frac{\rho_s}{\rho_w} = \frac{m_s V_w}{V_p m_w} = \frac{1 - \delta^*}{X} \quad (4.5)$$

Now, Equation 4.4 can be arranged into an integrable form,

$$\frac{d\delta^*}{1 - \delta^*} = \frac{-dX}{X} \quad (4.6)$$

Integrating Equation 4.6 yields:

$$\frac{\delta}{b} = \delta^* = \left( 1 - \frac{X}{X_0} \right) \quad (4.7)$$

Equation 4.7 states that the evaporative front position is a linear function of the moisture content for this particular case.

Case 2. Volume of the wet region remains constant. The moisture content is spatially uniform; in other words,

$$\frac{\partial X}{\partial x} = \frac{\partial X}{\partial y} = \frac{\partial X}{\partial z} = 0 \quad (4.8)$$

This particular case was observed by Lyons [13] when he subjected a bundle of wet cotton yarn to microwave heating. Throughout the experiment, the moisture distribution was uniform inside the material (See Figure 4.2). For this case, Equation 4.2 reduces to

$$A N_v = -V_w \frac{\partial \rho_w}{\partial t} \quad (4.9)$$

and going through the same procedure,  $\delta^* = 0$  (no evaporative front is present).

Most materials are expected to behave somewhere between Case 1 and Case 2 depending on their permeability, dielectric heating rate and air temperature. Low permeability and high power will generate pressure inside the material which will tend to keep the surface wet and  $\delta$  small. Also, if boiling is occurring within the wet region, the boiling action tends to push the water towards the surface. This behavior has been observed experimentally in drying of beds of glass beads under microwave irradiation [20]. Also for low surface temperature, continuous vapor condensation in the dry region will keep this region wet, raising the front position. In addition, if the permeability of the material is low, pressure build-up and capillary forces will drive moisture toward the surface, hindering the establishment of an evaporative front.

Based on the above observations, the following model is proposed:

$$\delta^* = 1 - \left( \frac{X}{X_o} \right)^\beta \quad (4.10)$$

where  $\beta$ , the evaporative front coefficient, is a function of the permeability, surface temperature and microwave power. In general:

$\beta \rightarrow 1$  for granular nonhygroscopic materials with a high surface temperature;

$\beta \rightarrow 0$  for low permeability materials and low surface temperature.

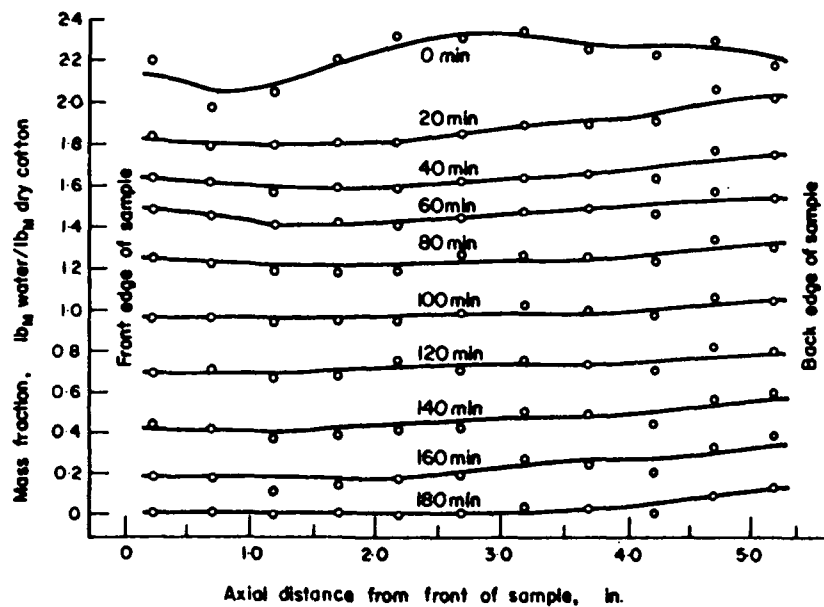


Figure 4.2 Moisture distribution in Lyons' experiment [13].

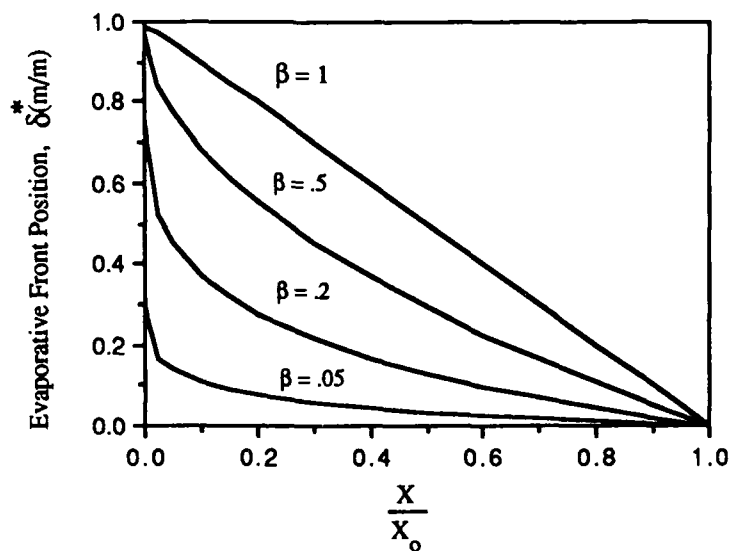


Figure 4.3 Evaporative front position as a function of X

Figure 4.3 shows the position of the evaporative front measured from the surface. If  $\delta^* = 1$ , the entire product is dry; if  $\delta^* = 0$ , the moist region encompasses the whole product volume.

For convective drying, an equation for  $\delta^*$  is given by Suzuki [14] as:

$$\delta^* = 1 - \sqrt{\frac{\Phi}{f_r}} = 1 - \left[ \frac{X}{X_{cr}} \right]^{\frac{(1-n)}{2}} \quad (4.11)$$

The relationship  $f_r = \Phi^n$  was used to develop Equation 4.11 in terms of  $X$ , assuming constant moisture diffusivity in a porous nonhygroscopic material. Note that Equations 4.10 and 4.11, are similar in nature. Evaluation of  $\beta$  for different types of materials as a function of their moisture transport characteristics is not within the scope of this report. Efforts are presently being devoted by others to developing models for drying kinetics of solids which will permit direct estimation of  $\beta$  from fundamental material characteristics [23].

#### 4.1.2 Governing dryer equations.

The dielectrically assisted, convective tunnel dryer was divided into three control volumes as depicted in Figure 4.4. Control Volume I encompasses the humid air inside the dryer, Control Volume II corresponds to the dry region left behind by an evaporative front moving into the product, and Control Volume III is the wet region of the product. A lumped parameter analysis was made for the  $y$  direction thermal and mass transport between the regions [2]. Due to the small temperature gradients, heat conduction in the  $z$  and  $x$  directions was neglected in the analysis. Equations 4.12, 4.13, and 4.14 are the energy balance equations for Control Volumes I, II, and III, respectively. The complete derivations of these equations is found in Appendix B.

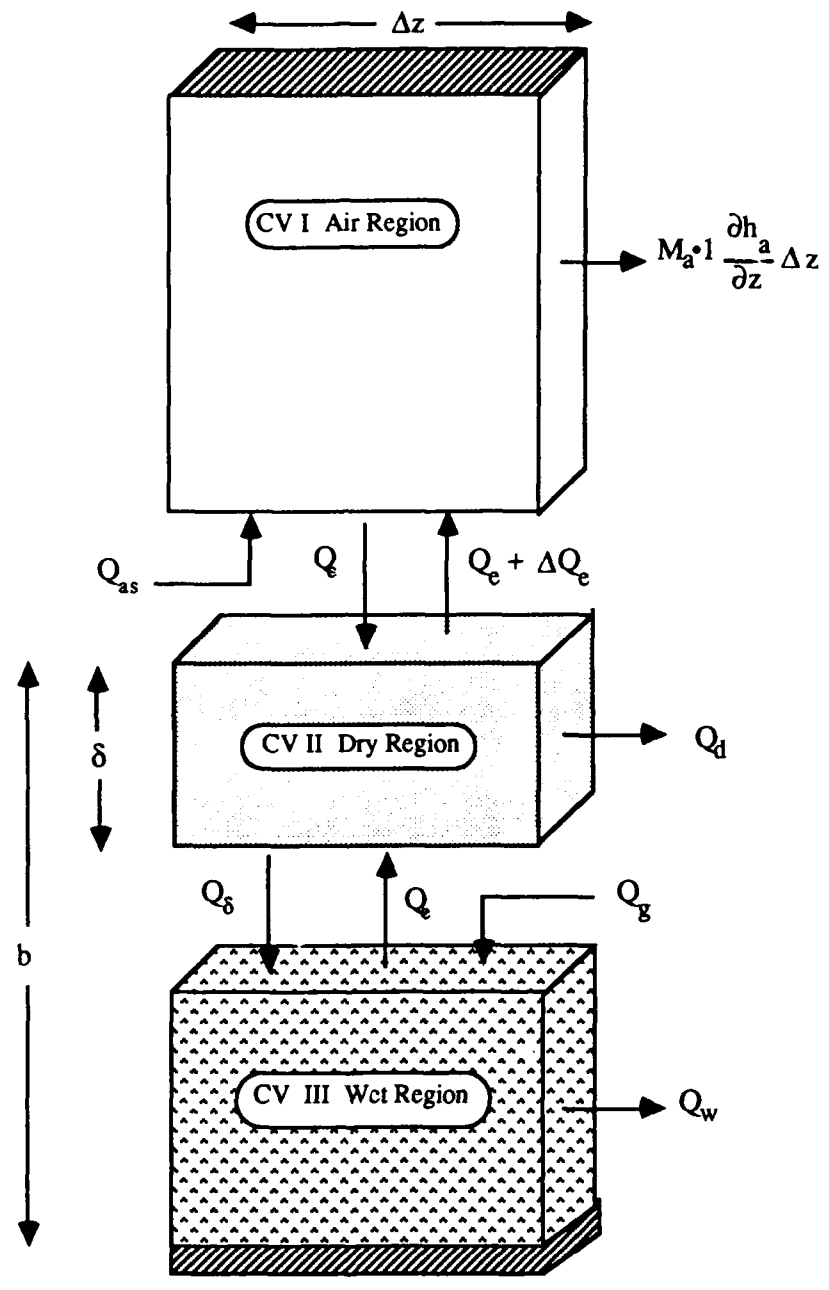


Figure 4.4 Control volumes and energy terms

$$N_v h_v + Q_{as} = M_a \frac{\partial h_a}{\partial z} + h(T_a - T_s) \quad (4.12)$$

$$h(T_a - T_s) = N_v C_v (T_m - T_p) + \frac{M_s \delta C_s}{b} \frac{\partial T_m}{\partial z} - \frac{N_v C_s T_p}{b} \frac{\partial \delta}{\partial X} + \lambda_s \frac{T_s - T_p}{\delta} \quad (4.13)$$

$$\lambda_s \frac{T_s - T_p}{\delta} + Q_g = N_v \Delta h_v + \frac{N_v h_s}{b} \frac{\partial \delta}{\partial X} + M_s (\zeta C_s + X C_w) \frac{\partial T_p}{\partial z} \quad (4.14)$$

where  $\zeta = 1 - \delta^*$ . Equation 4.13 incorporates two new terms into the existing dryer model.  $N_v C_v (T_m - T_p)$  is the change in enthalpy experienced by the water vapor while it is being transported from the evaporative interface to the surface. This term was initially neglected by Flake [2] because  $N_v$  and  $(T_m - T_p)$  are relatively small in convective drying. The incorporation of dielectric heat generates a larger  $N_v$ , and the temperature difference  $(T_m - T_p)$  is larger when  $T_a \gg T_B$  or  $T_a \ll T_B$ . These two factors make the change in the vapor enthalpy term an influential one.

The third term in the RHS of Equation 4.13 accounts for the dry product enthalpy influx into the control volume due to the moving evaporative plane. This term was also neglected by Flake [2] because it is proportional to  $N_v$  and  $T_p$  which are relatively small for convective drying. Examining this term for the case where  $\beta = 1$ , the differential term is

$$\frac{\partial \delta}{\partial X} = \frac{-b}{X_0} \quad (4.15)$$

Therefore,

$$\frac{N_v C_{s,p} T}{b} \frac{\partial \delta}{\partial X} = \frac{-N_v C_{s,p} T}{X_o} \quad (4.16)$$

Equation 4.16 reveals that the third term in Equation 4.11 is most significant for less porous and denser materials when experiencing relatively high drying rates at relatively high temperatures.

Finally, Equation 4.14 states that the heat conducted into the wet region plus the heat generated must equal the evaporative heat loss plus the energy associated with the dry product leaving the control volume due to the movement of the evaporative front plus the change in sensible heat of the wet region.

From a composite mass balance on Control Volumes I, II, and III

$$N_v = M_a \frac{\partial Y}{\partial z} = -M_s \frac{\partial X}{\partial z} \quad (4.17)$$

The energy and mass balance relations expressed in Equations 4.12 through 4.14 and Equation 4.17 must be supplemented by a number of additional constitutive relations to complete the formulation of the problem. The equations to complete the analysis were provided by Flake [2] and are summarized in Appendix B.

#### 4.1.3 Temperature profile

Although drying is a transient phenomenon, quasi-steady analyses may be valid if the time scale for the rate of recession is large compared to the time required for a steady state response of the temperature and humidity gradients to the moving boundary [2]. This is generally valid for convective drying in which the drying time is relatively long, the air temperature is higher than the product temperature, and the effect of vapor convection in the dry region's temperature profile can be reasonably neglected. When dealing with dielectrically enhanced drying, there will be many cases where the product temperature is higher than the air temperature (subcooled drying), vapor fluxes are much larger than in convective drying, and

drying rate is much higher. It has been observed in recent experiments that the vapor flow through the dry region tends to shift the temperature profile towards a more uniform state, depending on the air temperature and dielectric power. Figure 4.5 shows the temperature history for drying of glass beads at  $T_a = 65^\circ\text{C}$  for 1.0 kW. The equilibrium temperature for the surface was around  $80^\circ\text{C}$  even though  $T_a = 65^\circ\text{C}$ . The conduction heat flux from the evaporative plane to the surface is not expected to have a large effect on the surface temperature because of the very low thermal conductivity of the glass beads ( $\approx 0.0004 \text{ kW/m-K}$ ). Therefore, it is concluded that for these two cases,  $T_s > T_a$  and  $T_s$  approaches  $T_p$  because the vapor flux through the dry region keeps this region at a more uniform temperature. This behavior depends on  $T_a$  and  $\phi$ ; their effect on the assumed linear temperature profile inside the dry region can be stated as follows:

- If  $T_a \gg T_B$  and  $\phi \gg 2$ , the temperature profile is not significantly affected, and the dry region temperature profile may be assumed linear.
- If  $T_a \gg T_B$  and  $\phi \approx 1$ , the vapor flux tends to cool down the dry region of the product and keep it near saturation temperature. In this case, it is reasonable to assume that the wet and dry region are approximately at the same temperature.
- If  $T_a = T_B$ ,  $\phi$  becomes unity automatically, and the temperature profile throughout the product is uniform.
- If  $T_a \ll T_B$ , and  $\phi \ll 1$ , the temperature profile is not affected, and the temperature inside the dry region is not uniform.
- If  $T_a \ll T_B$  and  $\phi \approx 1$ , the vapor transport through the region will tend to heat up the dry region and establish a uniform temperature throughout the product.



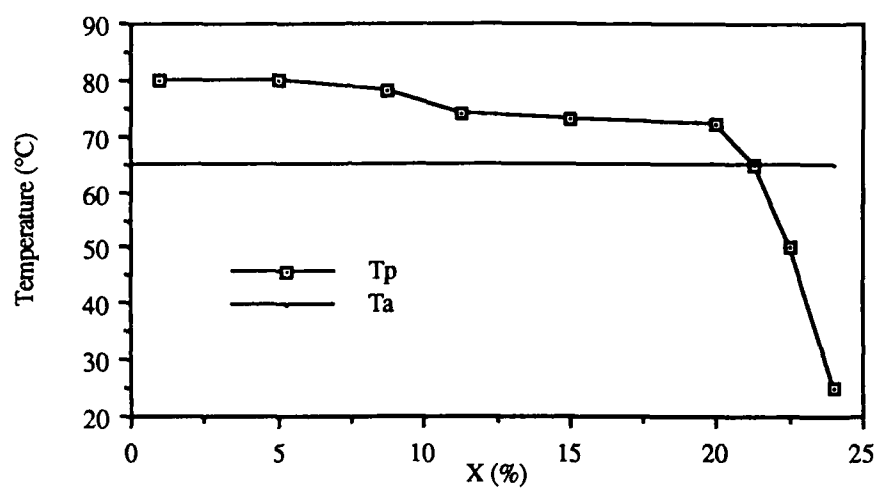


Figure 4.5 Temperature history for drying glass beads with 1.0 kW and 65°C air.

In summary, when  $\phi \approx 1$ , it can be assumed that the dry region temperature equals that of the wet region.

Flake [2] assumes that the dry region is at a mean temperature  $T_m$ , derived from the arithmetic average of  $T_s$  and  $T_p$ . This assumption is suitable for low intensity convective drying where a front is observed only in the late stages of drying, and any error due to the assumption of a linear temperature profile in the dry region is negligible. However, for coarse nonhygroscopic materials under dielectric heating, a front may occur from the beginning and the dry product entering the control volume in the  $y$  direction can have a significantly higher enthalpy than the rest of the dry region. This observation has been incorporated into the governing equations of the product model. Appendix B contains a more detailed derivation of the analytical expression to account for this "extra" enthalpy carried into the control volume by the dry product.

#### 4.2 HEAT GENERATION TERM

Schmidt and Acaad [9] performed a series of model studies which considered a pan of water subjected to simultaneous dielectric heating and convection. The volumetric heat generation term was plotted against the water volume, and a quasi-linear dependence between the heat generation and the water volume was observed, as discussed in Chapter 2. From this behavior, it is assumed, that if  $X = f(z)$  then  $Q_v = \Gamma f(z)$ , where

$$\Gamma = \frac{Q_v}{X} = \frac{P}{V_p X_0} = \frac{1}{X} \frac{\partial P}{\partial V_p} \quad (4.18)$$

The initial conditions are used to determine  $\Gamma$ . Since  $\Gamma$  is constant, it also represents the ratio of  $Q_v/X$  for a differential control volume element as expressed by the last term of Equation 4.18. Solving this equation for  $dP$ :

$$dP = \Gamma X dV_p = \Gamma X b dA \quad (4.19)$$

It is desirable to express the rate of heat generated on a per unit of surface area since the other heating terms in the dryer model are represented on a flux basis (i.e., heating rate per unit of product surface area); therefore,

$$\frac{\partial P}{\partial A} = Q_g = \Gamma X b = \frac{P X}{A X_0} \quad (4.20)$$

A representation of Equation 4.20 is given in Figure 4.4A;  $Q_g$  is a maximum at  $X_0$  and then decreases linearly to zero. Recent experimentation has shown, however, that  $Q_g$  tends to be constant for some time prior to this linear decline; therefore, Equation 4.20 needs to be modified as follows.

If the product moisture level is higher than the "saturation point" of the dielectric oven (i.e., the moisture content above which all of the incident power is absorbed), it can be assumed that  $Q_g$  is constant. The hypothesis in Equation 4.18 can now be modified to reflect this observation. Instead of using the ratio  $Q_v/X$ , the ratio  $Q_v/\Phi$  is used where  $\Phi$  is  $X$  normalized by the "saturation point" (moisture content at which the drying rate first begins to decline). This value of  $X$  plays the role of  $X_c$  for dielectric drying and will be termed  $X_{cd}$ . Now, the volumetric heat generation per unit mass of water is constant until the critical moisture content is reached. Following the same procedure as before,

$$\frac{Q_v}{\Phi} = \Gamma = \frac{P}{\Phi A b} = \frac{\partial P}{\Phi \partial V} \quad (4.21)$$

$$\partial P = \Gamma \Phi \partial V = \Gamma \Phi b \partial A \quad (4.22)$$

$$\frac{\partial P}{\partial A} = Q_g = \Gamma \Phi b = \frac{\Phi P}{A} \quad (4.23)$$

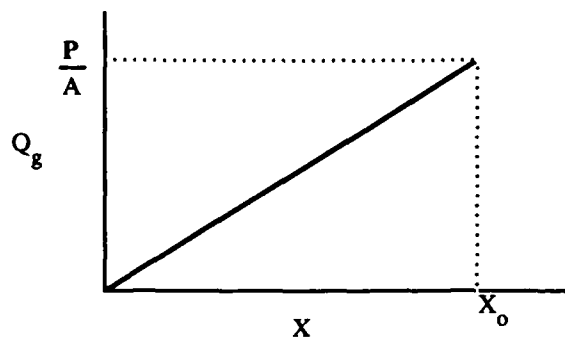


Figure 4.4A

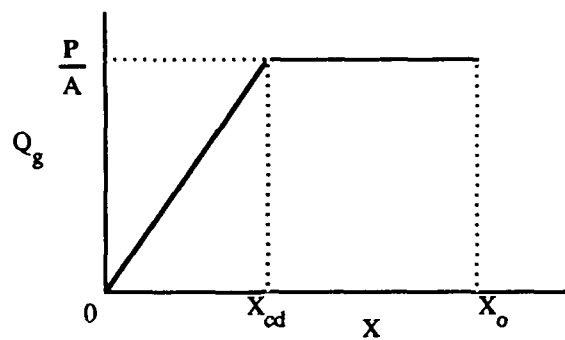


Figure 4.4B

Figure 4.4 Graphical representation of the heat generation model.

For  $\Phi \geq 1$ ,  $Q_g$  is constant; for  $\Phi < 1$  (i.e., below  $X_{cd}$ ),  $Q_g = \Gamma\Phi$ . Now  $Q_g$  will remain constant until  $X_{cd}$ , and then will fall linearly to zero for  $X < X_{cd}$ , as represented in Figure 4.4B.

If the moisture level is less than the saturation point of the dielectric oven, a decay of the absorbed power will be observed. If the product temperature is at equilibrium (sensible heat is negligible), an energy balance yields

$$\phi Q'_g = f_r N_v \Delta h_v = f_r Q_g \quad (4.24)$$

where the primed  $Q_g$  refers to the dielectric heat flux in the falling rate period. Therefore, the heat generation term will decay proportionally according to

$$Q'_g = \frac{f_r}{\phi} Q_g \quad (4.25)$$

In the dryer model it is proposed that Equation 4.25 be used for the falling rate period and Equation 4.23 for the warm-up and constant rate periods to represent the dielectric heat flux as a function of the material properties.

## CHAPTER 5

### THE MODIFIED DRYER CODE

#### 5.1 INTRODUCTION

The dryer code developed by Flake [2] has been modified to handle dielectric heating and boiling point drying. The basic computational procedure used in Flake's model is essentially unchanged. It is convenient to take  $X$  as the independent variable and step through the length of the dryer in  $\Delta X$  increments from the known initial moisture content to the desired exit moisture content, calculating the required dryer length for each increment. The original dryer code has been well documented in Reference [2]; thus, only significant changes made in the code are reported here.

The most important subprograms of the enhanced code are described. The code is validated using experimental data from different sources, and its performance is evaluated by means of running hypothetical cases representative of different drying regimes. A listing of the code and a variable dictionary are presented in Appendix A.

#### 5.2 SUBPROGRAMS IN THE ENHANCED DRYER CODE

##### Main Program

The main program initializes and passes all the variables to a non-linear equation solver, called NLSYST, where new values are determined. The main program writes the new values for the variables and re-initializes them for another computational step. Figure 5.1 shows the relationship between the main program and its subroutines. COMMON blocks were extensively used to avoid transferring arguments and to facilitate the "debugging" of the Fortran code.

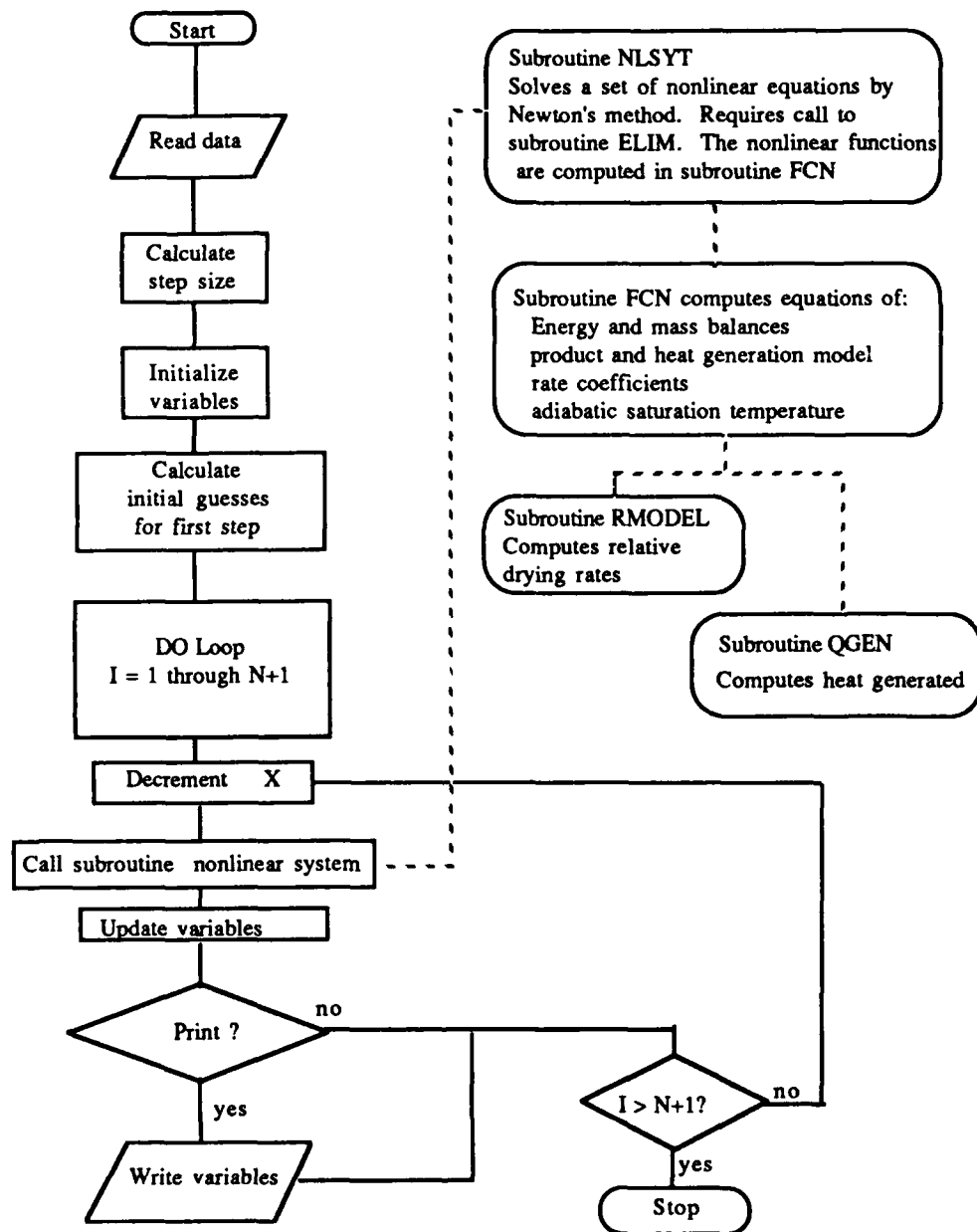


Figure 5.1 Computational flow chart for the modified University of Texas dryer code. Adapted from Reference [2].

### Subroutine FCN

This subroutine contains all the governing equations describing the drying problem. A summary of these equations is given in Appendix B. The major modifications made to this subroutine were:

- Incorporation of "IF" statements and local variables that reduced the sub-program to half of its original length.
- Incorporation of a subroutine called ASSIGN, which allows governing equations to be written using the variables' real names instead of meaningless subscripted variables as required by the subroutine NLSYST.

### Subroutine RMODEL

This subroutine represents the product model in the dryer code. When called, it computes the normalized moisture content, the relative drying rate, and the evaporative front position, taking into consideration whether or not the product is in the warm-up rate, constant rate, or falling rate period. For dielectrically enhanced drying, the user must enter a flag to indicate whether the behavior of the drying curve during the warm-up rate and falling rate periods is linear, parabolic, or cubic. These functions are given by Equations 3.32-3.34, and are already incorporated in the code.

### Subprogram QGEN

This program models the dielectric heating within the wet product. Equations 4.25 and 4.23 are currently used in the code, but any other model could be used.



### 5.3 VALIDATION OF THE DRYER CODE

#### 5.3.1 Introduction

Validation studies of the original dryer code were carried out by Flake [2] for purely convective cases. To validate the modified code, three cases were designed in which experimental data from the literature and experimental drying data generated in the Process Energetics Laboratory of the University of Texas at Austin were used for comparison and illustration. The cases are intended to demonstrate the attributes and shortcomings of the code. Case 1 examines the code for drying without an evaporative front. The experimental data for this case was published by Lyons [13] et al. Case 2, which includes an evaporative front, gives a step by step explanation in how to apply the code to existing experimental data. Case 3 is an exercise to determine the amount of dielectric power necessary with ambient air to attain the same drying time as purely convective drying with air at 150°C.

#### 5.3.2 Case 1: Drying without an evaporative front

Experimental data presented by Lyons et al. was used to check the modified dryer code. The material used was absorbent cotton yarn with the following thermophysical properties:

Density, $\rho_s$	80 kg/m <sup>3</sup>
Thermal conductivity, $\lambda_s$	0.00006 kW/m K
Specific heat, $C_s$	1.3 kJ/kg K
Surface area, A	0.0872 m <sup>2</sup>
Mass, $m_s$	1.474 kg

Air conditions were not documented; Lyons does not mention an air heater when discussing his experimental apparatus. He attributes minor losses to natural convection around the sample; for computational purposes, an ambient air velocity of 0.4 m/s was specified. The ambient air temperature, humidity and flow rate were specified to avoid condensation of moisture.

Lyons et al. did not document the microwave power level; therefore, it was estimated from the temperature history of the sample. This approximation should be reasonably accurate at the beginning of the drying process because both the air and the wet product are at the same temperature, thereby minimizing convective losses. Deriving  $\partial T/\partial t$  from the temperature history graph and applying the pertinent conversion factors, the temperature rate of change was

$$\frac{\partial T}{\partial t} = 0.0555 \frac{^{\circ}\text{C}}{\text{sec}} \quad (5.2)$$

Performing an energy balance on the sample and neglecting the convective term:

$$P = Q_w A = M_s (C_s + X C_w) \frac{\partial T}{\partial t} = 0.8 \text{ kW} \quad (5.3)$$

This value is consistent with the size of the commercial microwave oven used in the tests.

#### Data normalization

Under ordinary circumstances, data are normalized using the normalizing code, NORM. This code calculates the boiling drying rate,  $N_{v0}$ , the drying mode factor,  $\phi$ , and the relative drying rate,  $f_r$ . The relative drying rate is plotted against  $X$  and a curve fit is obtained. Finally, the function  $f_r$  vs.  $X$  is input into the dryer code in the subroutine "RMODEL". A different approach was used for the warm-up period in this case study because the temperature history of the product as a function of moisture content was not documented. It was assumed that  $N_v$  vs.  $X$  was linear during the warm-up period, and the normalized moisture content was defined according to Equation 3.14.

In Lyons et al.'s experiment it was observed that sample weight loss at the beginning of the experiment was due to water "gushing" out and not to actual evaporation. This "liquid movement period", as they defined it, is not modeled by

the present dryer code; thus, it was decided to start the normalization after the liquid movement period. The  $X_O$  was fixed, and  $X_B$  was iterated on until  $T_p = 100^\circ\text{C}$  and  $f_r = 1$  at  $X = X_B$ .

### Results

The results are plotted in Figures 5.2 and 5.3. The predicted drying rate agreed with the experimental data for the region past the liquid movement period. The experimental data for the liquid movement period was included to show that even though the simulation was started at a lower moisture content, the slope for the drying rate curve during the warm-up period was similar to that of the experimental drying curve as it was established in Chapter 3.

The temperature history agreed with the experimental data to a reasonable degree. The small discrepancy may be due to two reasons: first, it was assumed in the code that the whole product was at a uniform temperature; and second, the experimental temperature data plotted in Figure 5.2 was taken from the center of the product which may be different from an average temperature across the sample.

#### 5.3.3 Case 2: Drying with an evaporative front

This section demonstrates how the modified code is applied to existing experimental data in order to predict drying rates, drying times and dryer length for other drying conditions. Experimental data were collected by Armstrong [24] for a polyurethane foam bed with a surface area of  $0.1 \text{ m}^2$  and a thickness of 5 cm. In this test,  $T_a = 150^\circ\text{C}$ ,  $P = 0.5 \text{ kW}$ , and  $U_a = 3 \text{ m/s}$ . Temperature and sample mass measurements were taken as explained in Section 3.3. To obtain the characteristic drying function, the drying rate curve, which is illustrated in Figure 5.4, was normalized according to the procedure listed in Section 3.3.3.

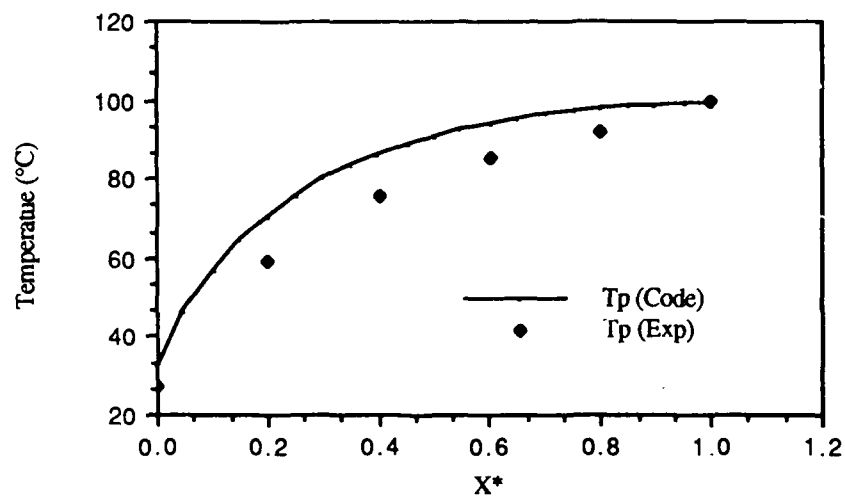


Figure 5.2 Temperature history prediction for Case 1. Experimental data extracted from Reference [13].

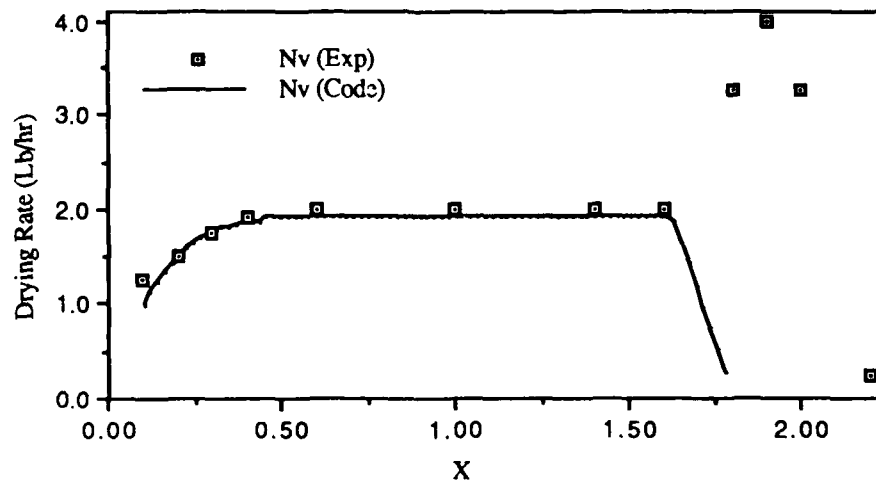


Figure 5.3 Drying rate prediction for Case 1. Experimental data extracted from Reference [13].

Several key points were selected from the drying rate curve and the temperature history curve, and a data file was generated. The most important points to consider are the initial and final conditions, and points identifying peaks and curvatures with their respective surface and product temperatures. Presently, the normalizing code looks for a data file named DATA, in which the values of  $X$ ,  $N_v$ ,  $T_s$  and  $T_p$  are stored. An input file, which is presently called INPUT, is generated with the following information (see variable dictionary in Appendix A for definitions and units):

A	B	POWER	N	EFC	TAIR
VEL	NUC1	NUEXP1	LENGTH	KD	IPRINT

For the case study the following conditions were used:

0.1	0.05	0.5	300	0.05	150
3	0.055	0.8	0.38	0.000021	10

The evaporative front coefficient  $\beta$ , (EFC) was set to 0.05 since capillary forces are expected to maintain the evaporative plane close to the surface.

Data generated by the normalizing code are presented in Figure 5.5, from which  $X_0$ ,  $X_B$ ,  $X_{cd}$ ,  $f_0$ , and  $f_f$ , the data points necessary to develop the product model, are extracted. The characteristic drying curve for the warm-up and falling rate period is categorized in the present code as either linear, parabolic or cubic; the shapes of these functions were illustrated in Figure 3.6. Based on Figure 5.5, a linear function was chosen for the warm-up period, and a cubic relation was chosen for the falling rate period; the cubic function (Equation 3.34) is plotted with the experimental data in Figure 5.6.

The input file for the dryer code is now generated. The parameters are read in the following order:

ISO	MWP	N	IPRINT	DELTA	SW	SF	
XMCL	XMCR	TAL	TPL	YAL	G	L	POWER
XCR	XCD	XB	EXPON	EQUILF	FI	FF	EFC
CPS	PA	B	KD	RHODS	A		
VEL	NUC1	NUEXP1	LENGTH	QAS			

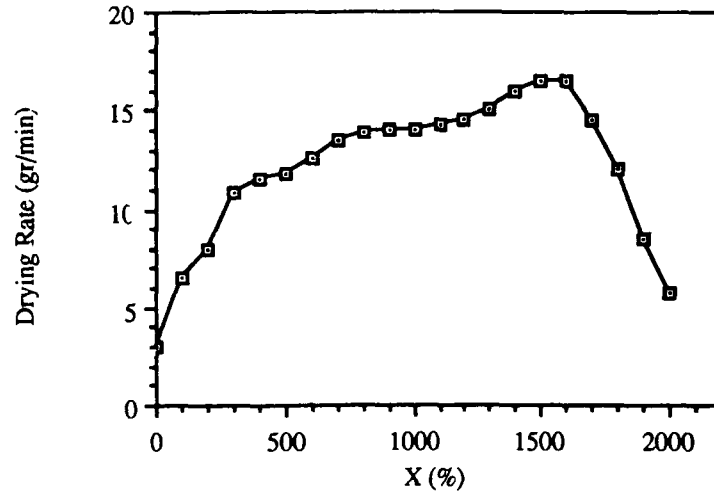


Figure 5.4 Drying rate curve for polyurethane foam,  $P = 0.5 \text{ kW}$ ,  $T_a = 150 \text{ }^\circ\text{C}$

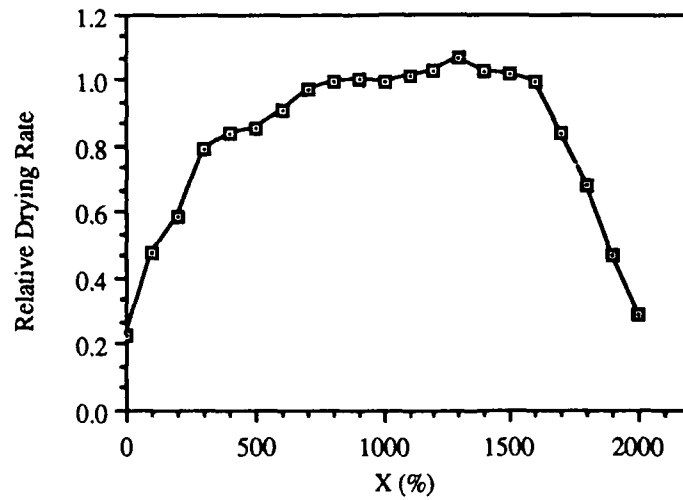


Figure 5.5 Normalized drying curve for Case 2

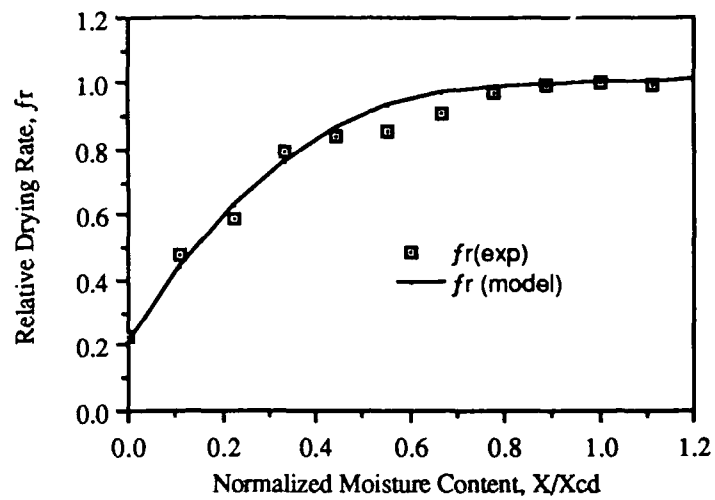


Figure 5.6 Characteristic function in the falling rate period for Case 2

For the Case 2 study, the input parameters were determined as follows. Since the air temperature was held constant at 150 °C, ISO was set to 1 to represent isothermal conditions inside the dryer. MWP was set to 1 because dielectric heating was used. Delta was set to 0.01. SW was set to 1 to cause the product model to use the linear characteristic relation between  $X$  and  $N_v$  for the warm-up period, and SF was set to 3 to cause the product model to use the cubic characteristic function for the falling rate period. In the second row, G was set to a very large number to simulate isohumid conditions inside the dryer. L was calculated based on a conveyor belt velocity of 0.3 meters per minute. The third row contains the parameters associated with the product model. These parameters were obtained from the characteristic drying curve. The fourth and fifth rows are the product properties and convection parameters, respectively. Documentation of the convective parameters is given by Flake [2]. Thus, the input file for this case is:

1	1	300	10	0.01	1	3	
19.2	0.06	150	25	0.01	30000	0.01	0.5
10	9	15.54	0.99	0	0.3	0.2	0.05
3	0.055	0.8	0.38	0			

Note that the units used in the code are: kg, kJ, kW, °C, seconds and meters.

After running the code, an output file is generated as shown in Table 5.1. The second column of the output file is the running sum of the required dryer length increments as the moisture content is decremented. YA/YSAT gives the level of saturation inside the dryer. The fifth column is the drying mode factor. Note that the drying process is dielectrically dominated towards the end. This behavior was observed in all the runs made.

To check the code for internal consistency,  $X$  vs.  $t$  was plotted for the experimental data and the dryer model data. As shown in Figure 5.7, the agreement is very close. The drying time estimated by the code was within about 1% of the experimental drying time, and the predicted temperatures were also in close agreement with the experimental data, as illustrated in Figure 5.8.



TIME	ZPOS	X	YA/YSAT	PHI	TSURF	TP	NV	FREL
(min)	(meters)	(kg/kg)	--	--	(°C)	(°C)	(kg/sec/m <sup>2</sup> )	--
.95	.30	19.20	.17	1.6	27.0	27.0	.107E-02	.300
17.99	5.62	18.56	.17	1.4	65.7	57.5	.131E-02	.422
32.21	10.07	17.92	.17	1.3	88.4	76.6	.154E-02	.545
44.41	13.88	17.29	.17	1.2	102.2	88.7	.179E-02	.667
55.02	17.19	16.65	.17	1.2	110.6	95.9	.204E-02	.789
64.38	20.12	16.01	.17	1.1	115.4	99.4	.231E-02	.912
72.72	22.72	15.37	.17	1.1	117.7	99.9	.250E-02	1.000
80.92	25.29	14.73	.17	1.1	119.6	99.9	.248E-02	1.000
89.19	27.87	14.10	.17	1.1	121.4	99.9	.246E-02	1.000
97.52	30.48	13.46	.17	1.1	122.9	99.9	.244E-02	1.000
105.91	33.10	12.82	.17	1.1	124.4	99.9	.243E-02	1.000
114.34	35.73	12.18	.17	1.1	125.7	99.9	.241E-02	1.000
122.83	38.38	11.54	.17	1.1	126.9	99.9	.240E-02	1.000
131.36	41.05	10.91	.17	1.1	128.0	99.9	.239E-02	1.000
139.93	43.73	10.27	.17	1.1	129.1	99.9	.238E-02	1.000
148.62	46.44	9.63	.17	1.1	122.9	99.9	.233E-02	1.000
157.41	49.19	8.99	.17	1.1	124.0	99.9	.232E-02	1.000
166.22	51.94	8.35	.17	1.1	125.0	99.9	.231E-02	1.000
175.05	54.70	7.72	.17	1.0	126.0	99.9	.230E-02	.998
183.95	57.48	7.08	.17	1.0	127.0	99.9	.229E-02	.992
192.94	60.29	6.44	.17	1.0	128.1	99.9	.226E-02	.981
202.08	63.15	5.80	.17	1.0	129.3	99.9	.221E-02	.963
211.46	66.08	5.16	.17	1.0	130.6	99.9	.215E-02	.937
221.18	69.12	4.53	.17	1.0	132.0	99.9	.206E-02	.900
231.41	72.32	3.89	.17	1.0	133.6	99.9	.194E-02	.850
242.38	75.74	3.25	.17	1.0	135.3	99.9	.179E-02	.787
254.42	79.51	2.61	.17	1.0	137.3	99.9	.161E-02	.708
268.13	83.79	1.97	.17	1.0	139.6	99.9	.139E-02	.612
284.58	88.93	1.34	.17	1.0	142.0	99.9	.112E-02	.496
306.15	95.67	.70	.17	1.0	144.7	99.9	.811E-03	.359
337.97	105.62	.09	.17	1.0	147.5	99.9	.467E-03	.209

DRYER LENGTH = 105.62 METERS  
GENERATED POWER = 5.00 KW/SQ.METER

DRYING TIME = 337.97 MINUTES  
AIR TEMP.= 150.0 DEGREES C

Table 5.1 Output file for Case 2

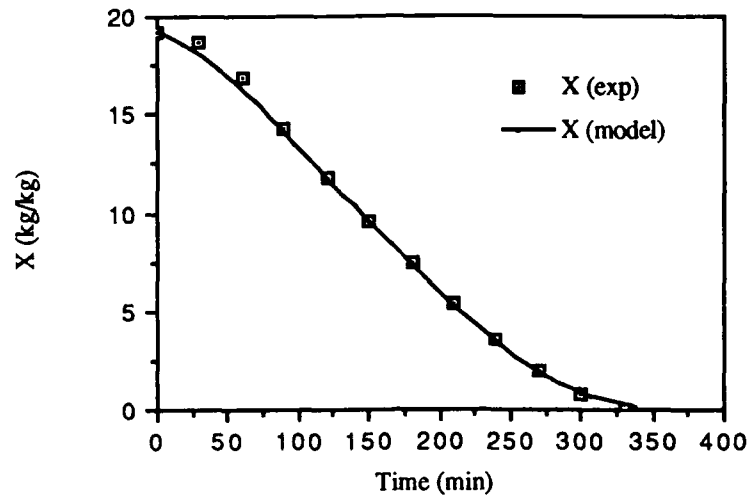


Figure 5.7 Moisture content history for Case 2.

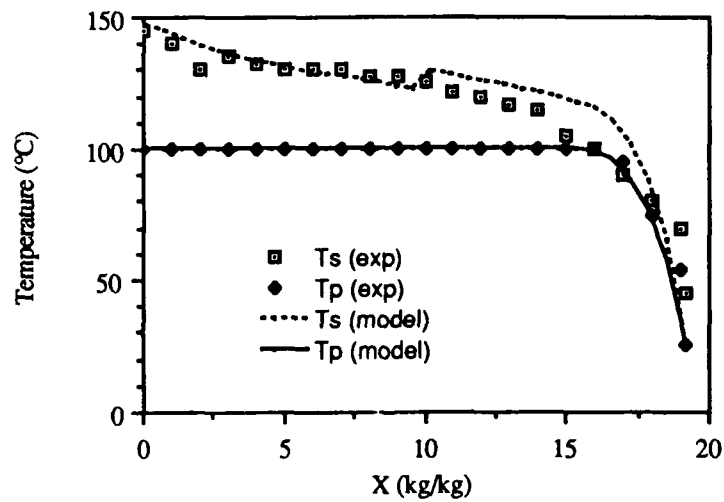


Figure 5.8 Temperature history as a function of moisture content for Case 2.

### Case 3: Determination of P for equivalent hot air drying rates

Case 3 considers the same drying conditions and material in Case 2, but without dielectric heating. A drying test was performed by Armstrong [24] for these conditions; it took approximately 57 hours for the foam to dry from 2000% to 0% moisture. The objective of this case is to estimate the dielectric power that would be necessary to achieve the same drying time using ambient temperature air.  $T_a$  is set to 25°C, MWP is set to one, and the dielectric power is iterated until the same drying time is attained. For this case the code predicted that the required power would be 1.47 kW/m<sup>2</sup>.

This case illustrates one of the advantages of dielectric heating for drying. For the convective case, the wet product reached a maximum temperature of 70°C, while the surface temperature reached 125 °C. For the hybrid case, the dryer code predicted that the wet product will reach a maximum of 100°C while the surface temperature only reaches 73.5°C. Dielectric heating can play an important role in drying temperature sensitive materials, producing equivalent drying rates at lower temperatures than pure convective drying.

Drying can also be accelerated using higher power densities, still without requiring high air temperature. To see the effect of dielectric heating on the drying time, the dielectric power input was doubled while maintaining  $T_a = 25^\circ\text{C}$ . The drying time was reduced to 818 minutes, a 76% reduction, but the predicted surface temperature increased by only 0.5°C.

## 5.4 DRYER PERFORMANCE UNDER VARYING DRYING REGIMES

### 5.4.1 Dryer code results for different drying mode factors

Several hypothetical cases were specified based on the drying regimes defined in section 3.2 to test the code under different drying conditions. Table 5.2 is a compilation of the results. The first three columns in the table are the initial drying conditions relevant to dielectric heating. The maximum surface temperature,

maximum wet product temperature, and drying time are tabulated for comparison purposes. The first row of Table 5.2 (pure convective) is experimental data published by Armstrong [24] as discussed in Case 3 above.

The trends observed in the drying times and temperatures behaved as expected. The most interesting result occurs in the subcooled dielectrically dominated region. The predicted drying time was more than twenty times lower than the drying time for the purely convective case and the convectively dominated case; however, the surface temperature reached a temperature of 78°C, considerably lower than the other two cases.

Results could not be obtained for the subcooled convectively dominated case due to instability problems with the numerical nonlinear equation solver. For the pure convective cooling regime and the dielectrically dominated cooling regime the code behaved erratically. The number of computational steps was increased with no positive results. To simulate the cooling regime, the initial product temperature was set to 80°C, and while the code did run for these conditions, it generated unreasonable data, indicating instability for these drying conditions.

#### 5.4.2 Vapor flux effect in dry region

The code was modified to account for the effect of vapor flux on the dry region temperature profile as discussed in Section 4.1.2. To determine the effect of this change, the code was run with and without the modification using the drying conditions specified for Case 2, but at a much higher microwave power level. The results are tabulated in the last two rows of Table 5.2. There was a small difference in the maximum predicted surface temperature and a large difference in the final surface temperature at the end of the drying process. Despite these differences, the drying time was not significantly affected. This is not surprising, since at high dielectric heating levels, the convective cooling term, which is the one most affected by the predicted product surface temperature, is negligible.

REGIME	T <sub>o</sub> (°C)	T <sub>a</sub> (°C)	Q <sub>g</sub> (kW/m <sup>2</sup> )	T <sub>s</sub> (°C)	T <sub>p</sub> (°C)	Drying Time (hr)
Pure Convective	25	150	0	125	70	57
Convectively Dominated	25	150	0.5	148	100	34.5
Mixed	25	150	2	148	100	12.5
Dielectrically Dominated	25	150	20	145	100	1.5
Subcooled	25	25	20	78	100	1.6
Subcooled	25	25	0.5	*	*	*
Cooling	80	25	0	*	*	*
Cooling	80	25	0.5	*	*	*
Modified	25	25	50	87	100	37.6
Non-Modified	25	25	50	82.7	100	37.7

Table 5.2 Computer results for dryer performance.

## CHAPTER 6

### CONCLUSIONS AND RECOMMENDATIONS

The conclusions and recommendations presented in this section are associated with development of predictive tools for evaluation of applications of dielectrically enhanced dryers.

#### 6.1 CONCLUSIONS

In general, it is concluded that the characteristic drying curve concept should be applicable to dielectric drying. Specifically in this study:

- A unique characteristic drying curve was obtained for dielectrically assisted drying of a bed of glass beads.
- A dimensionless energy balance equation was formulated for dielectrically assisted drying, and used to define a dimensionless parameter, the drying mode factor, which was used to define drying regimes.
- Relative drying rate and relative warm-up rate functions were defined which depend only on the moisture content and the material properties.
- An equation was developed to estimate the position of the evaporative front in drying capillary-porous materials.
- Governing equations were modified to account for the thermal effect of vapor transport in the product's dry region.
- A heat generation term model was developed and incorporated into the dryer code.

- The existing computer code was modified to accept dielectrically assisted drying. Sanity checks were performed on the computer code by comparing the results obtained using the code to published data found in the literature and to experimental data attained in the Process Energetics Laboratory at the University of Texas at Austin.

It was concluded from the dimensional analysis of the energy balance equation that the relative drying rate and the relative warm-up rate were independent of power level and air temperature. This concept was experimentally confirmed by applying the normalizing scheme to drying data taken at two microwave power levels (0.5 kW, 1.0 kW) with different air temperatures (65°C, 100°C, 120°C, 150°C).

## 6.2 RECOMMENDATIONS

Presently, the code uses the conditions at the entrance of the dryer as input; for countercurrent air flow the air conditions are unknown at the dryer entrance, and therefore, the exiting air temperature must be estimated until the computed initial air conditions match the given initial air conditions. Currently this iteration is performed manually. It is recommended that the necessary programming instructions be incorporated into the code so that iterations are performed automatically.

It is important to further modify the dielectrically enhanced drying model to handle multi-zone drying. Drying data are needed to evaluate the behavior of the drying rate in the transition from dielectric to conventional drying and vice versa. In principle, each drying zone can be treated as a different drying problem whose input data is obtained from the exit conditions of the prior zone. The main difficulty rests in developing a product model to handle the transition from one zone to the other; in other words, the product model must be independent of the moisture content to allow the code to compute a relative drying rate from the characteristic drying function assigned to a particular drying zone. The enhanced code developed

here has been structured in modular form to permit extension to the multi-zone problem. This assumes, however, that the material's characteristic drying curve will respond instantaneously to a sudden change in boundary conditions. This question has not been investigated.

The characteristic drying curve also needs to be correlated to the initial moisture content and initial product temperature. These two parameters are very significant for the development of a multi-zone dryer model because the initial conditions are going to be different for each different zone encountered by the product.

It is recommended that  $\phi$  be used as a management tool for the planning of dielectric drying experiments. Existing hardware would have to be modified to allow lower microwave power levels and higher air temperatures in order to achieve the convection dominated regime ( $\phi > 2$ ) and the subcooled regime ( $\phi < 1$ ). Knowing more about the convective regime is important because it concerns the incorporation of dielectric power into existing convective dryers. The subcooled regime is of interest because it permits drying with ambient air. Table 6.1 shows a proposed matrix for the experimental runs.  $\Delta T$  is the equilibrium temperature difference between the air and the product surface. The table is symmetrical about the parameter  $\alpha$ , the ratio of  $Q_c/Q_g$ , where

$$\phi = 1 + \alpha \quad (6.1)$$

Note that  $\alpha$  is negative for convective cooling and positive for convective heating which generates a mirror image of the table to the left of  $\Delta T = 0$ . Some different combinations of  $\Delta T$  and  $P$  provide the same  $\phi$ , so while Table 6.1 reflects 55 experiments, only 37 are necessary to cover the range of  $\phi$ 's. Values for  $P$  and  $\Delta T$  should be selected according to the experimental equipment capacity. To generate Table 6.1, it was assumed that the convective heat transfer coefficient stays relatively constant when going from  $-5\Delta T$  to  $5\Delta T$ .



## EQUILIBRIUM TEMPERATURE DIFFERENCE

POWER	0 $\Delta$ T	$\pm \Delta$ T	$\pm 2\Delta$ T	$\pm 3\Delta$ T	$\pm 4\Delta$ T	$\pm 5\Delta$ T
1P	1	$1 \pm \alpha$	$1 \pm 2\alpha$	$1 \pm 3\alpha$	$1 \pm 4\alpha$	$1 \pm 5\alpha$
2P	1	$1 \pm 0.5\alpha$	$1 \pm \alpha$	$1 \pm 1.5\alpha$	$1 \pm 2\alpha$	$1 \pm 2.5\alpha$
3P	1	$1 \pm 0.33\alpha$	$1 \pm 0.67\alpha$	$1 \pm \alpha$	$1 \pm 1.33\alpha$	$1 \pm 1.67\alpha$
4P	1	$1 \pm 0.25\alpha$	$1 \pm 0.5\alpha$	$1 \pm 0.75\alpha$	$1 \pm \alpha$	$1 \pm 1.25\alpha$
5P	1	$1 \pm 0.2\alpha$	$1 \pm 0.4\alpha$	$1 \pm 0.6\alpha$	$1 \pm 0.8\alpha$	$1 \pm \alpha$

Table 6.1 Drying mode factor matrix for dielectrically enhanced drying tests.

The present code provides critical input information for economic comparison of conventional and hybrid dryers. All parameters that might affect the ultimate economic efficiency (\$/Kg of removed water) of the dryer should be taken into account. As mentioned in Chapter 2, Pourhiet [12] developed an expression to convert dielectric drying transfer units in a hybrid system to conventional drying transfer units. A similar concept could be incorporated into this model to aid in comparing the two approaches.

One of the assumptions made when developing the model was that a linear temperature profile exists in the dry region. This implies that the dry region's thermal capacitance is small. This assumption is not valid when the thermal capacitance of the product is relatively high. Not knowing the temperature profile inside the dry region precludes estimating the amount of heat being conducted through the dry region into the wet region. It is recommended that the dry region model be modified by discretizing it in the y direction and by using the heat diffusion equation to determine the temperature profile, subject to the following boundary conditions:

$$T_p = T \Big|_{y=\delta} \qquad Q_c = \lambda_s \frac{\partial T}{\partial y} \Big|_{y=0}$$

After discretizing the diffusion equation, n equations in n unknowns are added to the already existing equations in the dryer model. The calculation of the temperature profile inside the dry region could be incorporated into an optional subroutine. An alternative approach has been suggested in which a comprehensive physical predictive product model is interfaced with the empirical approach to generate a characteristic drying curve for convective and enhanced drying. Such models are being developed as part of the overall drying research program at the University of Texas at Austin.

The model used to predict the position of the evaporative front must be experimentally validated. Knowing  $\delta$  is crucial, especially when drying thick low thermal conductivity materials with air at temperatures much higher or lower than the boiling temperature.

The validation studies performed on the dryer code produced positive results within the limited range of available drying data. Experiments need to be run to test the predictive capability of the modified code for a wider range of drying conditions. For example, a drying test should be performed on polyurethane foam for the same initial moisture content and initial product temperature as in Case 2, but at a microwave power level of  $15 \text{ kW/m}^2$  and air temperature of  $65^\circ\text{C}$ . A characteristic drying function for foam is already documented in this report; an immediate follow-on should be to confirm its ability to extrapolate to conditions beyond the range of the data used to generate the function.

The problem of numerical instability of the code during cooling of the product must be investigated and resolved. It is unclear whether the problem lies in the inadequacy of the nonlinear equation solver routine or in inconsistency of the basic product model in the cooling regime. Since cooling conditions might commonly occur in multi-zone dryers, this question is critical to successful development of a multi-zone model.

## **APPENDIX A**

**A.1 VARIABLES DICTIONARY**

**A.2 LISTING OF THE ENHANCED DRYER CODE**

**A.3 LISTING OF THE NORMALIZING CODE**

### A.1 VARIABLE DICTIONARY FOR THE COMPUTER CODES

- A - Products surface area, ( $m^2$ )
- ASSIGN - Subroutine that assigns a subscripted variable to the unknowns as required by NLSYST and viceversa.
- ATM - Air pressure in dryer, (atmospheres).
- B - Product thickness, (meters)
- BETA - Coefficient used in heat and mass transfer analogy, (dimensionless)
- CPA - Dry air specific heat, ( $kJ/kg^{\circ}C$ )
- CPAF - Function subroutine used to calculate dry air specific heat, CPA, as a function of temperature.
- CPAI - Dry air specific heat under isothermal drying conditions. This is separately defined because it remains constant throughout the dryer.
- CPF - Specific heat of saturated liquid water, ( $kJ/kg^{\circ}C$ )
- CPFA - Same as above, evaluated at  $T_{dp}$  for use in air enthalpy equation,
- CPFF - Function subroutine used to calculate saturated liquid water specific heat
- CPS - Specific heat of the (solid) product, an input variable, ( $kJ/kg^{\circ}C$ ).
- CPV - Specific heat of water vapor, ( $kJ/kg K$ )
- CPVA - Same as above, evaluated at  $T_a$  for use in air enthalpy equation,
- CPVF - Function subroutine used to calculate water vapor specific heat
- D - Ratio of molecular weights of air to water, (dimensionless).
- DAB - Diffusivity of water vapor in air,  $D_{ab}$ , ( $m^2/s$ ).
- DAB1 - Same as above, except computed according to Eq. B-12 of Reference [2].

- DELTA - Input variable used to calculate perturbation value in nonlinear equation solver subroutine, NLSYST, where for a given unknown variable  $X(I)$ , the perturbation amount for that variable is  $DELTA * X(I)$ . See discussion at end of Chapter 3 of Reference [2]
- DELTA X - Equivalent to DELTX (below), except at end nodes  $DELTA X = DELTX/2$ .
- DELTX - Decrement value of moisture content, ( $\Delta X$ ), equivalent to  $X_{in} - X_{out}/N$ , where  $N$  is the number of nodes, (kg/kg).
- DELTY - Air humidity increment (or decrement in countercurrent case), where  $DELTY = (L/G) DELTX$ , (kg/kg).
- DELZ - Increment value of dryer length,  $\Delta z$ , (m) See ZPOS.
- DMF - Drying mode factor,  $\phi$ , (dimensionless)
- DRYTIM - Drying time, function of dryer position and product flow rate, (s).
- EFC - Evaporative front coefficient,  $\beta$  (dimensionless)
- EFG - Change of  $\delta$  with respect to  $X$ , (m-kg solid/kg water)
- ENTHAL - Humid air enthalpy,  $h_a$ , at  $i^{th}$  step, (kJ/kg).
- ENTHO - Humid air enthalpy at  $i-1$  step, set equal to computed air enthalpy, ENTHAL, after each step, (kJ/kg).
- EQUILF - Equilibrium moisture content factor. Used to determine the equilibrium moisture content for hygroscopic materials, which is the product of the equilibrium factor and the air humidity.
- EXPON - Exponent  $n$ , in the function for the characteristic drying curve,  $f = \Phi^n$ .
- F - Array of equations which, with  $X(I)$  unknowns, is solved by NLSYST.
- F(1) - Mass balance, composite CV I, CV II.
- F(2) - Energy balance, air control volume, CV I.
- F(3) - Air enthalpy equation.

- F(4) - Dew point temperature function.
  - F(5) - Energy balance for adiabatic saturation process.
  - F(6) - Saturated humidity function.
  - F(7) - Energy balance, wet region, CV III.
  - F(8) - Energy balance, dry region, CV II. .
  - F(9) - Drying rate equation.
  - F(10) - Surface energy balance for wet bulb conditions.
- 
- FCN - Subroutine containing equations of heat and mass balances, etc, solved at each step by NLSYST.
  - FF - Final relative drying rate.(dimensionless)
  - FI - Initial relative drying rate.(dimensionless).
  - FKAIR - Function used to compute thermal conductivity of air,  $k_a$ , (kW/m K).
  - FRACT - Relative depth of evaporative plane (dimensionless).
  - FREL - Relative drying rate  $f_r$ .(dimensionless)
  - FT - Array of dew point and wet bulb equations solved by initial call to NLSYST.
  - FTOL - Tolerance parameter used by NLSYST to determine convergence. As a solution converges, the equations being solved F(I) approach zero. Convergence is reached when  $F(I) < FTOL$ . See Reference [2].
  - G - Air mass flow rate, dry air weight basis, ( $\text{kg}_{\text{dry air}}/\text{s-m}$ ). Positive value indicates concurrent air flow, and a negative value, countercurrent.
  - HC - Convective heat transfer coefficient,  $h$  ( $\text{kW}/\text{m}^2\text{C}$ )
  - HCF - Function subroutine used to calculated convective heat transfer coefficient.

- HFGA - Latent heat of vaporization evaluated at  $T_{dp}$ , used in air enthalpy equations.
- HFGS - Same as above, evaluated at wet bulb temperature used in wet bulb equation.
- HFGW - Same as above, evaluated at adiabatic saturation temperature,  $T_{as}$ , used in adiabatic saturation energy balance equation.
- HFGF - Function used to calculate latent heat of vaporization of water.
- I - Counter, steps from 1 to  $N+1$ .
- IFLAG - Flag set when air humidity is greater than saturation value. Saturation will occur when air flow rate is not sufficient to entrain moisture removed from product, when specified entering air humidity is at or greater than saturated humidity or when entering product temperature is less than the dew point temperature (condensation).
- IP - Printing counter reset to 1 after each print. See IPRINT below.
- IPRINT - Counter used to determine printing increments. For example, if IP is set to 4, variables are printed every fourth step (1,5,9,13, ..... $N+1$ ).
- ISO - Flag set to 1 if program is to be run in an isothermal configuration, set to 2 if drying configuration is nonisothermal.
- K - Flag sent to NLSYST. If set to one, values of the solved variables and equations will be printed at each iteration. If solution fails to converge, the equations or variables which did not converge may be found by examining the output. As currently configured, these values are printed only on the first call to NLSYST.
- KD - Thermal conductivity of dry product, an input variable, ( $\text{kW/m}^\circ\text{C}$ )
- L - Mass flow rate of product, dry mass basis, ( $\text{kgdry product/s-m}$ )
- LE - Lewis number.
- LENGTH - Characteristic length used in Nusselt number correlation, an input variable.
- MAXIT - Maximum number (limit) of iterations to be made in NLSYST.
- MWP - Flag set to 1 if dielectric power is on; set to zero for conventional drying.



- N - Number of nodes, input variable.
- NEQ - Number of equations to be solved by NLSYST
- NTQ - Number of equations to be solved by NLSYST in initial call for finding wet bulb and dew point temperatures (NTQ=2).
- NTU - Number of transfer units.
- NUC1 - Coefficient , C,used in Nusselt number correlation.
- NUEXP1 - Exponent , m, of Reynolds number used in Nusselt number  
NLSYST - Subroutine used to solve a system of nonlinear equations.
- NUL - Nusselt number.
- NV - Drying rate flux,  $N_v$ , (kg/m<sup>2</sup>s).
- NVO - Maximun drying rate if all the dielectric heat is used for evaporation. Convective heat is not included. (kg/sec-m<sup>2</sup>)
- PA - Air pressure in Pascals.
- PD - Dielectric power deposition in the wet material, (kW/m<sup>3</sup>).
- PEN - Argument used in subroutine WRITER. When set to zero, the headings of the output files are written; when set to one, the variables for each moisture content decrement are written; when set to two, the dryer length, drying time and NTU are written.
- PHIH - Correction to convective heat transfer coefficients due to high mass transfer rates.
- POWER - Forward dielectric power, (kW)
- PR - Prandtl number.
- PVEL - Velocity of product through dryer, (m/s).
- PWA - Partial pressure of water vapor in air, (Pascals).
- PWS - Saturated partial pressure of water vapor (Pascals).

- QAS - Air heating source flux  $Q_{as}$ , (kW/m<sup>2</sup>), an input variable. For isothermal configuration, the air heating necessary to provide constant temperature air is calculated and the input value of QAS is not used.
- QCOND - The heat conducted through the dry region (kW/m<sup>2</sup>).
- QCONV - The heat convected at the surface (kW/m<sup>2</sup>).
- QEVAP - The total rate of latent heat of vaporization,  $N_v \Delta h_v$  (kW/m<sup>2</sup>).
- QGEN - Dielectric heat flux, (kW/m<sup>2</sup>)
- QGENF - Subroutine used to calculate QGEN
- QSENSD - Sensible heating in the dry region control volume, (kW/m<sup>2</sup>).
- QSENSW - Sensible heating in the wet region control volume, (kW/m<sup>2</sup>).
- QSOL - Enthalpy flux carried in by the dry solid due to the displacement of the evaporative front, (kW/m<sup>2</sup>)
- QVAP - Change in enthalpy of the water vapor when transported through the dry region, (kW/m<sup>2</sup>)
- REL - Reynolds number,  $Re_L$ , used in Nusselt number correlation.
- RELHUM - Relative humidity, (dimensionless).
- RHOA - Air density,  $\rho_s$ , (kg/m<sup>3</sup>).
- RHODS - Density of the dry product (solid), an input variable, (kg/m<sup>3</sup>).
- RKO - The mass transfer coefficient,  $K_o$ , (Kg/m<sup>2</sup>s)
- RKOF - Function subroutine used to calculate mass transfer coefficient  $K_o$ .
- RMODEL - Product model subroutine used to calculate relative drying rate,  $f_r$ , as a function of normalized moisture content.
- SC - Schmidt number.
- SW - Flag used to specify whether the characteristic function during the warm-up period is linear, parabolic or cubic.

- SF - Flag used to specify whether the characteristic function during the falling rate period is linear, parabolic or cubic.
- TA - Air temperature,  $T_a$ , in nonisothermal configuration ( $^{\circ}\text{C}$ ).
- TADSAT - Adiabatic saturation temperature,  $T_{as}$ , ( $^{\circ}\text{C}$ ).
- TAI - Air temperature in isothermal case, constant throughout the dryer, ( $^{\circ}\text{C}$ ).
- TAIR - Local variable used in FCN to represent air temperature, ( $^{\circ}\text{C}$ ).
- TAL - Air temperature at product inlet (left), an input variable, ( $^{\circ}\text{C}$ ). This is the entering air temperature in concurrent configuration, exiting air temperature in countercurrent.
- TALF - Same as above but in  $^{\circ}\text{F}$ . Used in initial calculations of the wet bulb temperature.
- TDEW - Dew point temperature,  $T_{dp}$ , ( $^{\circ}\text{C}$ ).
- TEVAPO - Evaporative plane temperature at previous iteration (old), ( $^{\circ}\text{C}$ ).
- TFCN - Subroutine containing functions for dew point and wet bulb temperature, called by NLSYST.
- TGU - Initial guess of wet bulb temperature ( $^{\circ}\text{F}$ ), before calling NLSYST to solve for wet bulb and dew point temperatures.
- TGUC - Same as above, but in  $^{\circ}\text{C}$ .
- TMEANO - Mean temperature in dry product region ( $^{\circ}\text{C}$ ), at previous iteration (old).
- TNITIAL - Subroutine that sets flags and initializes variables.
- TP - Product temperature,  $T_p$ , ( $^{\circ}\text{C}$ ).
- TPL - Product temperature at product inlet (left), an input variable ( $^{\circ}\text{C}$ ).
- TPOLD - Product temperature at previous iteration, ( $^{\circ}\text{C}$ ).
- TSURF - Product surface temperature,  $T_s$ , ( $^{\circ}\text{C}$ ).
- TSURFO - Product surface temperature at previous iteration, ( $^{\circ}\text{C}$ ).
- TWB - Wet bulb temperature,  $T_{wb}$ , ( $^{\circ}\text{C}$ )

- TWMIN - Minimum wet bulb temperature ( $^{\circ}\text{F}$ ), used in initial guess calculation for wet bulb temperature.
- VEL - Air velocity, an input variable (m/s). Used to compute Reynolds number in heat transfer correlation calculations.
- VISC - Air viscosity, kinematic,  $\nu_a$ , ( $\text{m}^2/\text{s}$ ).
- VISCF - Function used to calculate air viscosity, defined above.
- WETBULB - Subroutine that estimates the wet bulb and adiabatic saturation temperature.
- WRITER - Subroutine containing write and format statements for output files.
- X - Variable array,  $X(I)$ , representing the unknown variables to be solved with equations  $F(I)$ , given in subroutine FCN.
- XB - Moisture content at which boiling point is reached.
- XCD - Critical moisture content,  $X_{cd}$ , for dielectric heating; an input variable, (kg/kg).
- XCR - Critical moisture content,  $X_c$ , an input variable, (kg/kg).
- XMC - Product moisture content at current step,  $X$ , (kg/kg).
- XMCL - Product moisture content at inlet (left), an input variable (kg/kg).
- XMCR - Desired product moisture content at outlet (right), an input variable (kg/kg).
- XNORM - Normalized moisture content,  $\Phi$ .
- XT - Variable array where  $XT(1)$  is  $T_{dp}$ , and  $XT(2)$  is  $T_{wb}$ . Solved with equation array FT by NLSYST.
- XTOL - Tolerance value used by NLSYST to determine convergence. Iteration is stopped at  $X(I) - X(I)_{old} < XT$
- YA - Current air humidity,  $Y$ , (kg/kg).
- YAL - Air humidity at product inlet (left), an input variable, (kg/kg).
- YS - Surface humidity,  $Y_s$ , (kg/kg).
- YSAT - Saturated air humidity,  $Y_{sat}$ , (kg/kg).

- YWF - Function subroutine used to calculate saturated humidity as a function of temperature.
- YWSAT - Saturated air humidity evaluated at wet bulb temperature,  $Y_w$ , (kg/kg).
- ZPOS - Current position in dryer, measured from the product inlet, (m).  
Computed by summation of  $\Delta z$ .

## A.2 LISTING OF THE ENHANCED DRYER CODE

```

PROGRAM DRYER (INPUT,TAPE4,TAPE6,TAPE7,TAPE8,TAPE5,TAPE9=INPUT,
* TAPE10,TAPE11,TAPE12,TAPE1,TAPE2,TAPE3,TAPE13,TAPE14,TAPE15,
* TAPE16,TAPE17,TAPE18,TAPE19,TAPE20,TAPE21,TAPE22,TAPE23,
* OUTPUT,TAPE24=OUTPUT)
C
C*****
C
C           ENHANCED TUNNEL DRYER
C
C           THIS PROGRAM SIMULATES PROCESS CONDITIONS IN A
C           CONTINUOUS CONVECTIVE, DIELECTRICALLY ENHANCED, TUNNEL DRYER
C           UNDER ADIABATIC OR ISOTHERMAL AIR CONDITIONS.
C
C           AT PRESENT, THE CODE SUCCESSFULLY HANDLES PRODUCT
C           MODELS OF PURELY CONVECTIVE OR HIBRIDLY DRIED MATERIALS AND IS
C           STRUCTURED SUCH THAT FUTURE EDITIONS CAN INCORPORATE
C           EQUIPMENT MODELS FOR MULTI-ZONE DRYING.
C
C           THE ACCOMPANYING VARIABLE DICTIONARY PROVIDES INFORMATION
C           ON VARIABLES AND SUBROUTINES FOR USE OF THE CODE.
C*****
C
C           EXTERNAL FCN,TPCN
C           DIMENSION F(16),X(16),XT(2),FT(2)
C           REAL KD,L,LE,LENGTH,NUC1,NUEXP1,NUL,NTU,NV,NVO
C
C           COMMON/FUNCT/DELZ,DRYTIM,ENTHAL,ENTHO,DMF,NEQ,NTU,NV,NVO,PD,
*           QAS,QCOND,QCONV,QEVAP,POWER,QGEN,QSENSD,QSENSW,TA,TADSAT,
*           TDEW,TMEANO,TP,TPOLD,TSURF,TSURFO,TWB,YSAT,ZPOS,QVAP,QSOL
C           COMMON A,B,D,DELTA,X,G,I,ISO,L,MWP,PWS,RELHUM,TAL,XMC,PA,YA
C           COMMON/NLSYS/MAXIT,DELTA,XTOL,FTOL
C           COMMON/PROP/CPA,CPAI,CPF,CPFA,CPS,CPV,CPVA,FKA,HFGA,HFGS,
*           HFGW,KD,RHODS,VISC
C           COMMON/PMODEL/EQUILF,SW,EXPON,FRACT,FREL,XCR,XNORM,SF,EFC,EFG,
*           FLXB,XCD,FF
C           COMMON/CONV/ATM,BETA,CPRAT,CPY,DAB,HC,LE,LENGTH,NUC1,NUEXP1,NUL,
*           PHIH,PR,PSYRAT,REL,RHOA,RHOMA,RKO,SC,VEL,YDA,YDS,YS
C           COMMON/TINIT/IFLAG1,IFLAG2,K,YAL,XMCL,XMCR,TPL,TAL,IFLAG
C
C           CALL WRITER(0.)
C           D = 0.62198
C
C           -----READ INPUT PARAMETER.STATEMENTS ARE DIVIDED AS-----
C           (1)FLAGS,
C           (2)INITIAL CONDITIONS, DRYER CONDITIONS
C           (3) PRODUCT MODEL'S COEFFICIENTS,
C           (4) THERMOPHISICAL PROPERTIES,
C           (5) CONVECTIVE PARAMETERS.
C
C           READ (9,*) ISO,MWP,N,IPRINT,DELTA,SW,SF

```

```

READ (9,*) XMCL,XMCR,TAL,TPL,YAL,G,L,POWER
READ (9,*) XCR,XCD,XB,EXPON,EQUILF,FI,FF,EFC
READ (9,*) CPS,PA,B,KD,RHODS,A
READ (9,*) VEL,NUC1,NUEXP1,LENGTH,QAS
C
C----- CALCULATE ΔX AND ΔY, PRESSURE IN PASCALS-----
C
  IP = IPRINT
  DELTX = (XMCR-XMCL)/FLOAT(N)
  DELTY = -(L/G)*DELTX
  DELTAX = DELTX
  PA = PA*101325.0
  PVEL = L/(RHODS*B)
C
C----INITIALIZE VARIABLES, SET FLAGS, AND CALCULATE WET BULB TEMPERATURE----
C
  CALL TINITIAL
  CALL WETBULB
C
C----- SPECIFIC HEATS AND TRANSPORT COEFFICIENTS ARE FOUND FOR
C           ESTIMATION OF DRYING RATE AND CONTROL VOLUME LENGTH-----
C
  CPA = CPAF(TAL/2.)
  CPF = CPFF(TPL/2.)
  HC = HCF(TAL,0.0001,TPL)
  CALL RMODEL
  CPV = CPVF(TPL/2.)
  YSAT = YWF(TWB)
  RKO = RKOF(TAL,YSAT,FREL,TDEW,TWB)
  NV = RKO*(YSAT-YA)
  DELZ = (-L*DELTX)/(NV)
C
C----- ESTIMATION OF DRYING RATE AND CONTROL VOLUME LENGTH FOR
C           DIELECTRIC DRYING-----
C
  IF (MWP.EQ.1) THEN
    PD = POWER/(B*A)
    NVO = POWER/(A*HFGF(100.))
    DMF = 1.+ HC*A*(TA-TSURF)/POWER
    QGEN = QGENF(PD,B,DMF)
    NV = FREL*NVO*DMF
    DELZ = (-L*DELTX)/(NV)
  ENDIF
C
  ENTHAL = CPAF(TAL/2.)*TAL+YAL*(HFGF(TDEW)+CPVF((TAL+TDEW)/2.)*
* (TAL-TDEW)+CPFF(TDEW/2.)*TDEW)
  ENTHO = ENTHAL
C
  IF (ISO.EQ.1) THEN
    QAS = NV*(HFGF(TAL)+CPVF(TAL/2.)*TAL-CPVF(TPL/2.)*TPL)+
* HC*(TAL-TPL)
  ENDIF
C
  K = 0
C
  DO 100 I = 1,N+1
    IF (I.EQ.N+1) THEN
      XMC = XMCL+DELTX*FLOAT(I-1)-DELTX/2.

```

```

      YA = YAL+DELTY*FLOAT(I-1)-DELTY/2.
      DELTAX = DELTX/2.
      ELSEIF (I.EQ.1) THEN
        XMC = XMCL
        YA = YAL
        DELTAX = DELTX/2.
      ELSE
        XMC = XMCL+DELTX*FLOAT(I-1)
        YA = YAL+DELTY*FLOAT(I-1)
        DELTAX = DELTX
      ENDIF
C
      CALL RMODEL
      CALL ASSIGN (X,0.)
      CALL NLSYST (FCN,X,F,NEQ,K)
      CALL ASSIGN (X,1.)
C
      ZPOS = ZPOS+DELZ
      NTU = NTU+DELTY/(NV/RKO)
      DRYTIM = ZPOS/PVEL
      IF (YA.GT.YSAT) IFLAG1 = 1
      IF (TADSAT.GE.100.) IFLAG2 = 1
C
      TMEANO = (TSURF+TP)/2.
      ENTHO = ENTHAL
      TPOLD = TP
      TSURFO = TSURF
C
      IF (IP.EQ.IPRINT.OR.IFLAG1 .EQ.1 .OR.IFLAG2 .EQ.1) THEN
        IP = 1
        YS = (YSAT-YA)*FREL+YA
C
C-----WRITE VALUES OF VARIABLES FOR CURRENT STEP-----
C
      CALL WRITER (1.)
      ELSE
        IP = IP+1
      ENDIF
C----- IF AIR IS SATURATED, EXIT LOOP -----
C
      IF (IFLAG1 .EQ.1 .OR.IFLAG2 .EQ.1) GO TO 110
      100 CONTINUE
      110 CONTINUE
C
C----- WRITE DRYER LENGTH,DRYING TIME AND NTU -----
C
      CALL WRITER(2.)
      IF (IFLAG1 .EQ.1) STOP 'CONDENSATION Y-AIR > Y-SURFACE'
      IF (IFLAG2 .EQ.1) STOP 'ADIABATIC TEMP.IS G.E.100 C'
      STOP 'END OF PRGM.'
      END
C

```



```

C*****
C  ----- FCN SUBROUTINE CONTAINS EQNS SOLVED BY NLSYST
C*****
C  SUBROUTINE FCN (X,F)
C    DIMENSION X(10),F(10)
C    REAL NVO,KD,L,NV
C
C    COMMON/FUNCT/DELZ,DRYTIM,ENTHAL,ENTHO,DMF,NEQ,NTU,NV,NVO,PD,
C    * QAS,QCOND,QCONV,QEVAP,POWER,QGEN,QSENSD,QSENSW,TA,TADSAT,
C    * TDEW,TMEANO,TP,TPOLD,TSURF,TSURFO,TWB,YSAT,ZPOS,QVAP,QSOL
C    COMMON A,B,D,DELTA,X,G,I,ISO,L,MWP,PWS,RELHUM,TAI,XMC,PA,YA
C    COMMON/PROP/CPA,CPAL,CPF,CPFA,CPS,CPV,CPVA,FKA,HFGA,HFGS,
C    * HFGW,KD,RHODS,VISC
C    COMMON/PMODEL/EQUILF,SW,EXPON,FRACT,FREL,XCR,XNORM,SF,EFC,EFG,
C    * FL,XB,XCD,FF
C
C    -----RENAME SUBSCRIPTED VARIABLES WITH THE NAMES USED IN THIS CODE
C
C    CALL ASSIGN (X,1.)
C
C    IF (ISO.EQ.1) THEN
C      TAIR = TAI
C      CPA = CPAI
C    ELSE
C      TAIR = X(2)
C      CPA = CPAF(TAIR/2.)
C    ENDIF
C
C    CPF = CPFF(TP/2.)
C    CPV = CPVF(TP/2.)
C    CPVA = CPVF((TAIR+TDEW)/2.)
C    CPFA = CPFF(TDEW/2.)
C    HFGW = HFGF(TP)
C    HFGS = HFGF(TWB)
C    HFGA = HFGF(TDEW)
C
C    -----COMPUTE NORMALIZED MOISTURE CONTENT, RELATIVE DRYING RATE,
C    AND THE EVAPORATIVE FRONT POSITION-----
C
C    CALL RMODEL
C    HC = HCF(TAIR,NV,TSURF)
C
C    -----COMPUTE THE FLUXES TO BE USED IN THE ENERGY BALANCE EQUATIONS.
C
C    QVAP = NV*CPV*(TSURF-TP)/2.
C    QSOL = NV*CPS*TP*EFG
C    QCONV = HC*(TAIR-TSURF)
C    QSENSW = L*((1-FRACT)*CPS+XMC*CPF)*(TP-TPOLD)/DELZ+QSOL
C    QSENSD = FRACT*L*CPS*(((TSURF+TP)/2.)-TMEANO)/DELZ-QSOL
C    QEVAP = NV*HFGW
C    RKO = RKOF(TAIR,YSAT,FREL,TDEW,TWB)
C    YWSAT = YWF(TWB)
C    IF (FRACT.GT.0.) QCOND = KD*(TSURF-TP)/(B*FRACT)
C
C    -----COMPUTE THE HEAT GENERATION TERM.-----
C
C    IF (MWP.EQ.1) THEN

```

```

IF (FRACT.LE.0.) THEN
  DMF = 1.+ QCONV*A/POWER
ELSE
  DMF = 1.+ QCOND*A/POWER
ENDIF
QGEN = QGENF(PD,B,DMF)
ELSE
  QGEN = 0.
ENDIF
C
C-----SET THE GOVERNING EQUATIONS TO BE SOLVED. F(1), F(3), F(4), F(5),
AND F(6) ARE CONSTITUTIVE EQUATIONS. F(2), F(7), AND F(8) ARE THE
ENERGY BALANCE EQUATIONS.-----
C
F(1) = L*DELTA X + NV*DELZ
F(2) = G*(ENTHAL-ENTHO)/DELZ+QCONV-QAS-NV*(CPF*TP+HFGW)
F(3) = CPA*TAIR+YA*(CPFA*TDEW+HFGA+CPVA*(TAIR-TDEW))-ENTHAL
F(4) = YWF(TDEW)-YA
F(5) = YWF(TADSAT)-(CPAF(TADSAT/2.)*TADSAT-CPA*TAIR-
* YA*(HFGA+CPVA*TAIR-CPFF(TADSAT/2.)*TADSAT))/(CPFF
* (TADSAT/2.)*TADSAT-HFGF(TADSAT)-CPVF(TADSAT/2.)*TADSAT)
IF (MWP.EQ.0) THEN
  F(6) = YWF(TWB) - YSAT
ELSE
  F(6) = YWF(TADSAT) - YSAT
ENDIF
C
IF (TPOLD.LT.99.9) THEN
  IF (FRACT.LE.0.) THEN
    F(7) = QCONV-QSENSW+QGEN-QEVAP
    F(8) = TSURF-TP
  ELSE
    F(7) = QCOND-QSENSW+QGEN-QEVAP
    F(8) = QCOND+QSENSD-QCONV + QVAP
  ENDIF
  IF (MWP.EQ.0) THEN
    F(9) = FREL*RKO*D*ALOG((D+YSAT)/(D+YA))-NV
    F(10) = RKO*ALOG((D+YWSAT)/(D+YA))*HFGS*D-HC*(TAIR-TWB)
  ELSE
    F(9) = FREL*NVO*DMF- NV
  ENDIF
C
C-----IF BOILING POINT DRYING DEVELOPS, THE FOLLOWING EQUATIONS NEED TO
BE USED.-----
C
ELSE
  IF (XNORM.LT.1.) THEN
    IF(FRACT.GT.0.)THEN
      F(7) = QCONV-QSENSD+QGEN-QEVAP - QVAP
      IF (MWP.EQ.1) F(8) = FREL*NVO*DMF - NV
      IF (MWP.EQ.0) F(8) = QCOND/HFGW - NV
    ELSE
      IF (MWP.EQ.1) F(7) = FREL*NVO*DMF - NV
      IF (MWP.EQ.0) F(7) = QCONV/HFGW - NV
    ENDIF
  ELSEIF(FRACT.GT.0.) THEN
    F(7) = QCONV-QSENSD+QGEN-QEVAP - QVAP

```

```

      IF (MWP.EQ.1) F(8)= FREL*NVO*DMF - NV
      IF (MWP.EQ.0) F(8)= QCOND/HFGW - NV
    ENDIF
  ENDIF
  RETURN
  END
C
C*****
C - SUPPORTING SUBROUTINES
C*****
C
C-----FUNCTION TO COMPUTE RELATIVE DRYING RATE AND
C      EVAPORATIVE FRONT POSITION-----
C
C  SUBROUTINE RMODEL
C  REAL NVO,KD,L,LE,LENGTH,NUC1,NUEXP1,NUL
C
C  COMMON A,B,D,DELTA X,G,I,ISO,L,MWP,PWS,RELHUM,TAI,XMC,PA,YA
C  COMMON/PMODEL/EQUILF,SW,EXPON,FRACT,FREL,XCR,XNORM,SF,EFC,EFG,
C  * FL,XB,XCD,FF
C  COMMON/TINTT/IFLAG1,IFLAG2,K,YAL,XMCL,XMCR,TPL,TAL,IFLAG
C  COMMON/FUNCT/DELZ,DRYTIM,ENTHAL,ENTHO,DMF,NEQ,NTU,NV,NVO,PD,
C  * QAS,QCOND,QCONV,QEVAP,POWER,QGEN,QSENSD,QSENSW,TA,TADSAT,
C  * TDEW,TMEANO,TP,TPOLD,TSURF,TSURFO,TWB,YSAT,ZPOS,QVAP,QSOL
C
C  IF (EQUILF.GT.0.0) THEN
C    RELH = RH(T,YA)
C    RELHUM = RELH
C    XEQ = EQUILF*RELHUM
C    IF (XEQ.GT.XMC) STOP 'XEQ > XMC'
C  ELSE
C    XEQ = 0.
C  ENDIF
C
C-----COMPUTE THE NORMALIZED MOISTURE CONTENT FOR THE FALLING RATE
C      AND WARM-UP PERIODS.-----
C
C  XNORM = (XMC-XEQ)/(XCR-XEQ)
C  XW = (XMC - XMCL)/(XB - XMCL)
C  XF = (XMC-XMCR)/(XCD-XMCR)
C
C  IF (XNORM.LT.0.) STOP 'XNORM .LT. ZERO'
C
C-----THIS BLOCK DEALS WITH THE FALLING RATE PERIOD-----
C
C  IF (XNORM.LT.1.0) THEN
C    IF (MWP.EQ.1) THEN
C      IF(SF.EQ.1) FREL = FF + (1.- FF)*XF
C      IF(SF.EQ.2) FREL = FF+2.*(1.-FF)*XF-(1.-FF)*XF**2
C      IF(SF.EQ.3) FREL = FF+3.*(1.-FF)*XF-3.*(1.-FF)*XF**2+
C      * (1.-FF)*XF**3
C      FRACT = 1.-(XMC/XMCL)**EFC
C      EFG = (-B*EFC/XMCL)*(XMC/XMCL)**(EFC-1)
C    ELSE
C      FREL = XNORM**EXPON
C      FRACT = 1.-SQRT(XNORM/FREL)
C      EFG = 0.
    
```

```

ENDIF
C
C-----THIS BLOCK DEALS WITH THE WARM-UP PERIOD-----
C
ELSEIF (MWP.EQ.1)THEN
  IF(SW.EQ.1) FREL = FI + (1.- FI)*XW
  IF(SW.EQ.2) FREL = FI + 2.*(1.- FI)*XW - (1.- FI)*XW**2
  IF(SW.EQ.3) FREL = FI+3.*(1.-FI)*XW-3.*(1.-FI)*XW**2+
  * (1.-FI)*XW**3
  IF (FREL.GT.1.) FREL=1.
  FRACT = 1.-(XMC/XMCL)**EFC
  EFG = (-B*EFC/XMCL)*(XMC/XMCL)**(EFC-1)
ELSE
  FREL = 1.
  FRACT = 0.
  EFG = 0.
ENDIF
RETURN
END
C
C*****
C-----FUNCTION TO COMPUTE THE VOLUMETRIC HEAT GENERATION.-----
C*****
FUNCTION QGENF(PD,B,DMF)
COMMON/PMODEL/EQUILF,SW,EXPON,FRACT,FREL,XCR,XNORM,SF,EFC,EFG,
* FL,XB,XCD,FF
IF (XNORM.LT.1) THEN
  QGENF = PD*FREL*B/DMF
ELSE
  QGENF = PD*B
ENDIF
RETURN
END
C
C*****
C-----SUBROUTINE TO CALCULATE INITIAL GUESS FOR WET BULB AND
DEW POINT TEMPERATURE -----
C*****
SUBROUTINE WETBULB
DIMENSION F(16),X(16),XT(2),FT(2)
REAL KD,L,LE,LENGTH,NUC1,NUEXP1,NUL,NTU,NV,NVO
EXTERNAL TFCN
C
COMMON/FUNCT/DELZ,DRYTIM,ENTHAL,ENTHO,DMF,NEQ,NTU,NV,NVO,PD,
* QAS,QCOND,QCONV,QEVAP,POWER,QGEN,QSENSD,QSENSW,TA,TADSAT,
* TDEW,TMEANO,TP,TPOLD,TSURF,TSURFO,TWB,YSAT,ZPOS,QVAP,QSOL
COMMON A,B,D,DELTA,X,G,I,ISO,L,MWP,PWS,RELHUM,TAI,XMC,PA,YA
C
K = 0
NTQ = 2
YWS = YWF(TA)
PWA = PA*YA/(D+YA)
TAF = (TA*9./5.)+32.
TWMIN = TAF*TAF*(-2.241468E-03)+.8315167*TAF-3.855549
TGU = TWMIN+(TAF-TWMIN)*PWA/PWS
TGUC = ((TGU-32.)*5./9.)*1.4
XT(1) = TGUC

```

```

      XT(2) = TGUC
C
      CALL NLSYST (TFCN,XT,FT,NTQ,K)
C
      TWB = XT(2)
      TDEW = XT(1)
      TADSAT = XT(2)
      RETURN
      END
C
C*****
C-----SUBROUTINE TO RENAME SUBSCRIPTED VARIABLES WITH THE NAMES
C      USED IN THIS CODE. THE VARIABLES AND NUMBER OF EQUATIONS
C      MUST MATCH THOSE OF SUBROUTINE FCN-----
C*****
      SUBROUTINE ASSIGN (X,T)
      DIMENSION X(16)
      REAL NV,NVO
C
      COMMON/FUNCT/DELZ,DRYTIM,ENTHAL,ENTHO,DMF,NEQ,NTU,NV,NVO,PD,
      * QAS,QCOND,QCONV,QEVAP,POWER,QGEN,QSENSD,QSENSW,TA,TADSAT,
      * TDEW,TMEANO,TP,TPOLD,TSURF,TSURFO,TWB,YSAT,ZPOS,QVAP,QSOL
      COMMON A,B,D,DELTA,X,G,I,ISO,L,MWP,PWS,RELHUM,TAI,XMC,PA,YA
      COMMON/PMODEL/EQUILF,SW,EXPON,FRACT,FREL,XCR,XNORM,SF,EFC,EFG,
      * FL,XB,XCD,FF
C
      IF (T.EQ.0.) THEN
      IF (TPOLD.LT.99.9) THEN
          X(1) = NV
          IF (ISO.EQ.0) X(2) = TA
          IF (ISO.EQ.1) X(2) = QAS
          X(3) = TP
          X(4) = DELZ
          X(5) = ENTHAL
          X(6) = TSURF
          X(7) = TDEW
          X(8) = TADSAT
          X(9) = YSAT
          IF(MWP.EQ.0) THEN
              X(10) = TWB
              NEQ = 10
          ELSE
              NEQ = 9
          ENDIF
      ELSE
          ELSE
          IF (ISO.EQ.0) X(1) = TA
          IF (ISO.EQ.1) X(1) = QAS
          X(2) = DELZ
          X(3) = ENTHAL
          X(4) = TDEW
          X(5) = TADSAT
          X(6) = YSAT
          IF (XNORM.LT.1.) THEN
          IF (FRACT.GT.0.) THEN
              X(7) = TSURF
              X(8) = NV
          
```

```
      NEQ = 8
    ELSE
      X(7) = NV
      NEQ = 7
    ENDIF
  ELSEIF(FRACT.GT.0.)THEN
    X(7) = TSURF
    X(8) = NV
    NEQ = 8
  ELSEF
    NEQ = 6
  ENDIF
ENDIF
ELSEIF (TPOLD.LT.99.90) THEN
  NV=X(1)
  IF (ISO.EQ.0) TA=X(2)
  IF (ISO.EQ.1) QAS=X(2)
  TP=X(3)
  DELZ=X(4)
  ENTHAL=X(5)
  TSURF=X(6)
  TDEW=X(7)
  TADSAT=X(8)
  YSAT=X(9)
  IF (MWP.EQ.0) THEN
    TWB = X(10)
  ENDIF
```

```
C
ELSE
  IF (ISO.EQ.0) TA = X(1)
  IF (ISO.EQ.1) QAS = X(1)
  DELZ = X(2)
  ENTHAL = X(3)
  TDEW = X(4)
  TADSAT = X(5)
  YSAT = X(6)
  IF (XNORM.LT.1.) THEN
    IF (FRACT.GT.0.) THEN
      TSURF = X(7)
      NV = X(8)
    ELSE
      NV = X(7)
    ENDIF
  ELSEIF(FRACT.GT.0.) THEN
    TSURF = X(7)
    NV = X(8)
  ENDIF
ENDIF
RETURN
END
```

```

C*****
C SUBROUTINE WRITER (PEN)
C REAL NTU,NV,NVO
C DIMENSION X(16)
C
C COMMON/FUNCT/DELZ,DRYTIM,ENTHAL,ENTHO,DMF,NEQ,NTU,NV,NVO,PD,
C * QAS,QCOND,QCONV,QEVAP,POWER,QGEN,QSENSD,QSENSW,TA,TADSAT,
C * TDEW,TMEANO,TP,TPOLD,TSURF,TSURFO,TWB,YSAT,ZPOS,QVAP,QSOL
C COMMON A,B,D,DELTA,X,G,I,ISO,L,MWP,PWS,RELHUM,TAI,XMC,PA,YA
C COMMON/PMODEL/EQUILF,SW,EXPON,FRACT,FREL,XCR,XNORM,SF,EFC,EFG,
C * FLXB,XCD,FF
C COMMON/CONV/ATM,BETA,CPRAT,CPY,DAB,HC,LE,LENGTH,NUC1,NUEXP1,NUL,
C * PHIH,PR,PSYRAT,REL,RHOA,RHOMA,RKO,SC,VEL,YDA,YDS,YS
C
C -----WRITE HEADERS FOR OUTPUTFILES-----
C
C IF (PEN.EQ.0.) THEN
C   WRITE (1,10)
C 10  FORMAT(2X,'TIME',3X,ZPOS',5X,'X',3X,'YA/YSAT',3X,'DMF',TSURF',
C * 4X,'TP',5X,'NV',5X,'FREL')
C   WRITE (2,20)
C 20  FORMAT(3X,T',5X,'XMC',9X,TA',9X,'YA',9X,TP',9X,'YSAT',9X,'RH')
C   WRITE (3,85)
C 85  FORMAT (1X,'XMC',8X,'NV',7X,'QGEN',8X,
C * 'DMF',6X,'FREL')
C
C -----WRITE VARIABLES FOR EACH STEP-----
C
C ELSEIF (PEN.EQ.1.) THEN
C   WRITE(1,120) (DRYTIM/60.),ZPOS,XMC,(YA/YSAT),DMF,TSURF,
C * TP,NV,FREL
C 120  FORMAT(1X,3(F7.2,''),F4.2,'',3(F6.1,''),E10.3,'',F7.3)
C   WRITE (2,70) LXMC,TA,YA,TP,YSAT,RELHUM
C 70  FORMAT (1X,I3,'',F7.4,'',F7.4,'',F8.4,'',F8.4,'',F7.4,
C * '',F7.4,'',F6.1,'',F6.1,'',E10.3,'',F5.2,'',F5.2)
C   WRITE (3,95) XMC,NV,QGEN,DMF,FREL,NVO
C 95  FORMAT (1X,9(E12.6,''))
C   WRITE (4,30) (DRYTIM/60.),XMC,TA,TP,TADSAT,TSURF,TAI
C 30  FORMAT (1X,7('F9.3))
C   WRITE (5,35) XNORM,XMC,(NV*7920.*A)
C 35  FORMAT (1X,3(F7.3,''),E9.3,'')
C
C   WRITE (7,95) ZPOS,HC,RKO,PSYRAT
C   WRITE(8,80) XMC,QCOND,QSENSW,QEVAP,QSENSD,QCONV,
C * QAS,QGEN,QVAP,QSOL
C 80  FORMAT (1X,10(F6.3,''))
C   WRITE (10,40) ZPOS,YA,YSAT,(YSAT-YA)
C 40  FORMAT (F11.4,'',F10.8,'',F10.8,'',F10.8)
C
C   WRITE (11,50) LXMC,YA,TWB,YSAT,(YSAT-YA),NV
C 50  FORMAT (I3,5('F11.7),E10.5)
C   WRITE (12,60) TA,YA,TDEW,TADSAT,TWB,QAS
C 60  FORMAT (1X,6(F6.2,''))
C   WRITE (13,*) PR,SC,LE,PHIH
C   WRITE (14,*) BETA,CPRAT,LE,PSYRAT
C   WRITE (15,*) YA,ENTHAL,FRACT
C   WRITE (16,*) ZPOS,TA,QCONV,QEVAP,QSENSW,QAS

```

```

WRITE (17,90) XMC,YA,XNORM,FREL,NV,TSURF,ZPOS
90  FORMAT (F7.4,',',F7.5,',',F7.5,',',F5.3,',',E12.4,',',F7.2,
*      ',F10.3)
C
C-----WRITE THE DRYER LENGTH, DRYING TIME, NTU, DIELECTRIC FLUX,
C      AND LATEST AIR TEMPERATURE.-----
C
ELSE
WRITE (1,77) ZPOS,(DRYTIM/60.),ABS(NTU),(QGEN*DMF/FREL),TA
77  FORMAT (/,1X,'DRYER LENGTH =',F11.2,' METERS',4X,'DRYING TIME
*      =',F12.2,' MINUTES',/, ' NUMBER OF TRANSFER UNITS, NTU =',
*      F7.2,4X,'GENERATED POWER =',F7.2,' KW/SQ.METER',/, 'AIR TEMP.=',
*      F7.1,' DEGREES C')
ENDIF
RETURN
END*
C*****
C----- FUNCTION TO COMPUTE SPECIFIC HEAT OF AIR -----
C*****
FUNCTION CPAF (T)
TK = 273.15+T
TK1 = TK/100.
CPAF1 = (.219+.342*(TK*9./5.)/1E4-.293*(TK*9./5.)**2/1E8)*4.1869
CPN2 = 39.06-512.79/(TK1*SQRT(TK1))+1072.7/TK1**2-820.4/TK1**3
CPO2 = 37.432+0.020102*TK1*SQRT(TK1)-178.57/(TK1*SQRT(TK1))+236.88
* /TK1**2
CPAR = .5203
CPAF2 = (.781*CPN2+.21*CPO2+.009*CPAR)/28.9645
CPAF = CPAF2
RETURN
END
C*****
C-----FUNCTION TO COMPUTE SPECIFIC HEAT OF SAT LIQUID WATER
C*****
FUNCTION CPFF (T)
C20 = 1.02493
C21 = (-4.149E-04)*2.
C22 = (3.07768E-06)*3.
C23 = (-1.2606E-08)*4.
C24 = (3.06581E-11)*5.
C25 = (-3.843E-14)*6.
C26 = (1.9907E-17)*7.
CPFF = (C20+C21*(T*9./5.+32.)+C22*(T*9./5.+32.)**2+C23*(T*9./5.
* +32.)**3+C24*(T*9./5.+32.)**4+C25*(T*9./5.+32.)**5+C26*(T*9.
* /5.+32.)**6)*4.1869
RETURN
END
C*****
C-----FUNCTION TO COMPUTE SPECIFIC HEAT OF WATER VAPOR -
C*****
FUNCTION CPVF (T)
TK = 273.15+T
TK1 = TK/100.
IF (TK.LT.0.0) STOP TEMP < 0.0 DEG CPVF
C
CPVF = (143.05-183.54*TK1**0.25+82.751*SQRT(TK1)-3.6989*TK1)/
* 18.01534

```



```

RETURN
END
C*****
C --- FUNCTION TO COMPUTE SATURATED HUMIDITY --
C*****
FUNCTION YWF (T)
REAL NVO,KD,L,LE,LENGTH,NUC1,NUEXP1,NUL
C
COMMON A,B,D,DELTA,X,G,I,ISO,L,MWP,PWS,RELHUM,TAI,XMC,PA,YA
C
TK = 273.15+T
TK = ABS(TK)
IF (T.LT.0.0) STOP 'EXPLODING SOLUTION, T < 0 K YWF'
C8 = -5800.2206
C9 = 1.3914993
C10 = -0.04860239
C11 = 0.4176478E-04
C12 = -0.14452093E-07
C13 = 6.5459673
C
PWS = EXP(C8/TK+C9+C10*TK+C11*TK**2+C12*(TK)**3+C13*ALOG(TK))
IF (PA.LE.PWS) THEN
YWF = 9999999.9
ELSE
YWF = .62198*PWS/(PA-PWS)
ENDIF
C
RETURN
END
C*****
C ----- FUNCTION TO CALCULATE LATENT HEAT OF VAPORIZATION
C*****
FUNCTION HFGF (T)
TAF = T*9./5.+32.
TAF = ABS(TAF)
IF (TAF.LT.0.0) STOP 'EXPLODING SOLN, TA < 0. HFGF'
HFGF = (1094.40516*EXP(-5.38822711E-04*TAF))*2.326
RETURN
END
C*****
C ----- FUNCTION TO CALCULATE RELATIVE HUMIDITY
C*****
FUNCTION RH (TN,YA)
REAL NVO,MU
IF (TN.GT.99.5) THEN
RH = YA/(YA+1.)
ELSE
YSAT = YWF(TN)
MU = YA/YSAT
PRR = YSAT/(.62198+YSAT)
RH = MU/(1.-(1.-MU)*PRR)
ENDIF
RETURN
END

```

```

C*****
FUNCTION DHFGF (TN)
  T = TN*.9/.5+.32.
  DHFGF = (-.59690355*EXP(-5.38822711E-04*T))*4.1868
RETURN
END
C*****
C----- FUNCTION TO COMPUTE CONVECTIVE HEAT TRANSFER COEFF. --
C*****
FUNCTION HCF (T,NVS,TS)
REAL NVO,KD,L,LE,LENGTH,NUC1,NUEXP1,NUL,NVS
COMMON/PROP/CPA,CPAI,CPF,CPFA,CPS,CPV,CPVA,FKA,HFGA,HFGS,
* HFGW,KD,RHODS,VISC
COMMON/CONV/ATM,BETA,CPRAT,CPY,DAB,HC,LE,LENGTH,NUC1,NUEXP1,NUL,
* PHIH,PR,PSYRAT,REL,RHOA,RHOMA,RKO,SC,VEL,YDA,YDS,YS
C
  TF = (T+TS)/2.
  VISC = VISCF(TF)
  REL = VEL*LENGTH/VISC
  NUL = NUC1*ABS(REL)**NUEXP1
  HC = NUL*FKAIR(TF)/LENGTH
  E = NVS*CPVF((TF)/2,)/HC
  IF (E.GT.1.E-9) THEN
    PHIH = E/(EXP(E)-1.)
  ELSE
    PHIH = 1.00
  ENDIF
  HCF = HC*PHIH
  HC = HCF
RETURN
END
C*****
C---- FUNCTION TO COMPUTE THERMAL CONDUCTIVITY OF AIR ----
C*****
FUNCTION FKAIR (T)
  FKAIR = (24.13022+.0749196*T-3.635783E-05*T**2+2.32043E-08*T**
  * 3)*1.E-06
RETURN
END
C*****
C----- FUNCTION TO COMPUTE AIR VISCOSITY -----
C*****
FUNCTION VISCF (T)
  VISCF = (13.28319+8.8032E-02*T+9.883066E-05*T**2-3.1548E-08*T**3)*
  * 1.E-06
RETURN
END
C*****
C----- FUNCTION TO COMPUTE MASS TRANSFER COEFFICIENT -----
C*****
FUNCTION RKOF (TA,YW,FC,TDP,TWB)
REAL KO,MW,MA,MBS,MBA
REAL NVO,KD,L,LE,LENGTH,NUC1,NUEXP1,NUL
C
COMMON A,B,D,DELTA,X,G,I,ISO,L,MWP,PWS,RELHUM,TAL,XMC,PA,YA
COMMON/PROP/CPA,CPAI,CPF,CPFA,CPS,CPV,CPVA,FKA,HFGA,HFGS,
* HFGW,KD,RHODS,VISC

```

```

C
COMMON/CONV/ATM,BETA,CPRAT,CPY,DAB,HC,LE,LENGTH,NUC1,NUEXP1,NUL,
* PHIH,PR,PSYRAT,REL,RHOA,RHOMA,RKO,SC,VEL,YDA,YDS,YS
C
YS = (YW-YA)*FC+YA
TF = (TA+TWB)/2.
YF = (YA+YW)/2.
IF (YA.LT.YW) THEN
  MW = .01801534
  MA = .0289645
  YDS = YW/(D+YW)
  YDA = YA/(D+YA)
  MBS = MW*YDS+MA*(1.-YDS)
  MBA = MW*YDA+MA*(1.-YDA)
  BETA = MBS*ALOG(MBS/MBA)/((MW-MA)*D*ALOG((D+YW)/(D+YA))/(D+YW))
ELSE
  BETA = 1.01
ENDIF
C
TK = 273.15
DAB = 1.1998806E-09*SQRT(TF+TK)*(TF+TK)*(TF+TK)**(.25)
TCA = 647.3
TCB = 132.48
PCA = 218.01
PCB = 37.10
RMA = 18.01534
RMB = 28.9645
DENOM = (PCA*PCB)**(1./3.)*(TCA*TCB)**(5./12.)*SQRT(1./RMA+1./RMB)
RAD = SQRT(TCA*TCB)
C1 = (1./RAD)**2.334
C = 3.64E-4*C1*DENOM
DAB1 = C*(TF+TK)**2.334*1.E-4
C
RHOA = 353.13/(TF+TK)
ATM = PA/101325.
YWDP = YA
DPP = YWDP/(D+YWDP)
RHOMA = RHOA*(ATM-.3783*DPP)
FKA = FKAIR(TF)
VISC = VISC(TF)
CPA = CPAF(TF)
CPY = CPA+YF*(CPVF(TF)+DHFGF(TDP))
CPRAT = CPY/(1.+YF)
PR = CPA*RHOA*VISC/FKA
SC = VISC/DAB
LE = PR/SC
PSYRAT = BETA*LE**(2./3.)/CPA
KO = HC*PSYRAT
RKOF = KO
C
RETURN
END

```

```

C*****
C-----SUBROUTINE CONTAINING EQUATIONS FOR DEW POINT AND WETBULB
C      TEMPERATURES. THIS SET OF EQS IS USED IN THE INITIAL CALL TO NLSYST.
C*****
      SUBROUTINE TFCN (X,F)
      DIMENSION F(2),X(2)
      REAL NVO,KD,L,LE,LENGTH,NUC1,NUEXP1,NUL
C
      COMMON A,B,D,DELTA,X,G,I,ISO,L,MWP,PWS,RELHUM,TAI,XMC,PA, YA
C
      PWA = PA*YA/(D+YA)
      YWDP = YWF(X(1))
      PWSDP = PWS
      YWSAT = YWF(X(2))
      PWSAT = PWS
      HC = HCF(TAI,0.0,X(2))
      RKO = RKOF(TAI,YWSAT,1.0,X(1),X(2))
      HFGS = HFGF(X(2))
C
      F(1) = PWA-PWSDP
      F(2) = RKO*ALOG((PA-PWA)/(PA-PWSAT))*HFGS*D-HC*(TAI-X(2))
C
      RETURN
      END
C*****
C-----SUBROUTINE THAT SETS FLAGS AND INITIALIZES VARIABLES.----
C*****
      SUBROUTINE TINITIAL
      COMMON/FUNCT/DELZ,DR YTIM,ENTHAL,ENTHO,DMF,NEQ,NTU,NV,NVO,PD,
      * QAS,QCOND,QCONV,QEVAP,POWER,QGEN,QSENSD,QSENSW,TA,TADSAT,
      * TDEW,TMEANO,TP,TPOLD,TSURF,TSURFO,TWB,YSAT,ZPOS,QVAP,QSOL
      COMMON A,B,D,DELTA,X,G,I,ISO,L,MWP,PWS,RELHUM,TAI,XMC,PA, YA
      COMMON/TINIT/IFLAG1,IFLAG2,K,YAL,XMCL,XMCR,TPL,TAL,IFLAG
      COMMON/PROP/CPA,CPAI,CPF,CPFA,CPS,CPV,CPVA,FKA,HFGA,HFGS,
      * HFGW,KD,RHODS,VISC
      COMMON/NLSYS/MAXIT,DELTA,XTOL,FTOL
      REAL NTU
      IFLAG = 0
      IFLAG1 = 0
      IFLAG2 = 0
      MAXIT = 120
      XTOL = 0.00001
      FTOL = 0.0003
      K = 0
      ZPOS = 0.0
      NTU = 0.0
      YA = YAL
      XMC = XMCL
      TSURF = TPL
      TA = TAL
      TAI = TAL
      CPAI = CPAF(TAL/2.)
      TMEANO = TPL
      TP = TPL
      TPOLD = TPL
      TSURFO = TPL
      RETURN

```

```

END
C
C*****
C-----NON-LINEAR EQUATIONS SOLVER. TAKEN FROM REFERENCE [15].-----
C*****
SUBROUTINE NLSYST (FCN,X,F,N,I)
DIMENSION X(N),F(N),A(10,11),XSAVE(11),FSAVE(11)
COMMON/NLSYS/MAXIT,DELTA,XTOL,FTOL
C
C LOGICAL PRINT
C
NEQ1 = N
IF (N.LT.2.OR.N.GT.15) GO TO 180
PRINT = .TRUE.
IF (I.NE.0) PRINT = .FALSE.
C
NP = N+1
DO 120 IT = 1,MAXIT
DO 10 IVBL = 1,N
XSAVE(IVBL) = X(IVBL)
10 CONTINUE
C
CALL FCN (X,F)
C
ITEST = 0
DO 20 IFCN = 1,N
IF (ABS(F(IFCN)).GT.FTOL) ITEST = ITEST+1
FSAVE(IFCN) = F(IFCN)
20 CONTINUE
C
IF (.NOT.PRINT) GO TO 50
WRITE (6,30) IT,X
30 FORMAT (1X,'AFTER ITERATION NUMBER',I3,' X AND F VALUES ARE '/
* ,1X,13F10.4)
WRITE (6,40) F
40 FORMAT (1X,13F10.4)
C
50 IF (ITEST.NE.0) GO TO 60
I = 2
RETURN
C
60 DO 80 JCOL = 1,N
X(JCOL) = XSAVE(JCOL)+DELTA*XSAVE(JCOL)
CALL FCN (X,F)
DO 70 IROW = 1,N
A(IROW,JCOL) = (F(IROW)-FSAVE(IROW))/(DELTA*XSAVE(JCOL))
70 CONTINUE
C
X(JCOL) = XSAVE(JCOL)
80 CONTINUE
C
DO 90 IROW = 1,N
A(IROW,NP) = -FSAVE(IROW)
90 CONTINUE
CALL ELIM (A,N,NP,10)
C
DO 100 IROW = 1,N

```

```

      IF (ABS(A(IROW,IROW)).LE.1.E-14) GO TO 160
100 CONTINUE
C
      ITEST = 0
      DO 110 IVBL = 1,N
        X(IVBL) = XSAVE(IVBL)+A(IVBL,NP)
        IF (ABS(A(IVBL,NP)).GT.XTOL) ITEST = ITEST+1
110 CONTINUE
C
      IF (ITEST.EQ.0) GO TO 130
120 CONTINUE
      I = -1
      RETURN
C
130 I = 1
      IF (.NOT.PRINT) GO TO 150
      WRITE (6,140) IT,X
140 FORMAT (1X,'AFTER ITERATION NUMBER',I3,
* ' X VALUES (MEETING XTOL) ARE ',1X,13F10.4)
150 RETURN
C
160 I = -2
      WRITE (6,170)
170 FORMAT (1X,'CANNOT SOLVE SYSTEM. MATRIX NEARLY SINGULAR')
      IF (I.EQ.-2) STOP 'NEARLY SINGULAR MATRIX'
      RETURN
C
180 I = -3
      WRITE (6,190) N
190 FORMAT (1X,'NUMBER OF EQUATIONS PASSED TO NLSYST IS INVALID. MU
*ST BE 1 < N < 13. VALUE WAS ',I3)
      RETURN
      END
C*****
      SUBROUTINE ELIM (AB,N,NP,NDIM)
      DIMENSION AB(NDIM,NP)
C
      NM1 = N-1
      DO 60 I = 1,NM1
C
        IPVT = I
        IP1 = I+1
        DO 10 J = IP1,N
          IF (ABS(AB(IPVT,I)).LT.ABS(AB(J,I))) IPVT = J
10 CONTINUE
C
        IF (IPVT.EQ.I) GO TO 30
        DO 20 JCOL = I,NP
          SAVE = AB(I,JCOL)
          AB(I,JCOL) = AB(IPVT,JCOL)
          AB(IPVT,JCOL) = SAVE
20 CONTINUE
C
        DO 50 JROW = IP1,N
          IF (AB(JROW,I).EQ.0) GO TO 50
          RATIO = AB(JROW,I)/AB(I,I)
          DO 40 KCOL = IP1,NP

```

```
      AB(JROW,KCOL) = AB(JROW,KCOL)-RATIO*AB(I,KCOL)
40  CONTINUE
50  CONTINUE
60 CONTINUE
C
  IF (ABS(AB(N,N)).LT.1.E-14) GO TO 100
C
  NP1 = N+1
  DO 90 KCOL = NP1, NP
    AB(N,KCOL) = AB(N,KCOL)/AB(N,N)
    DO 80 J = 2, N
      NVBL = NP1-J
      L = NVBL+1
      VALUE = AB(NVBL,KCOL)
      DO 70 K = L, N
        VALUE = VALUE-AB(NVBL,K)*AB(K,KCOL)
70    CONTINUE
      AB(NVBL,KCOL) = VALUE/AB(NVBL,NVBL)
80    CONTINUE
90 CONTINUE
  RETURN
C
100 WRITE (6,110)
110 FORMAT (1X,
  * 'SOLUTION NOT FEASIBLE. A NEAR ZERO PIVOT WAS ENCOUNTERED.
  WRITE (6,*) N,(AB(N,N))
  IF (ABS(AB(N,N)).LT.1.E-14) STOP 'NEAR ZERO PIVOT'
  RETURN
  END
```

### A.3 LISTING OF THE NORMALIZING CODE

```

PROGRAM NORM(INPUT,OUTPUT,DATA,TAPE1=DATA,TAPE9=INPUT,
* TAPE2,TAPE3,TAPE4,TAPE5,TAPE6,TAPE7,TAPE8,TAPE10,TAPE11)
C
C*****
C*
C          NORMALIZING CODE
C          THIS CODE REQUIRES NV VERSUS X AND TP VERSUS X DATA AS INPUT.
C          THE OUTPUT FILE, WHEN PLOTTED, GIVES THE CHARACTERISTIC DRYNG
C          CURVE FOR THE PRODUCT.
C
C          THE ACCOMPANYING VARIABLE DICTIONARY PROVIDES INFORMATION
C          ON VARIABLES AND SUBROUTINES FOR USE OF THE CODE.
C*****
C
C          COMMON/CONV/ATM,B      CPRAT,CPY,DAB,HC,LE,LENGTH,NUC1,NUEXP1,NUL,
*          PHIH,PR,PSYRAT,REL,RHOA,RHOMA,RKO,SC,VEL,YDA,YDS,YS
C          DIMENSION XMC(150),NV(150),TP(150),TSURF(150),NVD(150),XSTAR(150)
C          REAL NVO,KD,L,LE,LENGTH,NUC1,NUEXP1,NUL,NV,NVD
C
C          READ (9,*) A,B,POWER,N,EFC,XB,TAIR
C          READ (9,*) VEL,NUC1,NUEXP1,LENGTH,KD,IPRINT
C
C-----READ DATA OBTAINED FROM A BENCH SCALE DRYING TEST ON A SMALL
C          QUANTITY OF THE PRODUCT. THIS CODE ASSUMES DRYING RATE IS IN
C          GRAMS PER MINUTE-----
C
C          READ (1,*) (XMC(I),I=1,N),(NVD(I),I=1,N),(TSURF(I),I=1,N),(TP(I),I=1,N)
C
C          IP = IPRINT
C-----NORMALIZE EACH DATA POINT-----
C
C          DO 10 I=1,N
C              NV(I) = NVD(I)/60000.
C              XSTAR(I) = (XMC(I) - XMC(1))/(XB - XMC(1))
C              NVO = P/HFGF(TP1(I))
C              HC = HCF(TP1(I),NV(I),TSURF(I))
C              FRACT = 1. - (XMC(I)/XMC(1))**EFC
C              QCONV = HC*A*(TAIR - TSURF(I))
C              QCOND = *A*KD*(TSURF(I) - TP(I))/(FRACT*B)
C
C-----DETERMINE IF AN EVAPORATIVE FRONT IS PRESENT TO CALCULATE
C          THE DRYING MODE FACTOR-----
C
C          IF (FRACT .LT.0.02) THEN
C              DMF = 1. + QCONV/POWER
C          ELSE
C              DMF = 1. + QCOND/POWER
C          ENDIF
C

```



```

C-----COMPUTE THE RELATIVE DRYING RATE AND WRITE THE VALUES-----
C
      FREL = NV(I)/(NVO*DMF)
      IF (IP.EQ.IPRINT) THEN
          IP = 1
          WRITE(2,50) XMC(I),FREL,FRACT,DMF
          WRITE (3,50) XMC(I),QCONV,QCOND,TSURF(I),FRACT
          WRITE (5,50) XMC(I),XSTAR(I),NVD(I),NV(I),FREL
          WRITE (6,50) XMC(I),NVD(I),TP(I)
50      FORMAT(1X,7(F10.4,','))
          ELSE
              IP = IP+1
          ENDIF
10     CONTINUE
        STOP
        END
C*****
C-----SUPPORTING FUNCTIONS. SAME AS IN DRYER CODE
*****
C
      FUNCTION HFGF (T)
      TAF = T*9./5.+32.
      TAF = ABS(TAF)
      IF (TAF.LT.0.0) STOP 'EXPLODING SOLN, TA < 0.HFGF'
      HFGF = (1094.40516*EXP(-5.38822711E-04*TAF))*2.326
      RETURN
      END
C*****
      FUNCTION HCF (T,NVS,TS)
      REAL NVO,KD,L,LE,LENGTH,NUC1,NUEXP1,NUL,NVS
      COMMON/CONV/ATM,BETA,CPRAT,CPY,DAB,HC,LE,LENGTH,NUC1,NUEXP1,NUL,
      * PHIH,PR,PSYRAT,REL,RHOA,RHOMA,RKO,SC,VEL,YDA,YDS,Y5
C
      TF = (T+TS)/2.
      VISC = VISCF(TF)
      REL = VEL*LENGTH/VISC
      NUL = NUC1*ABS(REL)**NUEXP1
      HC = NUL*FKAIR(TF)/LENGTH
      E = NVS*CPVF((TF)/2.)/HC
      IF (E.GT.1.E-9) THEN
          PHIH = E/(EXP(E)-1.)
      ELSE
          PHIH = 1.00
      ENDIF
      HCF = HC*PHIH
C
      RETURN
      END
C*****
      FUNCTION VISCF (T)
      VISCF = (13.28319+8.8032E-02*T+9.883066E-05*T**2-3.1548E-08*T**3)*
      * 1.E-06
      RETURN
      END

```

```
C*****
  FUNCTION FKAIR (T)
  FKAIR = (24.13022+.0749196*T-3.635783E-05*T**2+2.32043E-08*T**
* 3)*1.E-06
  RETURN
  END
C*****
  FUNCTION CPVF (T)
  TK = 273.15+T
  TK1 = TK/100.
  IF (TK.LT.0.0) STOP 'TEMP < 0.0 DEG      CPVF'
  CPVF = (143.05-183.54*TK1**0.25+82.751*SQRT(TK1)-3.6989*TK1)/
* 18.01534
  RETURN
  END
```

## **APPENDIX B**

**B.1 HEAT AND MASS BALANCES**

**B.2 SUMMARY OF EQUATIONS USED BY THE  
DRYER MODEL.**

## B.1 HEAT AND MASS BALANCES

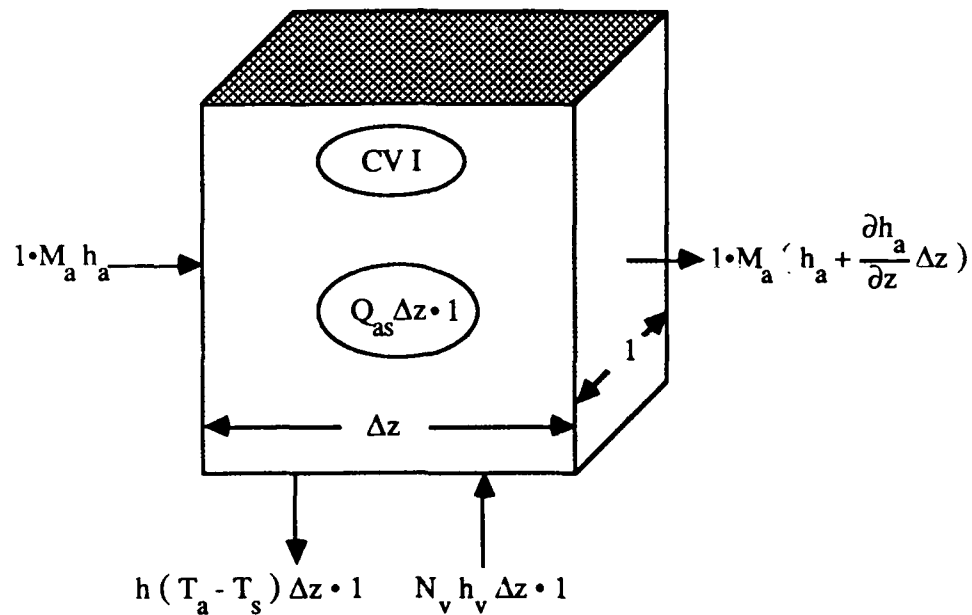
The control volume around the dielectric dryer was divided into three control volumes to represent the distinct regions inside the dryer and the product. The three control volumes correspond to the air region, the dry product region, and the wet product region. The following assumptions were used to perform the analysis:

- The process is steady-state, and the following conservation laws apply where M and E represent mass and energy respectively:

$$M_{in} + M_{source} = M_{out} \quad \text{and} \quad E_{in} + E_{source} = E_{out}$$

- No mass source is considered in this analysis.
- A uniform temperature profile exists in the wet region represented by  $T_p$ .
- A lumped parameter analysis may be used to represent thermal and mass transport in the y-direction.
- Dryer walls, and the top and bottom dryer boundaries are insulated and impermeable.
- Formulation was done on a per unit of dryer width basis.
- Dry product is transparent to electromagnetic energy.
- No heat conduction in the z and x direction
- No product is entrained in the air stream.
- The solid and air mass flow rates are considered constant.
- A linear profile exists between the surface temperature,  $T_s$ , and the evaporative plane temperature,  $T_p$ .

B.1.1 AIR REGION:



Performing an energy balance on CV I and dividing the equation by  $\Delta z \cdot 1$  yields:

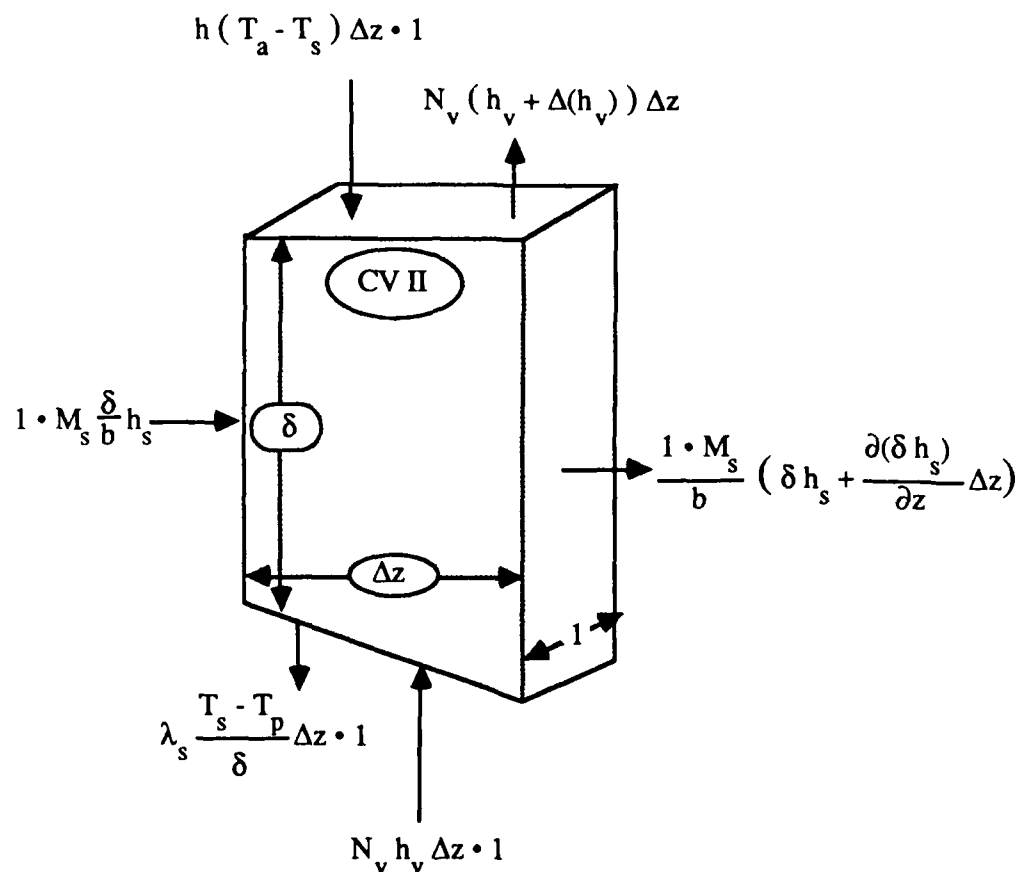
$$N_v h_v + Q_{as} = M_a \frac{\partial h_a}{\partial z} + h (T_a - T_s) \quad (\text{B.1})$$

Where  $h_a$ , the total dry air plus vapor enthalpy on a per unit dry air basis is given by Flake [2] as:

$$h_a = C_a T + Y [ C_w T_{dp} + \Delta h_v + C_v (T - T_{dp}) ] \quad (\text{B.2})$$

The energy input into the control volume, given by the evaporative heat flux and the supplemental air heat source, must equal the sensible heat gained plus the heat convected into the material.

### B.1.2 DRY PRODUCT REGION



Performing an energy balance on control volume II, cancelling common terms in both sides of the equation and dividing both sides by  $(\Delta z \cdot 1)$  yields:

$$h(T_a - T_s) = N_v \Delta(h_v) + \frac{M_s}{b} \left[ \frac{\partial(h_s \delta)}{\partial z} \right] + \lambda_s \frac{T_s - T_p}{\delta} \quad (\text{B.3})$$

where  $\Delta(h_v)$  is the enthalpy difference between the vapor at the evaporative interface and the vapor at the surface. Equation B.3 states that the heat convected into the material must equal the change in enthalpy of the vapor being convected

through the dry region plus the sensible heat gain of the dry region, plus the heat being conducted into the wet region.

Assuming that  $\delta$  is known as a function of  $X$  for the material,  $(\delta, z)$  can be transformed to  $(\delta, X)$  by means of the chain rule.

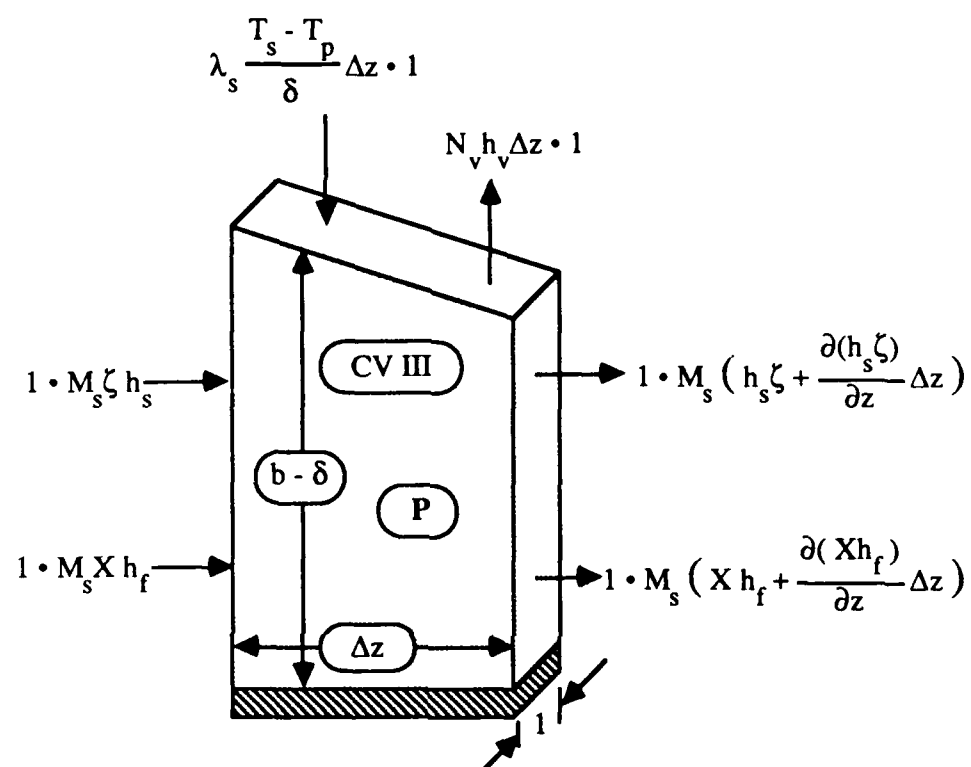
$$\frac{\partial \delta}{\partial z} = \frac{\partial \delta}{\partial X} \frac{\partial X}{\partial t} \frac{\partial t}{\partial z} = \frac{-N_v}{M_s} \frac{\partial \delta}{\partial X} \quad (\text{B.4})$$

Expanding the second term on the RHS of equation B.3, the resulting term with the rate of change of  $\delta$  with respect to  $z$  is related to the change of enthalpy of the dry region due to the enlargement of the control volume. This term is evaluated at  $T_p$  since the enlargement occurs at the evaporative interface, which is at  $T_p$ .

To calculate the change of enthalpy of the vapor going through the dry region, it will be assumed that the vapor leaves the material at the mean temperature of the dry region. Now the energy balance equation reads,

$$h(T_a - T_s) = N_v C_v (T_m - T_p) + \frac{M_s \delta C_s}{b} \frac{\partial T_m}{\partial z} - \frac{N_v C_s T_p}{b} \frac{\partial \delta}{\partial X} + \lambda_s \frac{T_s - T_p}{\delta} \quad (\text{B.5})$$

### B.1.3 WET PRODUCT REGION



Define the relative depth of the wet product as

$$\zeta = \frac{b - \delta}{b} \quad (\text{B.6})$$

Performing an energy balance on the control volume yields:

$$\lambda_s \frac{T_s - T_p}{\delta} \Delta z \cdot 1 + P = N_v h_v \Delta z \cdot 1 + 1 \cdot M_s \frac{\partial(h_s \zeta)}{\partial z} \Delta z + 1 \cdot M_s \frac{\partial(X h_f)}{\partial z} \Delta z \quad (\text{B.7})$$



Applying the chain rule, simplifying and using the following expressions:

$$M_s \frac{\partial X}{\partial z} = -N_v \quad \frac{\partial \zeta}{\partial z} = \frac{-\partial \delta}{b \partial z} = \frac{N_v}{b M_s} \frac{\partial \delta}{\partial X} \quad (\text{B.7})$$

$$\frac{P}{\Delta z \cdot 1} = Q_g \quad h_v - h_f = \Delta h_v \quad (\text{B.8})$$

equation B.7 becomes:

$$\lambda_s \frac{T_s - T_p}{\delta} + Q_g = N_v \Delta h_v + \frac{N_v h_s}{b} \frac{\partial \delta}{\partial X} + M_s (\zeta C_s + X C_w) \frac{\partial T_p}{\partial z} \quad (\text{B.10})$$

The second term on the RHS of Equation B.10, is the enthalpy associated with the dry product leaving the control volume because of the evaporative front. This enthalpy will be evaluated at  $T_p$ .

B.2 SUMMARY OF EQUATIONS USED BY THE DRYER CODE.

Energy Balance, Air Region, CVI

$$N_v h_v + Q_{as} = M_a \frac{\partial h_a}{\partial z} + h(T_a - T_s)$$

Energy Balance, Dry Region, CV II

$$Q_c = N_v C_v (T_m - T_p) + \frac{M_s \delta C_s}{b} \frac{\partial T_m}{\partial z} - \frac{N_v C_s T_p}{b} \frac{\partial \delta}{\partial X} + Q_\delta$$

Energy Balance, Wet Region, CV III

$$\lambda_s \frac{T_s - T_p}{\delta} + Q_g = N_v \Delta h_v + \frac{N_v h_s}{b} \frac{\partial \delta}{\partial X} + M_s (\zeta C_s + X C_w) \frac{\partial T_p}{\partial z}$$

Moisture Mass Balance, Air Region, and Product Region, CV I, II and III.

$$N_v = M_a \frac{\partial Y}{\partial z} = - M_s \frac{\partial X}{\partial z}$$

Humid Air Enthalpy Expression

$$h_a = C_a T + Y [ C_w T_{dp} + \Delta h_v + C_v (T - T_{dp}) ]$$

Dew Point Temperature Definition

$$Y_{sat}(T_{dp}) = Y_a$$

Drying Rate Equation for Convective Drying.

$$N_v = f_r K_o D \ln \left[ \frac{D + Y_w}{D + Y_a} \right]$$

Drying Rate Equation for Hybrid Drying.

$$N_v = f_r \phi \frac{Q_g}{\Delta h_v}$$

Surface Energy Balance Defining Wet Bulb Conditions

$$h(T_a - T_w) = K_o D \ln \left[ \frac{D + Y_w}{D + Y_a} \right] h_{fg}$$

Relationship Between Saturated Humidity and Temperature

$$Y_{sat} = Y_{sat}(T_a)$$

Characteristic Drying Curve Function

$$f_r = f(\Phi)$$

Evaporative Plane Position,  $\delta$ , for convective drying

$$\Phi = f \left[ 1 - \frac{\delta}{b} \right]^2$$

Evaporative Plane Position,  $\delta$ , for dielectric drying

$$\frac{\delta}{b} = \delta^* = \left( 1 - \frac{X}{X_o} \right)$$

Convective Heat Transfer Coefficient Correlation

$$\text{Nu} = C_2 \text{Re}^m$$

Heat and Mass Transfer Analogy Relating Transport Coefficients  $h$  and  $K_o$

$$K_o = h \frac{\beta \text{Le}^{2/3}}{C_p}$$

## REFERENCES

1. D.Reay. "Modeling Continuous Convection Dryers for Particulate Solids - Progress and problems." Engineering Sciences Division, A.E.R.E., Harwell, Oxfordshire OX11 0RA, England
2. B.A.Flake. "Process Design Model for a Single-Zone Tunnel Dryer." Master of Science in Mechanical Engineering Thesis, University of Texas at Austin, December 1987.
3. R.B. Keey. Introduction to Industrial Drying Operations, New York Pergamon Press, 1978.
4. R.B.Keey, T.A.G. Langrish, D.Reay. "The Application of the Characteristic Drying Curve to the Drying of Porous Particulate Material." Third Australasian Conference on Heat and Mass Transfer. The University of Melbourne, May 1985. PP 103-110.
5. R.B.Keey, M.Suzuki. "On the Characteristic Drying Curve." Int. J.Heat Mass Transfer. Vol.17 pp.1455-1464.
6. M.Suzuki, R.B.Keey and S.Maeda. "On the Characteristic Drying Curve." AIChE Symposium Series, 73 (163), 47-56 (1977).
7. A.C.Meiners "Development of an Empirical Model for the Drying of Hygroscopic and Non-Hygroscopic Materials." Masters of Science in Mechanical Engineering Thesis, University of Texas at Austin, May 1988.
8. A.L. Vankoughnett. "Fundamentals of Microwave Heating." Trans.IMPI 1973 paper no.3.
9. J.M.Accad and P.S.Schmidt. "Model Studies of Evaporation Under Combined Microwave and Convective Heating." Proceedings of the 8<sup>th</sup> International Heat Transfer Conference, San Francisco, Ca. August 17-22, 1986
10. P.S.Lefevre, A.Parsi, B.Mangin, W. Rezvan. "Industrial Materials Drying by Microwave and Hot Air." Microwave Power Symposium Digest, Ottawa,Ont., Jun 28-30 1978, pp 65-67.
11. R.M.Perkin. "The Drying of Porous Materials With Electromagnetic Energy Generated at Radio and Microwave Frequencies." Progress In Filtration and Separation 3,blz. 205-266. Electricity Council, Great Britain, 1983.

12. A.Le Pourhiet, S.Bories. "Analysis of the Role of a Microwaves Energy Contribution in Drying Porous Media." *Drying '80*, Vol 2 Proceedings of the International Symposium, 2nd, McGill University, Montreal, Que, Jul 6-9 1980, pp 186-194.
13. D.W.Lyons, J.D.Hatcher, J.E.Sunderland. "Drying of a Porous Medium With Internal Heat Generation." *Int. J. Heat Mass Transfer*. Vol. 15, pp. 897-905. 1972
14. M.Suzuki, S.Maeda. "On the Mechanism of Drying of Granular Beds." *Journal of Chemical Engineering of Japan*. Vol. 1, no. 1, 1968, pp. 26-31.
15. C.F.Gerald, Applied Numerical Analysis, Second Edition. Reading, Massachusetts: Addison-Wesley, 1980.
16. R.B.Keey, "Process Design of Continuous Drying Equipment." *AIChE Symposium Series*, 73 (163), 1-11(1977).
17. C.Moyne, A.Degiovanni, "Importance of Gas Phase Momentum Equation in Drying Above the Boiling Point of Water." *Drying '85*, pg 109-116, 1985
18. R.Panton, Incompressible Flow. John Wiley and Sons, Inc. 1984
19. E.R.G.Eckert, M.Faghri, "A Parametric Analysis of Moisture Migration in an Unsaturated Porous Slab Caused by Convective Heat and Mass Transfer." *Wärme- und Stoffübertragung*, Volume 20, pgs 77-87, 1986.
20. Conversation with J.Grolmes, M.S. candidate, who performed the experiment using a transparent container for the visualization of the behavior of the receding front.
21. D.A.van Meel, "Adiabatic Convective Batch Drying With Recirculation of Air." *Chemical Engineering Science*, Vol. 9, pg 36-44.
22. J.C.Ashworth, R.B.Keey, "The Evaporation of Moisture From Wet Surfaces." *Chemical Engineering Science*, 1972 Vol. 27, pp 1797-1806
23. P.Chen, P.Schmidt, "An Integral Model for Convective Drying of Hygroscopic and Nonhygroscopic Materials." 8<sup>th</sup> International Drying Symposium, Paris. September, 1988.
24. M.P.Armstrong, "Empirical Models of Convection Drying Rates Curves for Nonhygroscopic Industrial Materials." *Master of Science in Mechanical Engineering Thesis*, University of Texas at Austin, May 1988.